AALBORG UNIVERSITY
STUDENTS STUDYREPORT

Department of Energy Technology-Pontoppidanstraede 101
Aalborg University, Denmark

INTELLIGENT CONTROL FOR DISTRIBUTED SYSTEM

MASTER THESIS

WPS4

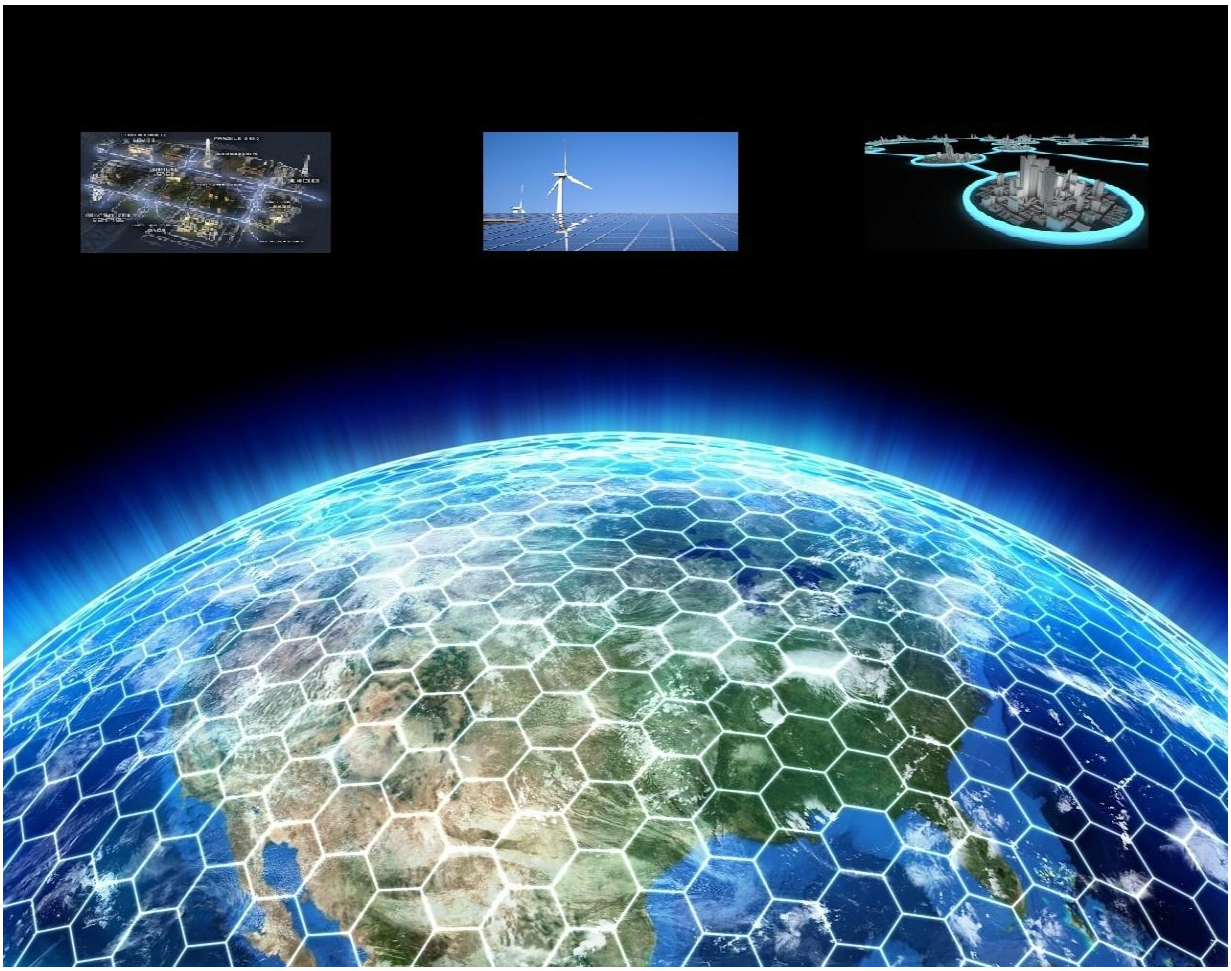

CONDUCTED BY GROUP WPS4 1054

SPRING SEMESTER 2012

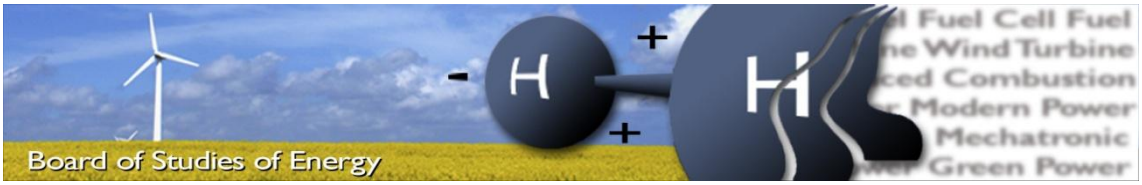

Title: **Intelligent Control for Distibuted System**

Semester: **4th**

Semester theme: **Master Thesis**

Project period: **01/02/2012 – 31/05/2012**

ECTS: **30**

Supervisor: **Prof. Zhe Chen**

Project group: **WPS4 - 1054**

SYNOPSIS:

An intelligent control strategy for a DC micro-grid system will be presented. The studied system consisting of renewable generations, one conventional generation, energy storages, loads and control units. The size of the micro-grid is determined on the base of the load and the renewable generations, the energy storages and the conventional generation have to be able to supply the DC loads when the weather conditions not are favorable to the PV and/or wind-turbine generations. The intelligent control method is used to regulate the DC voltage when the Microgrid is disconnected to the grid, i.e. islanded mode, due to disturbances, such as a fault and its subsequent switching incidents. Moreover the grid connected mode is considered to implement an intelligent energy management that will schedule the energy allocation at minimum cost on the base of the electricity market. The studied system with the control strategy have been implemented in a simulation tool, the results are presented and discussed in the thesis.

_____

Michele Martino

_____

Yamshid Farhat Quiñones

Copies: 3

Pages, total: 109

Appendix: 5

Supplements: 1 CD

By signing this document, each member of the group confirms that all group members have participated in the project work, and thereby all members are collectively liable for the contents of the report. Furthermore, all group members confirm that the report does not include plagiarism.

PREFACE

The present thesis entitled *Intelligent Control for Distributed System* was written by group WPS4-1054 in 10th Semester at the Department of Energy Technology, Aalborg University. This project has been carried out between 1st of February – 31th May 2012. On the base of the study and results of this thesis a paper was written, Intelligent Control for a DC Micro-grid. It was submitted at the 47th International Universities' Power Engineering Conference (UPEC 2012) in London, UK.

Reading instruction

In order to simplify the reading of the project some details about the way it is structured are presented. Detailed information about the literature used is illustrated in the bibliography. References are shown as a number in brackets [X]. Figures and tables are numbered in arithmetical order. Equations are represented like (X.Y), where X is the chapter number and Y is the equation number. Appendixes are assigned with capital letters and put in alphabetical order. For the values, the comma is used as a the thousand separator and the point as decimal separator.

Acknowledgement

The authors of the thesis would like to express their special thanks to the supervisors, Prof. Zhe Chen, for his endless support and invaluable information provided throughout the development of the project. Also the authors would like to express their appreciation and gratitude to PhD fellow Pietro Raboni for all the help provided during the entire project period.

Finally, they would like to thank to their families and girlfriends for their generous and continuous moral support in the past 2 years.

Aalborg, 31st May 2012

GROUP 1054

Summary

The thesis covers the aspect of the intelligent control for a distributed system and consists of sixth chapters.

In the first chapter a general introduction with the background and the goals of the thesis are presented.

In the second chapter a review of the state of art of the micro-grids was shown considering the development of the electrical networks in the last years and the introduction of DER sources. Focusing in the micro-grid concept and state of art, the currently control topology methods for these systems and the different implemented micro-grid and control topology used.

In the third chapter the implemented DC micro-grid has been presented, with the chosen voltage level and its intelligent control strategy. Also the participation of the micro-grid in the electricity market was considered and its economical profit was studied with an intelligent economical control. Different study cases are presented to evaluate the optimal participation in the electricity market.

In the fourth chapter, the DER units are shown with different kinds of control methods used for each unit, showing the fundamental concept of every technology used in the implemented system, the chosen model for every DER unit, the different kinds of control methods to increase the injected power, to balance the power flow and the voltage level of the micro-grid and the chosen power electronics for each unit.

The purpose of the fifth chapter is to build a series of scenarios by MATLAB/Simulink to simulate the implemented micro-grid. Four study cases are presented to show the behavior of the DC micro-grid in different scenarios. The behavior of the system in islanded mode, in grid connected mode, working with three master units and in a cascade faults are shown in this chapter.

As conclusion, it can be stated that the proposed intelligent control for the distributed systems has been tested and validated in four simulation cases and the overall project objectives were accomplished.

Contents

Figures

Tables

ABBREVIATIONS

Symbol	Meaning
AC	Alternating Current
ADA	Advanced Distribution Automation
BPL	Broadband over Power Line
CCM	Continuous Current Mode
CERTS	Consortium for Electrical Riability Technology Solution
CHP	Combined Heat and Power
DC	Direct Current
DER	Dustributed Energy System
DG	Distribute Genaration
ES	Energy Storage
ESMS	Economical Storage Management System
ESS	Energy Storage System
EV	Electrical Vehicle
GE	Gas Engine
IGBT	Isulated Gate Bipolar Transistor
LA	Lead-Acid
MPPT	Maximun Power Point Tracking
PI	Proportional-Integral
PMSG	Permanent Magnet Synchronous Generator
PV	Photovoltaic
PWM	Pulse Width Modulation
SISO	Single-Input Single-Output
SOC	State Of Charge
U.S.	United States
UPS	Uninterruplible Power Supply
VSC	Voltage Source Converter
WAMS	Wide Area Measurement System
WT	Wind Turbine

CHAPTER 1- INTRODUCTION

1. Background and Motivations

The use of renewable energy in the world in the period between the 2004 and 2008 [1] grew by an unprecedented manner, in this period the total production capacity of renewable energy increased by 75%, Fig. 1 shows the energy capacity in the countries that have invested more in this field according to the data published in 2009.

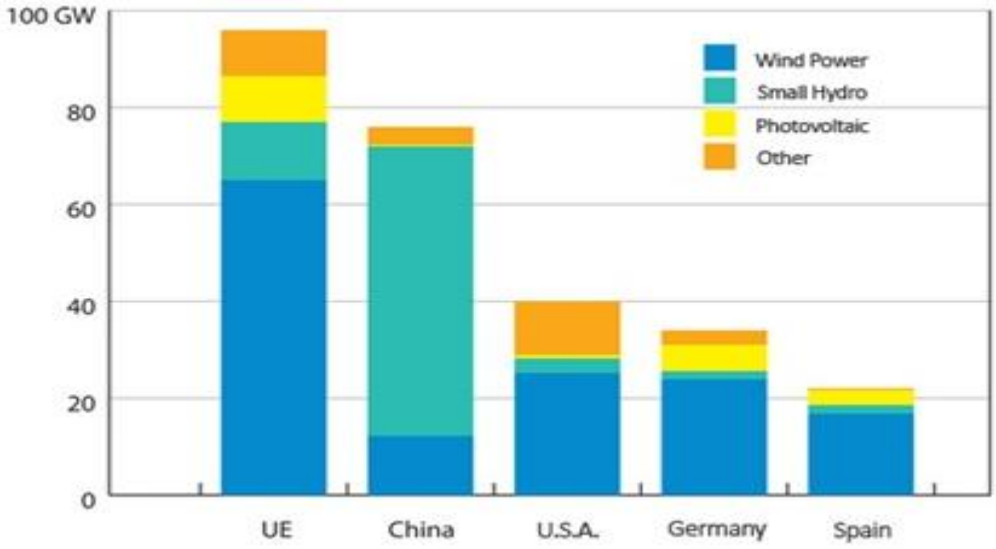

Fig. 1. Renewable Energy Capacity around the World[1]

So the distributed energy resources (DER) are emerged as a promising option to meet the growing customer needs for electric power with an emphasis on reliability and power quality, all in a context of evolutionary changes from the traditional electric utilities. The DER may be connected into a micro-grid and controlled in a self-intelligent way for each units[2].

AC and DC micro-grids may be very good elements for the integration of renewable and distributed energy resources. In the recent years, the increase attentions about these opportunities have been observed, so many studies on the AC micro-grid are done, and therefore a more thorough analysis on the DC micro-grid could be performed. The DC distribution system has some advantages over the AC distribution, the DC micro-grid can easily be operated in a simple coordination method because it controls only the DC bus voltage, moreover when the AC-grid, which is connected with the DC micro-grid has fault conditions the DC micro-grid is disconnected and operate in a stand-alone mode in which the generated power is supplied to the loads connected to the DC distribution system, another advantage is the possibility of reducing the system cost and loss thanks to the only single AC grid side inverter unit used[3][4].

Some of the more important characteristics of the DC micro-grid could be [5]:

- Super high quality power supplying is provided by distributed scheme of the load side converters contributes, so if a short circuit occurs at one load the other loads not are affected.
- It is suitable for DC output type distributed generations such as photovoltaic (PV) and energy storage (ES), i.e. batteries.
- If the power production is less than the power consumption, it can stop supplying power for some loads intentionality by load side converter in order to continue supplying power for high quality loads.

Nowadays, the losses in the distribution systems are an evident problem, as it is shown in Fig. 2, but in the modern digital economy, demand for power quality and reliability can vary significantly. Commercial customers with critical computer systems require high levels of power quality and are often willing to pay for it, while most residential consumers may not. This is evidenced investment in uninterruptible power supply (UPS) by commercial customers to protect computer and data systems from outages[6].

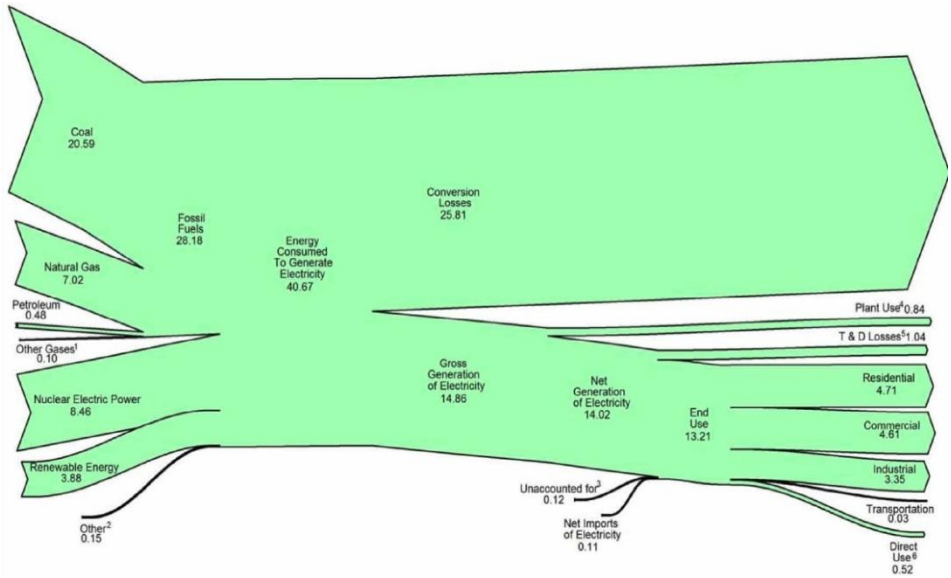

Fig. 2. US Electricity Flow, 2008, source: "US Energy Information Administration (2009)"

1.1 Subjects

In this thesis, an intelligent control strategy for a DC micro-grid system will be presented.

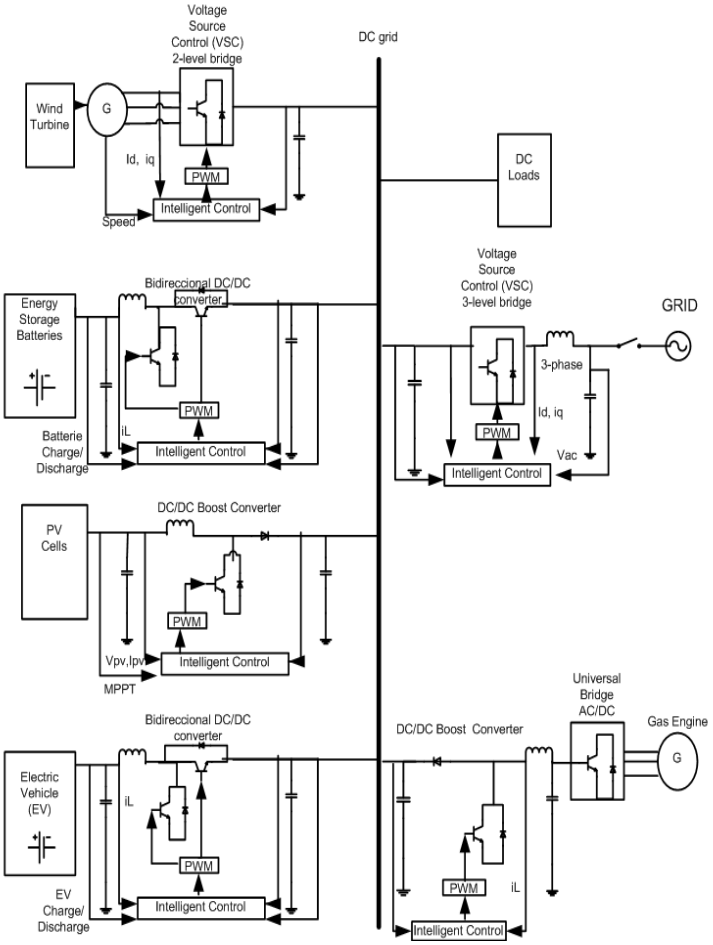

Fig. 3. Micro-grid Configuration

The thesis presents a studied system consisting of two renewable generations, one conventional generation, two energy storages, loads and control units; a Photovoltaic (PV) generation unit, a wind-turbine (WT) generation unit, a battery energy-storage unit, an Electrical Vehicle (EV) unit, a gas engine (GE) generation, an AC grid-connected power control unit and DC loads such are shown in the Fig. 3. The size of the micro-grid is determined on the base of the load and the renewable generations, the energy storages and the conventional generation have to be able to supply the DC loads when the weather conditions not are favorable to the PV and/or wind-turbine generations. This configuration is shown in the chapter 3.1.

1.1 Goals

The thesis proposes an intelligent control method to regulate the DC voltage and the power flow when the micro-grid is disconnected from the grid, i.e. islanded mode, due to disturbances, such as a fault and its subsequent switching incidents. The micro-grid is kept in operation to meet the corresponding load requirements [7].

Moreover the grid connected mode is considered to implement an intelligent energy management that will schedule the energy allocation at minimum cost on the base of the Danish electricity market. The expected output is constituted by the optimal economic dispatch of the generators in micro-grid by using an input pattern containing information about the energy price, the weather conditions and the forecast on the energy load demand by showing the benefit to use the energy storage.

The studied system with the control strategy have been implemented in MATLAB/Simulink, the results are presented and discussed in the paper.

CHAPTER 2 - MICROGRID

2. Introduction

The electrical network is the set of transformers and infrastructures that carry electricity from the centers of production to all consumers. These networks are responsible to transport and distribute the electricity generated from the source to the final point of consumption. They are designed to operate since the middle of last century, where main production centers were distant from the final costumers, therefore from the standpoint of consumers and the characteristics of plants based on renewable energy the actual network is redesigning to become more suitable. Since this, a new concept of power grid is appearing considering the capability to integrate an intelligent control. In this chapter the state of art of these new topologies of power grid is shown, called Smart Grids. It is making a new concept of power grid whose can intelligently integrate behavior and actions of all the actors connected to them to provide a supply of electricity safe, economical and sustainable. While many renewable power source are large-scale and are connected directly to the transmission system, also there are small-scale and distributed renewable sources (e.g. solar photovoltaic, energy storage, micro-wind farms, etc.), these sources, also known as distributed generations, have to be located near consumption points within low-voltage electric distribution to achieve efficient and economical requisites.. So the development of micro-grids can be one way to solve these questions. Nowadays, emerging power electronic technologies and digital control systems makes possible to build advanced micro-grids capable to operate independently from the grid and integrating multiple distributed energy resources. A review of micro-grid is presented[6], by showing the concept of AC and DC distributions mode and their advantages and disadvantages.

2.1 Smart grids

The European Technology Platform defines the Smart Grids as the electrical grid that can intelligently integrate the behavior and actions of all users connected to them (generators, consumers and those who generate and consume) in order to work efficiently, economically and ensure electricity supply [8].

A Smart Grid has innovated products and services, also intelligent monitoring control communication and self-healing technologies to improve the connection and operation of generators of all sizes and technologies, allow consumers to play a role in optimizing the system operation, giving consumers more information to choose the best option for them. Also reduce the environmental impact of electrical system supply and maintain or improve the existing levels of reliability, quality and safety system supply. An example of smart grid is shown in the Fig. 4.

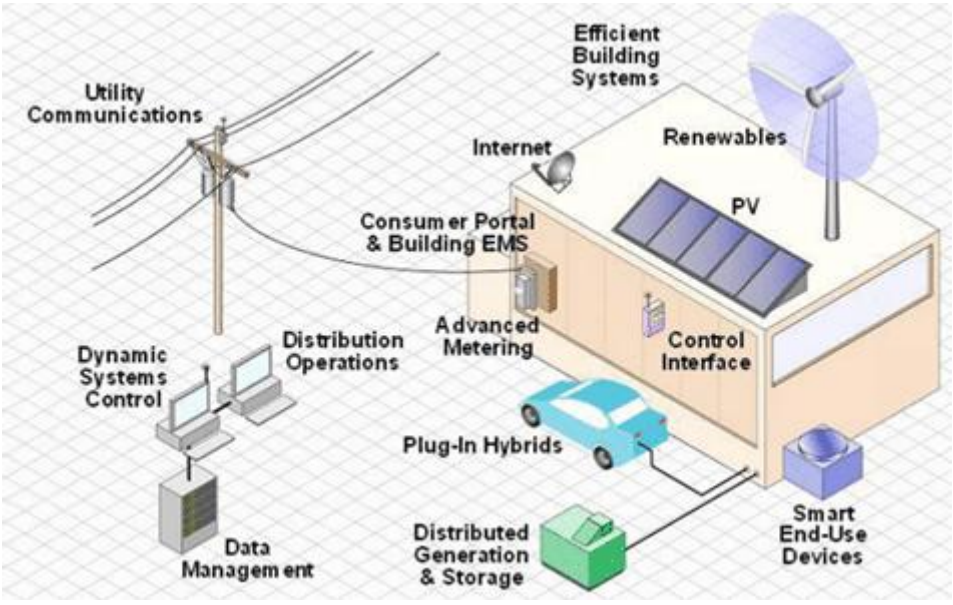

Fig. 4. Smart Grid example

Smart Grid technology stems from attempts to use consumption controls by measuring and monitoring systems. Since 1980, the meters breakers were used to monitor the load of millions of customers, and in 1990 an advanced infrastructure was implemented to determine the amount of energy used at different times per day.

In 2000, in Italy the first Smart Grid project was created spanning nearly 27 millions households using smart meters connected via a communication line.

The Smart Grid maintains constant communication, to be able to control the system in real time and it is able to be used as a bridge to the creation of intelligent systems for energy savings. One of the first implemented devices was the passive demand to determine the frequency variations in the provision of energy in homes[9].

Recent projects are those that use wireless technology, or Broadband Over Power Line (BPL). The network's monitoring and synchronization process evolved when the Bonneville Power Administration created a new prototype sensor. This sensor was able to analyze anomalies in the power quality of the electric system in large geographical areas. This led to the first Wide Area Measurement System (WAMS) in 2000. This technology has also been integrated by other countries. China is building it, expecting to complete it in 2016.

Nowadays, Smart Grids have a large amount of research activity. The EPRI IntelliGrid initiative has proposed to create a new electric power delivery infrastructure that integrates advances in communications, computing, and electronics to meet the energy needs of the future and to facilitate the transformation of the electric infrastructure to cost-effectively provide secure, high-quality, reliable electricity products and services[10].

The EPRI Advanced Distribution Automation (ADA) objective is to create the distribution system of the future. It has to be a highly automated system with a flexible electrical system architecture operated via open architecture communication and control systems. As the systems improve, they will provide increased capabilities for capacity utilization, reliability, and customer service options[10].

The Modern Grid Initiative focus on the modern grid as a new model of electricity delivery. It sees the modern grid as a system that utilizes the most innovative technologies in the most useful manner by creating an industry–DOE partnership that invests significant funds in demonstration projects. They will address key barriers and establish scalability, broad applicability, and a clear path to full deployment for solutions that offer compelling benefits[10].

Each project will involve national and regional stakeholders and multiple funding parties.

2.2 Micro-grids

Even though a standard protocol to define a micro-grid doesn't exist, there are certain characteristics in the existing micro-grid systems. They are composed of interconnected distributed energy resources which provide continuous energy capable of supplying the internal load demand. A micro-grid is self-controlled and capable of working in grid-connected mode and possesses independent control capable of controlling the micro-grid on islanding mode when a grid service interruption takes place [11].

These systems can maximize the use of renewable energy, increase the power quality and reliability level for local customer's loads[11][12].

Micro-grid concept has a long history. Thomas Edison's was the first one to implement a MG in 1882, the Manhattan Pearl Street Station, due to the actual centralized grid was not yet implemented. By 1886, fifty-eight direct current (DC) micro-grids were installed. However, the evolution of the electric market industry changed to a state-regulated monopoly AC market, ending with the micro-grid developments.

Nowadays, a variety of studies and investigations are converging to evolve the electric model to implement micro-grids. It has become clear that the fundamental architecture of the 20^{th} century electricity grid based on a unidirectional power flow is obsolete.

The first "modern" industrial micro-grid was built at the Whitling Refinery in Indiana, with 64 MW of installed power. This micro-grid was based on fossil-fueled generation.

Between now and 2015, over 3.1GW of new micro-grid capacity is projected to be implemented worldwide. As shown in the Fig. 5, the United States is the current leader, with exactly 626 MW operating at 2010, and that capacity is expected to increase to 2,352 MW by 2015[13].

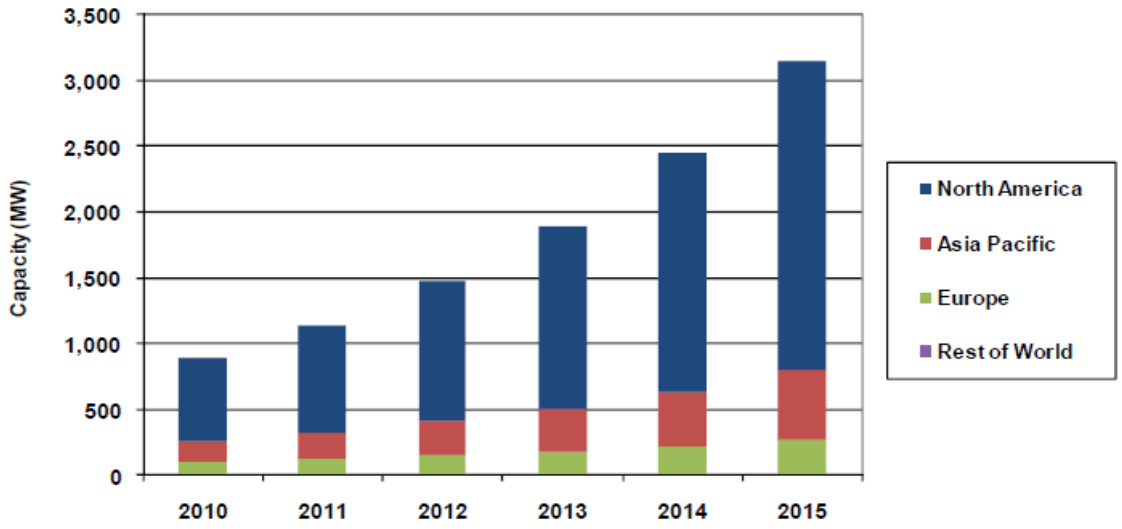

Fig. 5. World Capacity of Micro-grid [13]

At 2009, in the United States, 322 MW of college campus micro-grids were up. In the U.S., 40% of future micro-grids will be developed in this market segment, adding 940 MW of new capacity valued at $2.76 billion by 2015[13].

The micro-grid can be classified as AC micro-grid and DC micro-grid, depending by distributed sources and loads are connected on the basis of AC or DC power transmission. AC micro-grid has the advantage to utilize existing AC grid technologies, protections and standards, but also needs synchronization and stability for reactive power.

On the other hand, DC micro-grid has an easier control management and the benefit that could eliminate DC-AC or AC-DC power electronics converters required in AC micro-grid for the sources and DC loads, providing more efficiency, lower cost and system size. However, DC micro-grid needs further research about proper operating range of DC voltage and protection devices for the DC system [14].

To resume, the DC micro-grid has the following advantages over the AC systems:

Each Distributed generator connected to the DC micro-grid system can easily be operated in coordination because only the DC bus voltage is controlled.

When there is a fault or a interruption on the AC-grid system, the DC system is disconnected from the grid, and then it is switched to the islanded operation in which the generated power is supplying the loads connected to the DC distribution system, even if one load is disconnected, it doesn't affect to the stability of the micro-grid [2].

There is only a single AC grid-side inverter needed, therefore the unit system cost and the power losses can be reduced [2].

If power consumption becomes more than power production during long term isolation, DC micro-grid can stop supplying power for some loads intentionality by load side converters in order to continue supplying power for high priority loads. It is also

possible to form dc loop configuration at the dc distribution part and to share the power between other dc micro-grid systems[4][5].

From the viewpoint of the system extendibility, reliability and maintainability, the DC and AC micro-grid architecture and control allows to:

Connect or disconnect more loads to the active bus.

In the near future, no changes are needed if some units with different power ratings are connected to the grid.

Depending the kind of used control, no signal and data communication is needed among the existing units[3].

2.2.1 Control

A micro-grid has to be able to import or export energy from the grid, control the power flows, and balance the voltage bus level. To achieve these objectives, small generators, storage devices, and loads have to be controlled. Usually, the distributed sources (PV, small wind turbines, or fuel cells) or storage devices use power electronic interfaces to connect them with the micro-grid [15].

According to the "Characterization of the Micro-grid in the U.S", micro-grids are separated in different classes based on the control topology.

Proposals for micro-grid's control can be grouped into three types, depending on their topology[16][11].

a) Simple Class or Virtual 'Prime Mover'

In this topology a central controller measures micro-grid's state variables and dispatches the information to all the distributed generators using fast telecommunication. This topology creates one virtual power supply unit which controls all the system behavior. This control is based on the telecommunication system; if the communications fail a back-up control is needed. Also it is restricted by the limited numbers of telecommunications channels available, therefore if some DG is added and there isn't available more channels, the central controller has to be replaced.

b) Master Class or Physical 'Prime Mover'

In this topology a large central controller unit, usually an energy storage system or a generator, is controlled to act as a "master" to handle transient power flows and balance the voltage level in an islanded mode. The other sources act as a "slave" injecting current to the micro-grid's bus. The disadvantages of this control is the dependence on the master unit, therefore it has to be a reliability central source (i.e. overall system reliability), also if there are future changes in load or micro-generation, the central unit would have to be resized again.

c) Peer to Peer or Distributed Control

In this topology each units responds autonomously to variation in local state variables, as voltage magnitude or power flow. This local control determines transient and default behavior. The commutation frequency of each controller unit has to be enough fast to ensure stable operation of the micro-grid. An "intelligent" local control at each source's location ensures voltage and frequency stability. The power flow has to be controlled on islanded mode to balance sources and loads without voltage disturbance.

In the Table 1, the different control's methods and their characteristics are shown.

Table 1. Classification of micro-grid control's methods[17].

	Simple or "Virtual Prime Mover"	**Master Control or Physical "Primer Mover"**	**Peer to Peer Control or Distributed Control**
Specific Characteristics	All generators acts as one central power plant	One "Master" generator control the voltage level and the "Slave" generators acts as a current sources.	Without Master Control. Each generator has a local control controlling voltage, frequency and power.
Common Characteristics	Multiple sources injecting power on several loads in multiple locations. All the components are connected to the Microgrid's bus. Event detection and response control		

The control strategy for a Distributed Energy Resource unit in a micro-grid has to be selected depending the required functions and scenarios. The principal control functions for non-interactive control method are active/reactive power control (PQ control) and voltage/frequency control (V/F control). The droop control is used for interactive or distributed control when the system works in island mode. The control method of a DER unit depending to the scenario is shown in Table 2.

Table 2. DER control method depending the scenario [18].

Control Method	**Grid-Connected Mode**	**Islanded Mode**
Non-interactive	Power delivered by MPPTs converters (PQ control)	Voltage and frequency control (V/F control)
Interactive	Power dispatch, Active and reactive power support	Droop Control

In the Table 2 the control method is classified into non-interactive control and interactive control[18]. The "interactive" control method means that the output power of DER unit depends on the conditions of other sources or loads.

In the interactive control method, the power electronic converters have two separate operation modes, if they are connected to the grid they follow the grid inverter, acting as

a current source. And they act as a voltage source if the micro-grid is working in islanded mode.

With the aim of connecting several parallel converters, the droop method is usually implemented[19]. The applications of this control topology are typically industrial UPS systems or islanding micro-grids [20]. Droop control is a method to achieve the peer-to-peer or distributed control mentioned in Table 1. This technique is a way to make the inverters in the micro-grid system to perform a load sharing function in islanded mode. In the droop method, active and reactive-power flows can be controlled by the phase and the amplitude of the converter voltage.

The droop method can be expressed as the next equations shows[15]:

$$\omega = \omega^* - G_P(s) \cdot (P - P^*) \tag{2.1}$$

$$E = E^* - G_Q(s) \cdot (Q - Q^*) \tag{2.2}$$

Where E is the amplitude of the output voltage, ω is the frequency, ω^* and E^* are the values without loads (reference values), and $G_P(s)$ and $G_Q(s)$ the transfer functions.

The unbalance voltage between parallel controllers is caused by the current that circulates in the sources. To reduce this current, a virtual output impedance is programmed to emulate physical output impedance. This virtual impedance has not power losses[21].

2.2.2 Real micro-grid overview

Some examples of micro-grid implementations are shown below:

There are good examples like the Consortium for Electric Reliability Technology Solution (CERTS) micro-grid. Composed by three combined heat and power sources (CHP), driven by natural gas, connected in parallel with energy storage systems integrated by a bi-directional DC/DC converter. Each unit has their own control, made by P-f and V-Q droop line and PI control loops, this control topology is called Peer to Peer or Distributed Control, because there is not a central control[22], the micro-grid model is shown in Fig. 6.

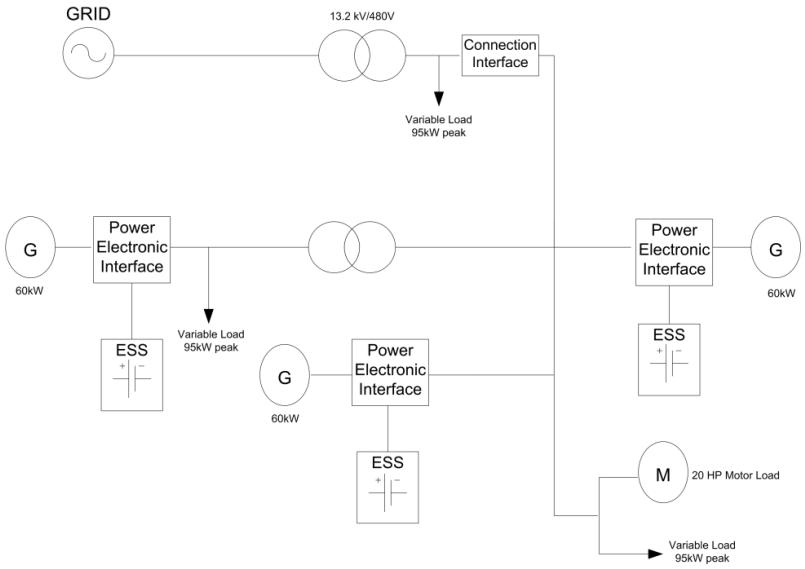

Fig. 6. CERTS AEP Micro-grid [16][22]

In Mad River a micro-grid has been built by the Northern Power Systems. A central MG controller controls the medium voltage switch and the loads. There isn't a Master unit like a Energy Storage System, then the control is Simple class or Virtual "Prime Mover", made by dispatching signals using fast telecommunications [13] [14], the Mad River micro-grid is shown in Fig. 7.

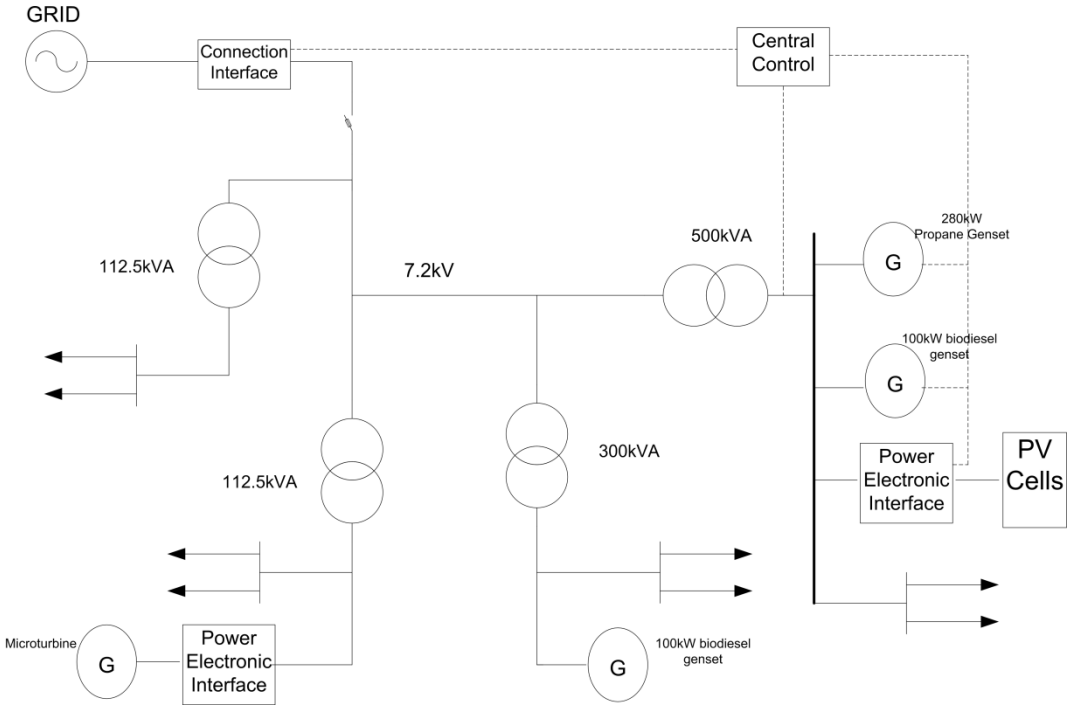

Fig. 7. MAD River Micro-grid [16], [23]

The British Columbia Hydro Boston Bar MG is able to supply a feeder with 3MW peak load, has an 8.6MVA of hydroelectric generation. The system effectively employs a single large generation station to control the net sub-system behavior. The topology of

the control is a Master class or Physical "Primer Mover" [16], [22], the micro-grid model is shown in Fig. 8.

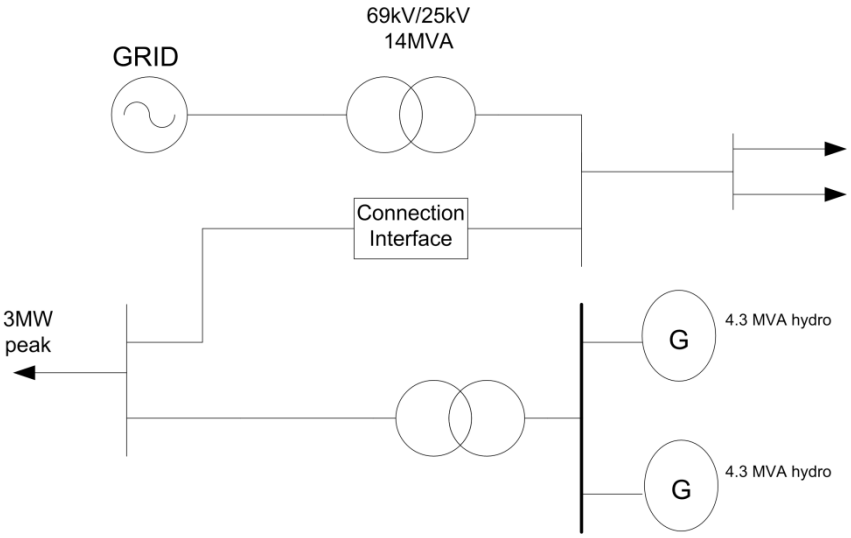

Fig. 8. BC Boston Bar Micro-grid [16], [22]

Japan is one of the modern leaders in the micro-grid sector, though most of its micro-grids include governmental and other institutional customers.

The Shimizu Corporation has built a large scale micro-grid in Tokyo, Japan. Composed by 4 Gas Engine models, a PV array and three ESS (a lead-acid battery, a NiMH battery and an ultracapacitor). All these sources feed the Shimizu laboratories. The control is made by a Central control without a Master unit, therefore is a Simple class or Virtual "Prime mover" [16], [24], the Shimizu micro-grid is shown in Fig. 9.

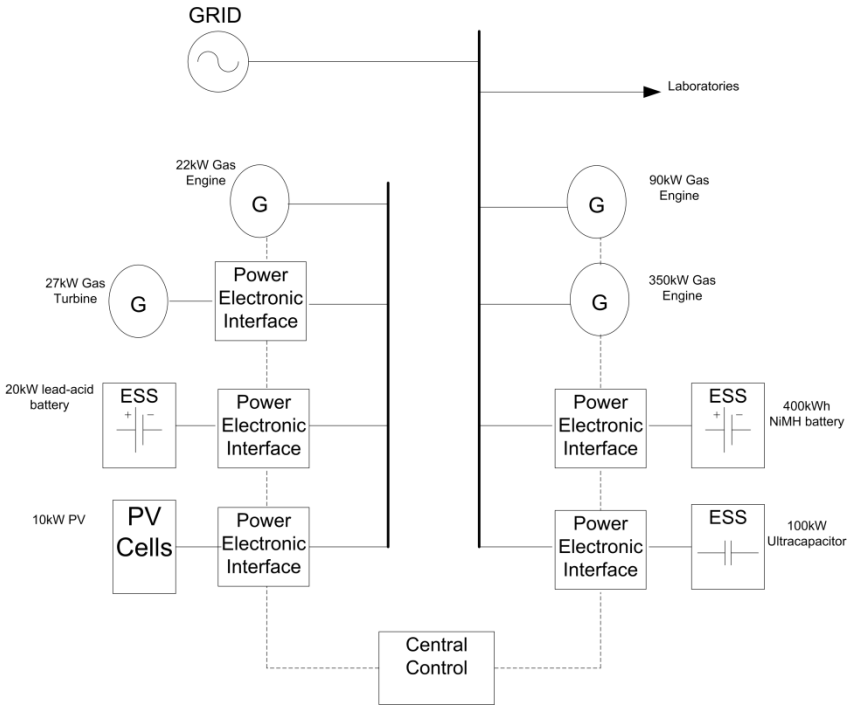

Fig. 9. Shimizu Extended Micro-grid [16], [24]

In Hachinohe is used a private 6kV feeder. The private distribution line was constructed to transmit electricity primarily generated by the gas engine system. Several PV systems and small wind turbines are also connected to the micro-grid. At the sewage plant, three 170-kW gas engines and a 50-kW PV system have been installed. The system is controlled by a Central Control System, without a Master unit, whose dispatches signals using fast telecommunications. Therefore, the control topology is a Simple class o Virtual "Primer Mover" [16], [25], the model is shown in Fig. 10.

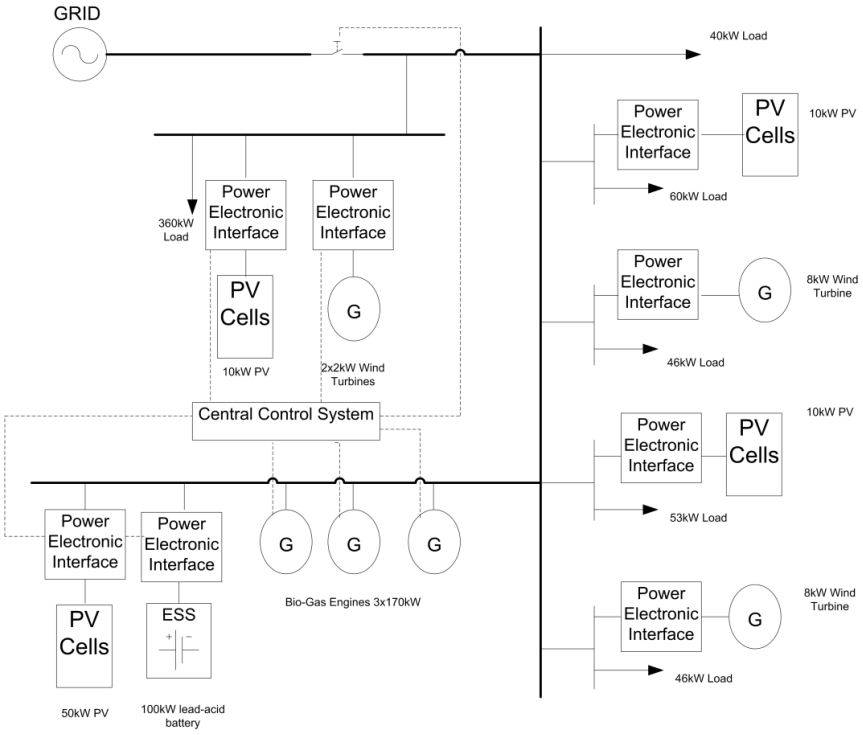

Fig. 10. Hachinohe System Micro-grid [16], [25]

Nowadays, DC micro-grids are an experimental issue, there is implemented a DC micro-Grid in Sendai, Japan, such it is shown in Fig. 11 [26]. This system is presently under-construction and is planned to include a 50 kW of PV micro-generation, two gas engines, a molten carbon fuel cell, also there is a battery backup fed through a DC/DC converter, to supply a full Uninterruptible Power Supply (UPS) back-up to part of the system and supplies some DC loads. This system is able to feed different kinds of power quality, a Premium power quality without voltage sags, a high quality power with voltage sags less than 15 ms, and the normal power quality, this system is shown in the Fig. 12 [26][16].

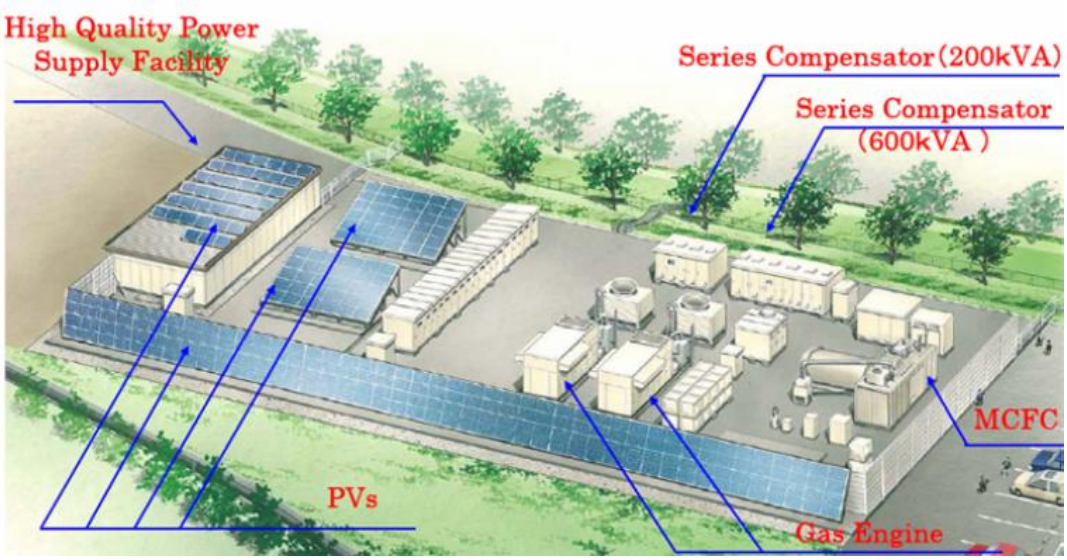

Fig. 11. A picture of Sendai DC Micro-grid [26]

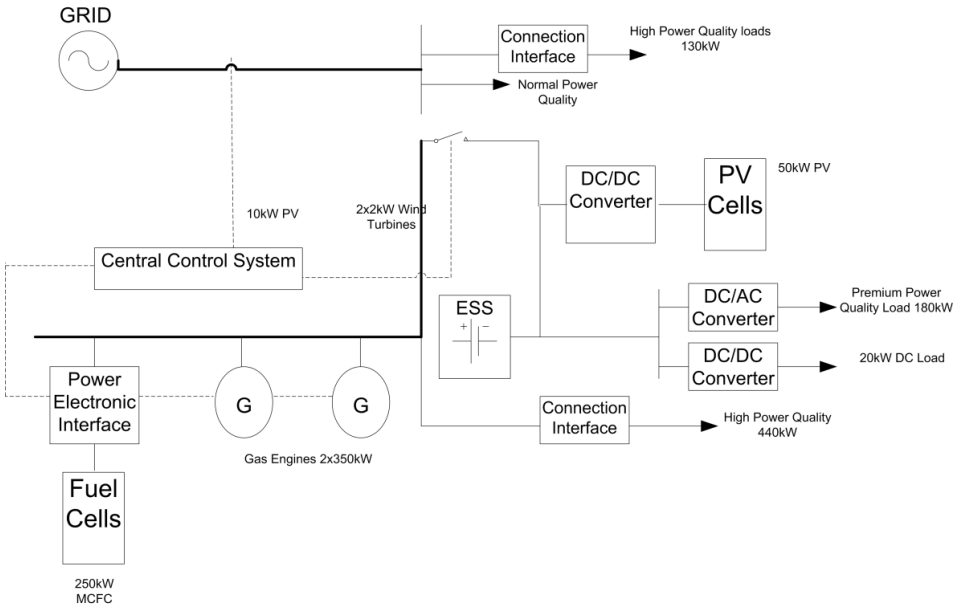

Fig. 12. Sendai Project: Multiple power quality supply system [16], [26]

Also in the Mayway Labs in Akagi (Japan) there is implemented a DC micro-grid of 10 kW composed by five units; the solar-cell generation unit, the wind-turbine generation unit, the battery energy-storage control unit, the flywheel power-leveling unit, and the ac-grid-connected inverter unit, Fig. 13 [27] .The power generated by the solar cell and the wind turbine is supplied to the dc load through the dc grid. The inverter sends the surplus power into the ac gird when the battery is a full charge. When the amount of the power generation is insufficient, the battery discharges the power into the dc grid. The inverter takes the power from the dc grid system when the battery has no power. The flywheel smoothes changes in power generation. The changes are caused by changes in the sun and/or wind conditions.

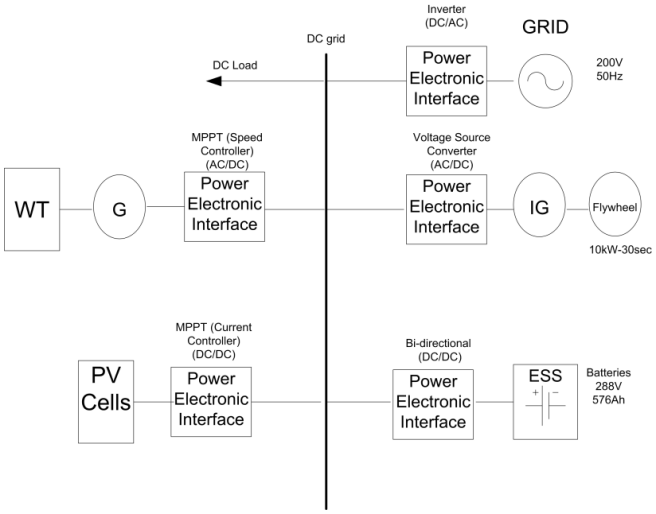

Fig. 13. Implemented Micro-grid in Mayway Labs, Akagi (Japan) [27]

CHAPTER 3 - TECHNICAL AND ECONOMICAL POINT OF VIEW FOR IMPLEMENTED MICRO-GRID

3. Introduction

To implement a micro-grid, the first step is to determine the structure and topology of the system. In this chapter, the overall concepts of the implemented micro-grid will be introduced; these can be classified as technical and economic concepts. On the technical side, the configuration of the DC micro-grid and the chosen DC voltage level are presented, including the control for the overall micro-grid in different scenarios.

On the economical side, an intelligent management of the micro-grid for the optimal participation with the electricity market is presented and different study cases are proposed. A study about the economical price of the different ESS technologies is needed to choose the optimal model for this application. Also a recompilation of files as the electricity market price, the wind speed and the irradiance for Aalborg (DK) in 2011 is needed and they are implemented by the HOMER software.

The results are shown in paragraph 3.3.1.

.

3.1 DC Micro-grid Configuration

The studied DC micro-grid consists of a cluster of generators, storages and loads and a power electronic interface to the three-phase AC grid. The regarded DGs are a 50kW WT, a 25kW PV, a 40kW back-up GE and stationary Lead-Acid battery and Lithium-Ion one, for Electric Vehicle usage, compose the ESS, which the power and technology chosen will be discuss in the chapter 3.3. In Fig. **3** at chapter 1.1, the implemented model is shown.

The voltage level on the DC bus will be defined on the base of the follow requirements[28]:

- little changes of the existing distribution system
- use of unified electrical cables or wire bidirectional energy transport
- electrical safety for people and equipment not lower than the actual level.

In Europe the most of the voltage power distribution networks (AC power supply system) are made with three phase cables lines, 400V $\pm$ 10% line voltage, 50Hz $\pm$ 2%.

The maximum current in the line has different limitations[28]:

- the temperature inside the cables should not exceed the limit by the characteristics of the cable itself
- the voltage drop has been to maintain into the range (the maximum voltage drop along the main LV back-bone feeders should not exceed 5%), this depend on the length of the cables.

So the followed configuration shown in Fig. 14 may be implemented [28]:

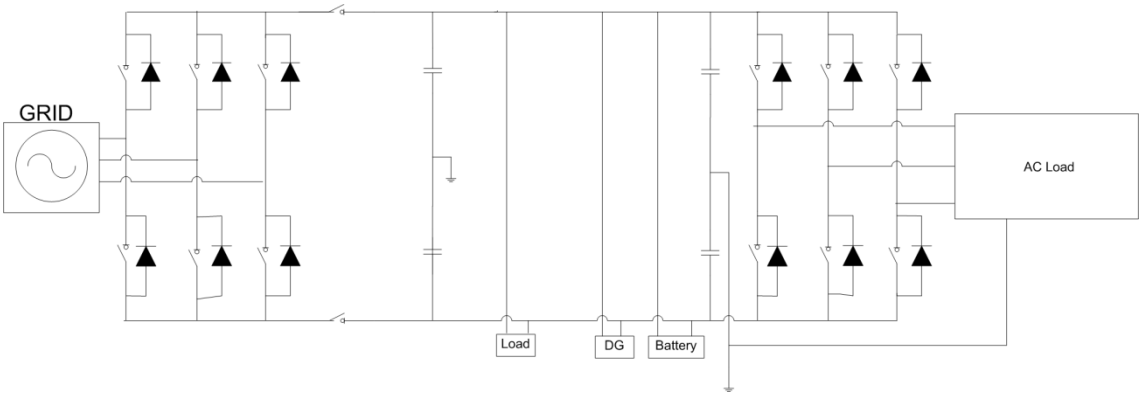

Fig. 14. Implemented wire configuration [28]

Regarding the power that can be transmitted, assuming the DC current equal to the RMS value of the AC one, this solution is profitable if the DC voltage is at least $\sqrt{3}\ \cos\Phi$ times the AC line to line voltage. In fact:

$$\frac{P_{DC}}{P_{AC}} = \frac{V_{DC}\cdot \mathrm{I}_{DC}}{\sqrt{3}\cdot V_{AC}\cdot \mathrm{I}_{AC}\cdot \cos\Phi} = \frac{V_{DC}}{V_{AC}\cdot\sqrt{3}\cdot\cos\Phi} \tag{3.1}$$

Assuming 0.9 as the minimum value of the power factor and $P_{DC} = P_{AC}$, the previous ratio is:

$$V_{DC} = 1.56 V_{AC} \tag{3.2}$$

which means a DC pole to pole voltage greater than:

$$V_{DC} = 1.56 \text{ x } 400\text{V} = 623V \tag{3.3}$$

Nevertheless a 800V pole-to-pole voltage has been assumed in order to ensure the operation of the grid tied inverter in the linear modulation region and for offering the opportunity to use two different voltage levels (pole-to-pole or pole-to neutral) to the loads.

3.2 Control Method

In the studied DC micro-grid, a "Master Class" control has been implemented to balance the DC voltage bus and to control the power supply to meet the load demand in islanded mode.

In this control, one unit source acts as a "Master" controlling the full system, while the rest of the units work as current sources (i.e. as "Slaves"). In this way, there will not be voltage different between the outputs of the DC sources, because the Master unit regulates the voltage values of all the output units, therefore will not circulate current between the sources[21].

The DC bus voltage in the micro-grid is sensed and compared with the reference voltage chosen in the chapter 3.1 (800V), the error is processed through a compensator (PI

block) to obtain the desired impedance current reference for the current loop. This compensator can be expressed in the following way:

$$I_{L_{REF}} = k_p(V_{REF} - V_{MG}) + k_i \int (V_{REF} - V_{MG})dt \quad (3.4)$$

The power flow is controlled by a current controller who compares the impedance current in the master unit with the reference current desired to stabilize the system, the error is processed through another PI block to obtain the desired duty cycle for the converter which acts as a Master. The PI block can be expressed as:

$$d = k'_p(I^*_L - I_L) + k'_i \int (I^*_L - I_L)dt \quad (3.5)$$

The problem of this control topology is the dependence on the Master unit, if there is a fault in this unit, the control will stop working properly[21]. To increase the reliability of the system, 3 different sources are able to act as a Master unit, decreasing the chance to have a fault in the micro-grid control.

In the studied model, the Voltage Source Converter (VSC) inverter of the grid will act as a "Master" when the micro-grid is connected to the grid, there are also implemented a voltage loop and a current loop to control the voltage level, so the VSC is not able to regulate the power flow.

The ESS is able to control the voltage level and the power flow through a bidirectional converter. When the micro-grid is working in islanded mode, this source will act as a "master" remaining the voltage at 800V and meeting the load demand.

If there is a fault in the ESS or the SOC level is not properly to control the micro-grid in islanded mode, the GE is able to act as a "master" controller too. There is a voltage controller implemented with a voltage and a current loop as it is shown in chapter 4.2.2.

3.2.1 Control Strategy

An Energy Management System (EMS) has been considered for the optimal operation of the micro-grid both in grid connected and islanded modes. The overall control is shown in Fig. 15 and an overview is given below.

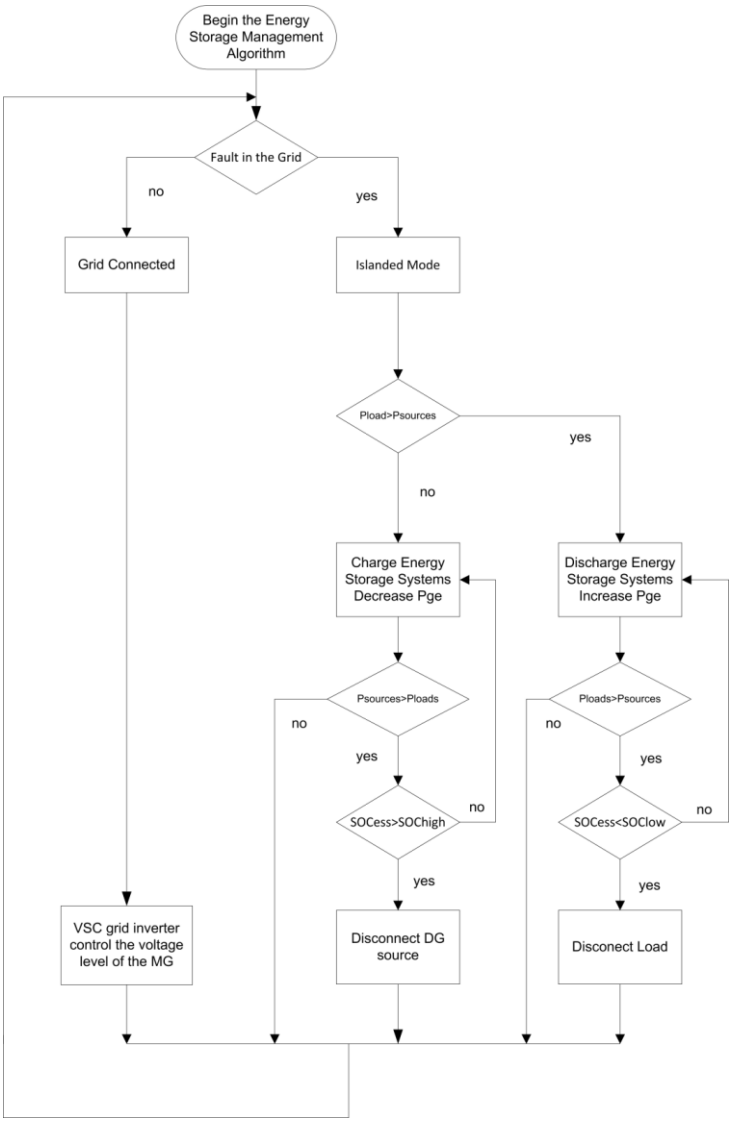

Fig. 15 Energy Management Control flow chart

In case of grid connected, the VSC grid inverter is able to work as “master” and all the sources from the micro-grid act as current source or as “slaves”. Therefore, the VSC is able to balance the DC voltage bus. In case of unplanned events as faults, the micro-grid has to be separated to the grid and work in islanded mode. In this case, the ESS will work as “master” controlling the voltage level and the power flow of the micro-grid. In all the operating conditions the PV and WT sources will be operating as slave ones. The Energy Management control copes the unbalances between power production from distributed generation (DG) units and load by means of the ESS, if their SOCs are sufficient, or with the GE. In this case it must be noticed that the GE response is slower than the ESS response due to the mechanical inertia and ramp-up time [27][29].

In case of ESS failure or an inappropriate SOC value, the master unit becomes the GE. If the control of the micro-grid is not able to balance the power flow of the system, the last countermeasure in case of load greater than the available generation is the load rejection. In case that the power generated by the sources would be bigger than the load

consumption, one of the distributed generators will be disconnected from the micro-grid.

3.3 Economical point of view

The aim of the Economical Storage Management System (ESMS) is to make the optimal decisions regarding the best use of the energy generated by the sources for balance the electric power in the micro-grid. Such decisions will be based upon the requirements of the local units, the weather, the demand of the load and many other considerations[30].

In particular, the capability of adapting the scheduling of generation to the availability of renewable sources is one of the major importance because it allows exploiting RES whose integration in the distribution system is worldwide supported by special programs[31][32].

The purpose of the implemented micro-grid system is to supply uninterruptible and maximum quality power to the DC loads in both modes, in grid connected and in islanded mode. But in this chapter, the price of the electricity market and the cost of the energy generated in the micro-grid are introduced as the points where the economical management decisions will be based.

The ESMS is based on the capacity of the ESS, to charge and discharge energy to obtain profit by an optimal participation in the electricity market. To be able to evaluate the advantage of this optimal participation, the cost of every kWh supplied by the ESS is needed.

3.3.1 Cost of ESS energy

The most important factors to calculate the costs and benefits ESS are the capital cost of the equipment, the cost for recharging energy and the replacements costs if they are needed. The benefits depend on the kind of use required by the user and the expected service of the ESS[33][34].

The frequency of operation (charge and discharge cycles) is one of the most important parameters to calculate the life-cycle. The applications for ESS can be categorized by whether frequent cycling is expected.

This is important because depending on the application, the number of cycles by year will change. For an arbitrage application the ESS will work more than 200 cycles by year. In the other hand, if the ESS is used only for power quality the ESS will work only 20 times by year. In Table 3, different operation/use categories are shown[35].

Table 3. Operation/Use Categories [35].

Category/Definition	Hours of Storage	Use/Duty Cycle	Representative Application
Long-duration storage, frequent discharge	4-8	1 cycle/day x 250 days/year	Load-leveling, Source following, arbitrage
Long-duration storage, infrequent discharge	4-8	20 times/year	Capacity credit
Short-duration storage, frequent discharge	0.25-1	4x15 min cycling x 250 days/year *	Frequency or area regulation
Short-duration storage, infrequent discharge	0.25-1	20 times/year	Power quality, momentary carry-over

*Only able to some technologies (with more than 10000 cycles)

In this chapter, some technologies are described and studied, for the studied micro-grid the economical study will be based on the Lead-acid batteries, and with the Li-ion batteries which have been developed during the last years to become one of the most promising technologies, as it is shown in the chapter 4.1. Also, the lead-acid batteries with carbon-enhanced electrodes are analyzed for the economical point of view, because they are the latest variation on asymmetric batteries.

- **The capital cost**, can be expressed as:

$$Cost_{total}(€) = Cost_{PCs}(€) + Cost_{ESS}(€) \tag{3.6}$$

Where $Cost_{PCs}$ is the cost of the full equipment, and $Cost_{ESS}$ the cost of charging the energy.

The cost of the full equipment depends on the power rating of the system:

$$Cost_{PCs}(€) = UnitCost_{PCs} * P_{kW} \tag{3.7}$$

For almost all the technologies, the cost of the storage unit depends on the amount of energy stored:

$$Cost_{ESS} = UnitCost_{ESS}\left(\frac{€}{kWh}\right) * E(kWh) \tag{3.8}$$

where E is the stored energy capacity.

All systems have some inefficiency at charging the ESS. To consider this losses, the last equation is modified and expressed as follows:

$$Cost_{ESS} = UnitCost_{ESS}\left(\frac{€}{kWh}\right) * \frac{E(kWh)}{\eta} \tag{3.9}$$

Where η is the round-trip efficiency of the ESS.

As shown, cost is calculated by adding the cost of the storage unit and the cost of the full equipment systems; these are treated separately because they depend on ratings, power and energy[35].

In [35–38], the cost of the power and energy storage is shown in Table 4. This values are used for comparative purpose, because the actual cost of storage systems depends on many factors and hypothesis, therefore the values shown are subjective and continue to be debated even among experts in the field.

Table 4. Cost and Performance Assumptions [35–38]

Technology	Power Subsystem Cost (€/kW)	Energy Storage Subsystem Cost (€/kWh)	Round-trip Efficiency (%)	Cycles
Advanced Lead-Acid Batteries	315,53	260,31	80	2000
Sodium/sulfur Batteries	276,09	276,09	75	3000
Lead-Acid with Carbon-enhanced electrodes	315,53	260,31	75	20000
Zinc/bromine Batteries	315,53	315,53	70	3000
Vanadium Redox Batteries	315,53	473,30	65	5000
Lithium-ion Bateries	315,53	473,30	85	4000
CAES	552,18	3,94	70	25000
Pumped hydro	946,59	59,16	85	25000
Flywheels	473,30	1262,13	95	25000
Supercapacitors	394,42	7888,30	95	25000

Considering the life-cycle of the batteries same as the total number of cycles that the battery can work, then the price for each kWh generated could be calculated as shown in the following equation.

$$Cost_{ESS}(\frac{€}{kWh}) = \frac{Cost_{PC}*kW+UnitCost_{ESS}*\left({E_{kWh}}/{\eta}\right)}{E_{kWh}*Cycles} \quad (3.10)$$

Using the values shown the Table 4, the cost of each kWh generated for the Lead-acid Batteries will be:

$$Cost_{ESS}\left(\frac{€}{kWh}\right) = \frac{Cost_{PC}*kW+UnitCost_{ESS}*\left({E_{kWh}}/{\eta}\right)}{E_{kWh}*Cycles} = \frac{315{,}53*40+260{,}31*\left({40}/{0.8}\right)}{40*2000} = 0{,}32046\frac{€}{kWh} \quad (3.11)$$

For Li-Ion Batteries will be:

$$Cost_{ESS}\left(\frac{€}{kWh}\right) = \frac{315{,}53*10+473{,}30*\left({40}/{0.85}\right)}{40*4000} = 0{,}21809\ €/kWh \quad (3.12)$$

The Lead-Acid batteries with Carbon-enhanced Electrodes are the energy storage device with more number of cycles, the cost of each kWh generated is:

$$Cost_{ESS}\left(\frac{€}{kWh}\right) = \frac{315{,}53*40+260{,}31*\left({40}/{0.75}\right)}{40*20000} = 0{,}0331€/kWh \quad (3.13)$$

Depending the application or use for the ESS, one technology is better than the other. In this case, an arbitrage and optimal participation application will be implemented. These references price for kWh generated had to be compared with the electricity

market price. In this case, the hour by hour price during 2011 in Denmark has been obtained from the website www.nordpoolspot.com.

The fluctuation of the electricity market price during 2011 is shown in Fig. 16. Where the electricity price fluctuates between 0.00€ and 0.11€ in the maximum peak. Therefore, to implement an optimal participation with the electricity market the price for each kWh generated by the ESS may not be higher than 0.11€.

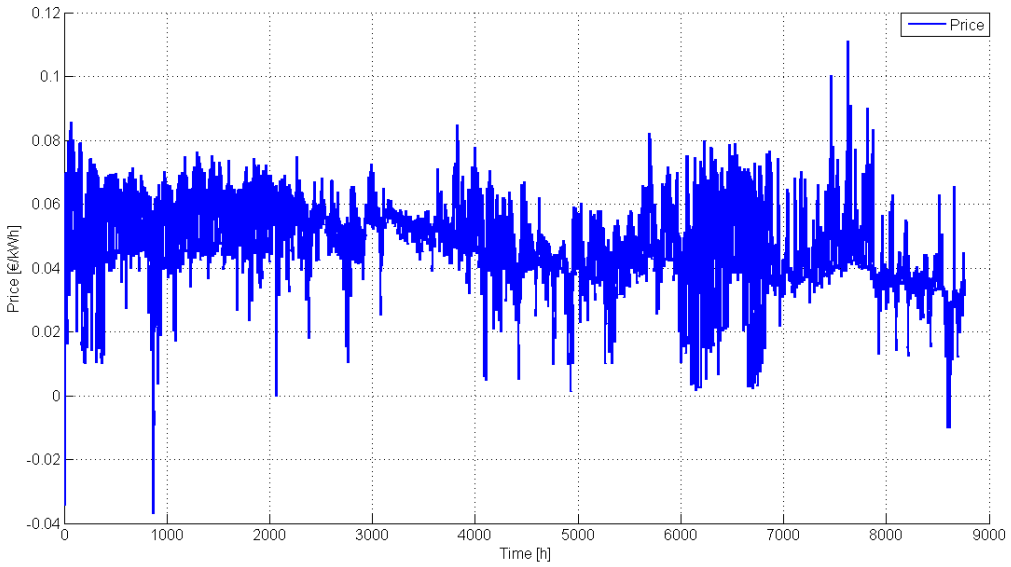

Fig. 16. Electricity price for every hour during 2011 in Denmark

For this reason, the Lead-acid battery with Carbon-enhanced Electrodes has been chosen to implement the Economical Storage Management, because the other technologies are not benefitting to be implemented for an optimal participation with the electricity market.

3.3.2 Economical Management System

An Economical Storage Management System (ESMS) algorithm has been implemented to optimize the exchange of energy with the grid. This control determines hour by hour the power injected into the micro-grid by an aggregated group of different kinds of DG and the electricity price market with the final goal of minimizing the global energy cost on the micro-grid. The micro-grid optimization is provided by this control that has to make the optimal decisions regarding the use of the generators for producing power in terms of minimum cost. ESMS algorithm is shown in Fig. 17.

The ESMS algorithm uses the information received about the wind speed and irradiance, to calculate the supplied power by the wind turbine and the photovoltaic array, and the price of the electricity market in every hour to choose the optimal option in terms of minimum cost for the system.

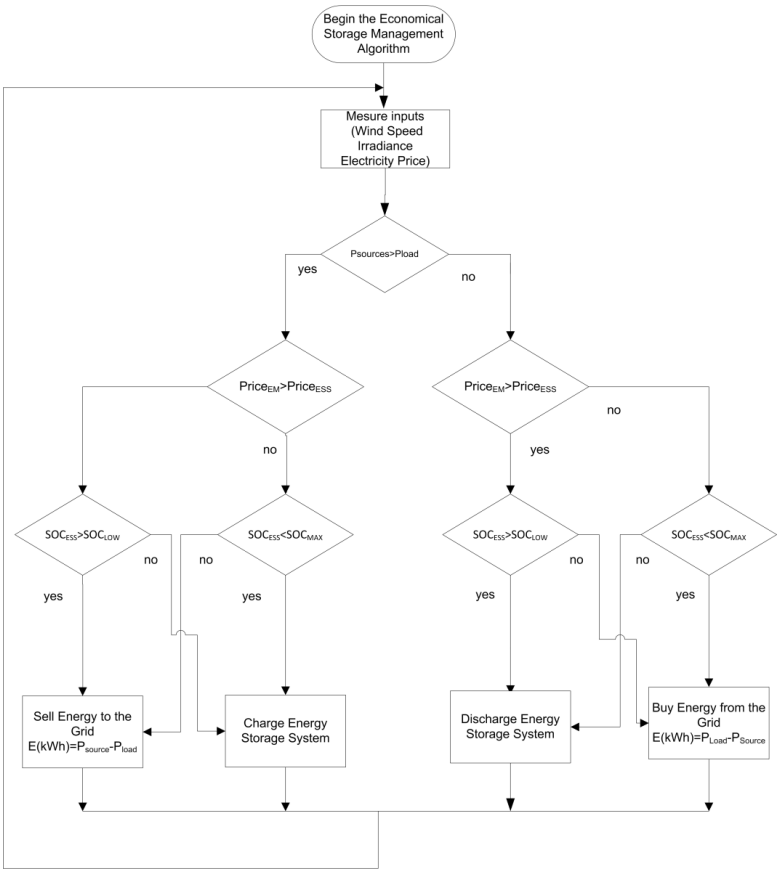

Fig. 17. Economical Storage Management System Algorithm flow chart

If the micro-grid is generating more power than the consumed by the loads, the algorithm compare the benefit of selling the energy to the grid with the benefit of charging the battery, for example when the price is lower than $Cost_{ESS}$, the micro-grid charge the ESS if the SOC is less than 85%, otherwise if the electricity market price is advantageous (higher than $Cost_{ESS}$), the energy is sold to the grid if the SOC is higher than 15%, these safety values of the SOC have been introduced to ensure the proper operation of the micro-grid in islanded mode.

The same occurs if the micro-grid needs external energy to supply the loads, depending on the electricity market price and the state of charge of the ESS the control will buy energy from the grid or discharge the batteries.

Some study cases are proposed in the chapter 3.3.3 to evaluate the benefit of implementing the ESMS in the studied micro-grid.

In the other hand, the concept of arbitraging will be explained and the benefits of using this application with the ESS will be shown too.

3.3.3 Study cases

The proposed study cases are designed to show the annual behavior of the implemented micro-grid in Aalborg (Denmark) during 2011.

To study the optimal participation of the micro-grid in the electricity market, several parameters are needed, they are the annual power flow of the system, the annual electricity market price and the price of charge and discharge the ESS.

To obtain the annual power flow of a system which includes a WT and a PV generator, the hour by hour data values of the wind speed and the irradiance are used. By the website www.tutiempo.net, the values of the daily average wind speed (m/s) and irradiance (kWh/m^2) have been obtained from the weather station 60300 (EKYT) located at 57.1N 9.86E with an altitude of 3 meters in Aalborg (DK).

These values have been introduced in the HOMER tool, which allows to obtain the final hour by hour annual values from daily or monthly averages for the studied stochastic process. In Fig. 18 is shown the wind speed values for every hour during 2011 in Aalborg.

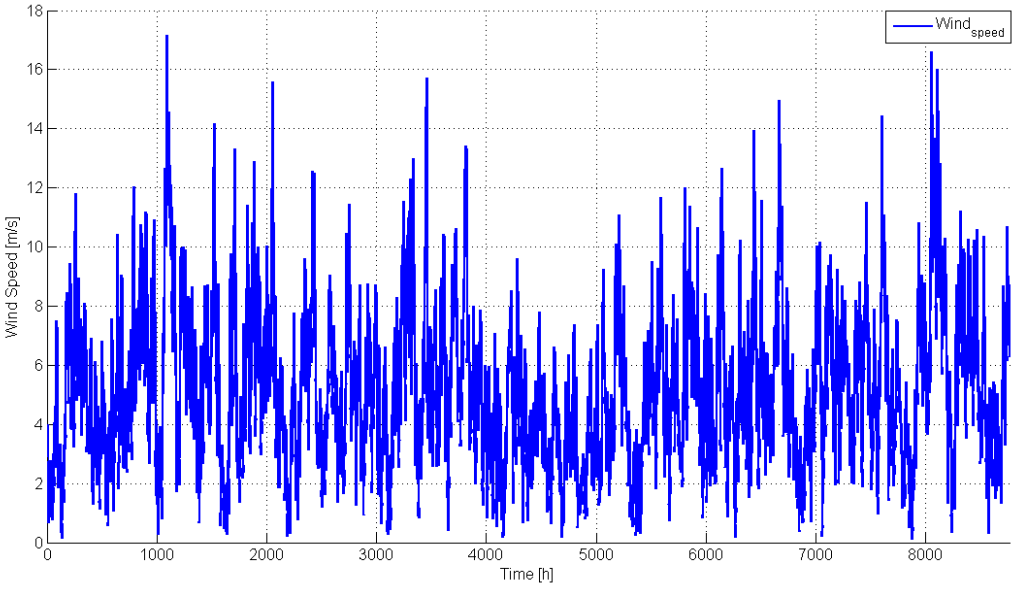

Fig. 18. Hourly wind speed in Aalborg during 2011

The hourly irradiance values are shown in Fig. 19, where is clear than the irradiance never reach 1000 W/m^2, therefore the PV array will never work at the nominal power.

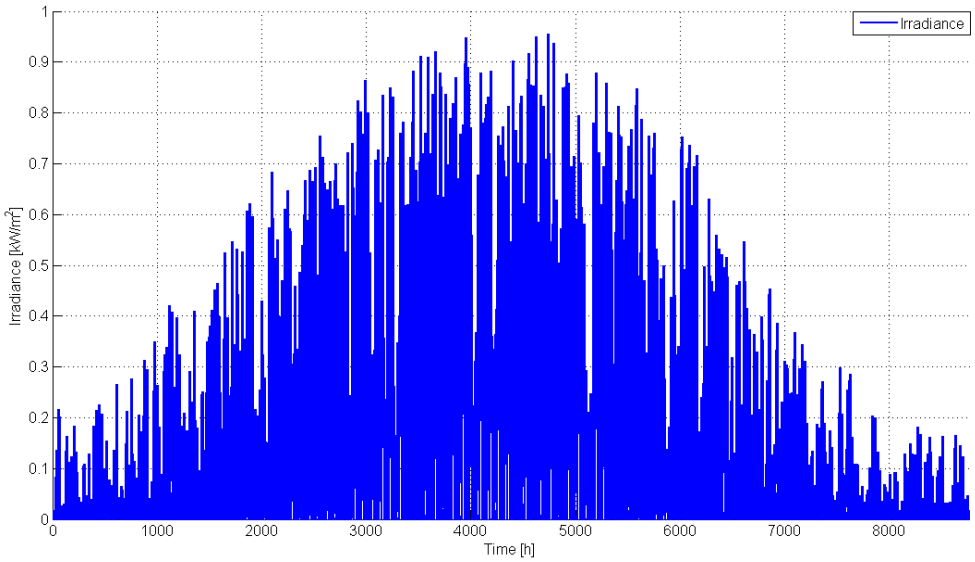

Fig. 19. Hourly Irradiance in Aalborg during 2011

With the annual wind speed and irradiance, the power generated for the PV and the WT can be calculated. The annual power generated by the PV is shown in Fig. 20, and the power generated by the WT during 2011 is shown in Fig. 21.

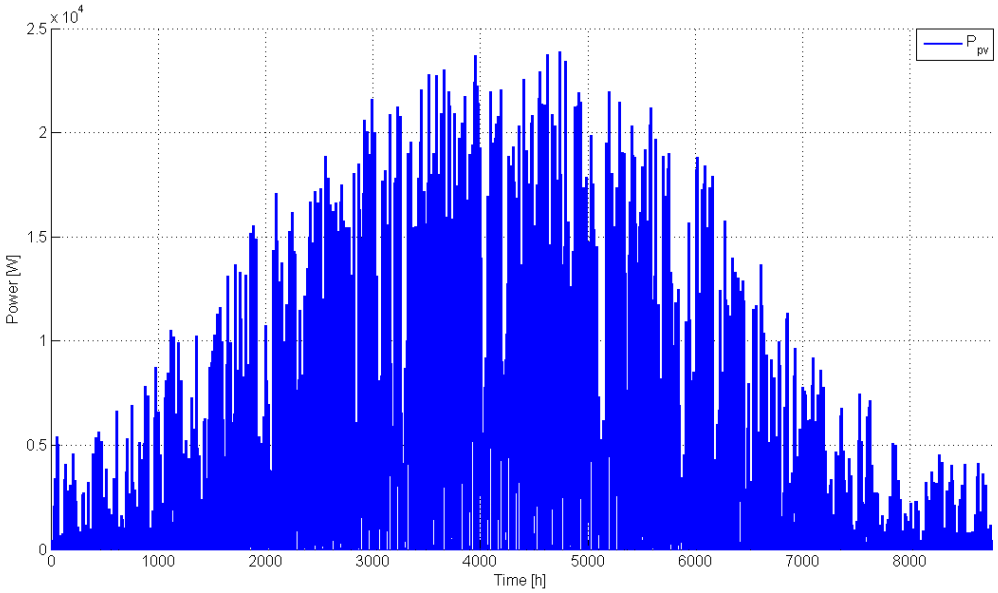

Fig. 20. Power generated by the PV for every hour during 2011

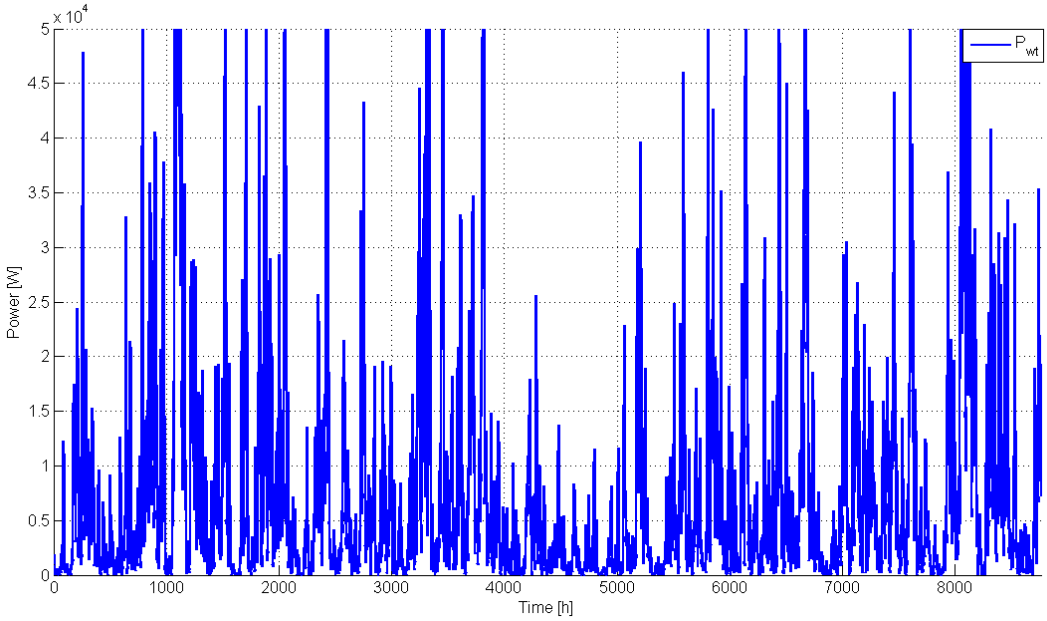

Fig. 21. Power generated by the WT for every hour during 2011

The electricity price for every hour during 2011 has been shown in Fig. 16. This price will be compared with the cost of generation for every kWh of the Lead-Acid battery with Carbon-enhanced electrodes that has been calculated in paragraph 3.3.1. A 40kW ESS has been considered with an energy capacity of 400kWh, therefore the batteries could discharge at nominal power a maximum of 10 hours.

By using MATLAB, three different study cases are implemented. The first two cases have the following three hypothesis:

a) Grid participation, the first actor is the grid that shares the power flow directly with the overall micro-grid
b) ES participation, the first actor is the ES that shares the power flow directly with the micro-grid on the base of SOC.
c) Optimal participation, by implementing the flow chart in Fig. 17

The third case will introduce the concept of arbitrage, and the benefits of the direct interaction of the ESS with the electricity market.

- **Case 1:**

In the first case, the ESMS will be implemented considering an uninterruptible DC load of 50 kW, this load has to be supplied during all the year at this power level. To achieve this objective the GE will work at the maximum power during all the year. Knowing the power supplied by the PV and the WT showed in Fig. 19 and Fig. 20, the annual power flow could be calculated comparing the energy generated by the sources with the energy consumed by the load. This power flow is shown in the Fig. 21.

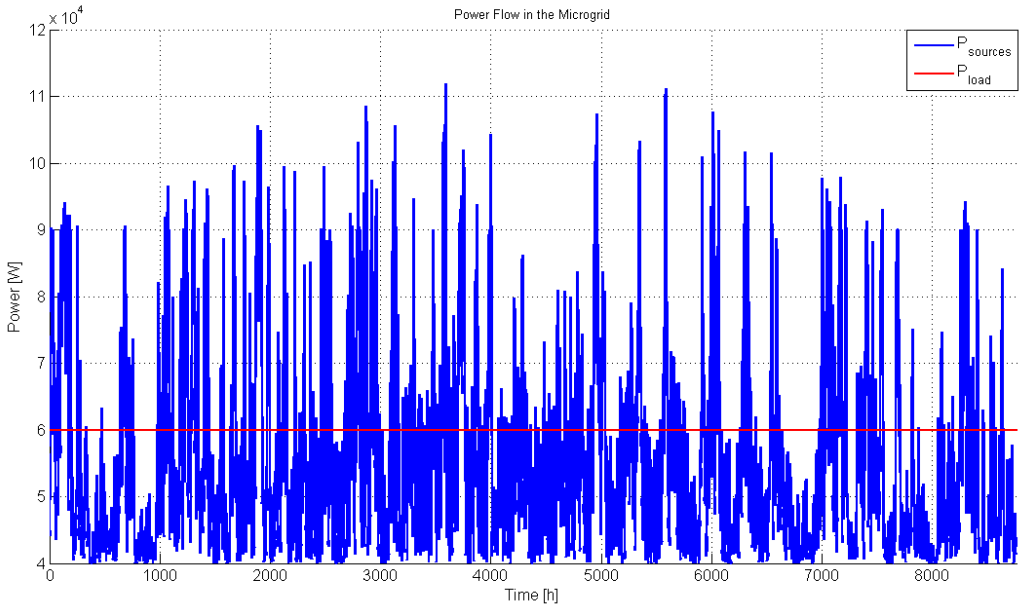

Fig. 22. Power flow in the micro-grid for the case 1

For the grid participation, the implemented algorithm only use the power flow in the micro-grid shown in Fig. 22 and the electricity market price shown in Fig. 16. When the generated energy is higher than the load demand, the micro-grid will sell the exceeded energy to the grid. Otherwise, when the micro-grid system needs energy to meet the load demand, the system will buy energy from the grid.

In the ES participation, the fluctuations of the power flow are controlled by the ESS as if the system was working in islanded mode. But in case of inappropriate SOC values which make impossible to meet the load demand, the electricity will be bought from or sold to the grid.

Fig. 23 shows the values of the SOC, the electricity price and the power flow for 2 days of the summer. When the sources generate more energy than the consumed by the load, the ESS is charged until reach the 95%, in that moment, if the sources still generating more energy this will be sold to the grid because the ESS is not able to be charged. Otherwise, when the load demand is higher than the energy generated by the sources, the ESS is discharged until the 5%, after that moment, the micro-grid buy energy from the grid.

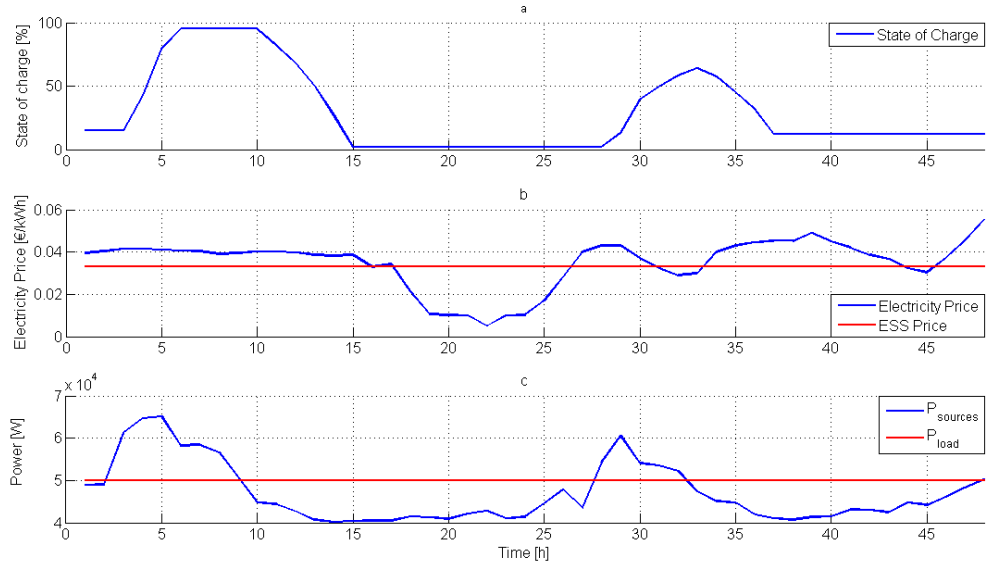

Fig. 23. Case 1, hypothesis B: a) SOC, b) comparison between electricity prices, c) comparison between power flow

The last hypothesis is the optimal participation with the electricity market, in this case the algorithm shown in Fig. 17 is implemented. In Fig. 24, the SOC level, the electricity price and the power flow are shown. When the power generated by the DGs are bigger than the consumed by the load, then the algorithm compare the electricity market price with the electricity price of the ES, if the first one is bigger than the second one, the energy is sold to the grid, if it is lower then the ESS is charged.

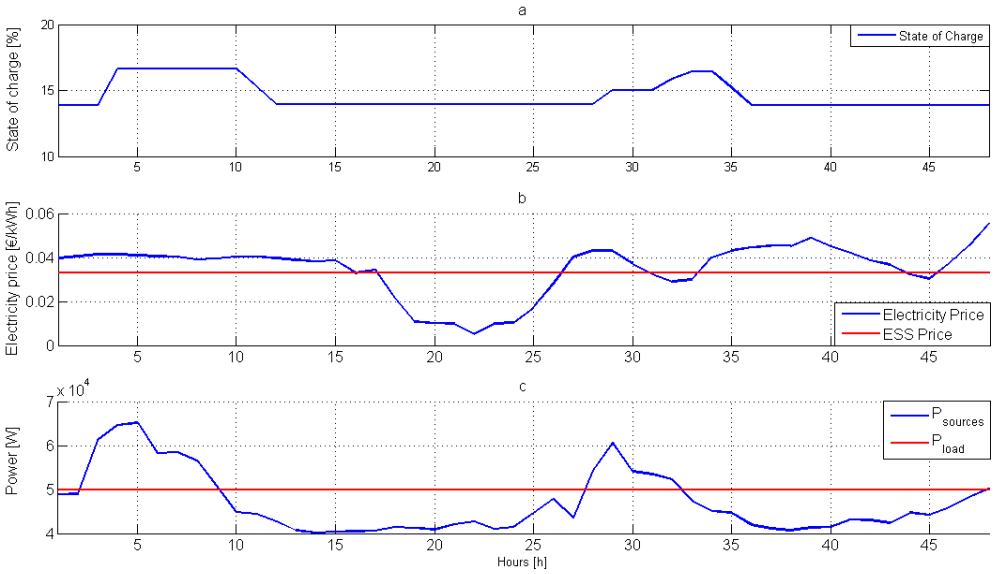

Fig. 24. Case 1, hypothesis C: a) SOC, b) comparison between electricity prices, c) comparison between power flow

Otherwise, if the load demand is bigger than the generated energy, the implemented algorithm compare the electricity price and decide to discharge the battery or buy energy from the grid.

In Table 5, the results of the annual benefit for the three hypotheses for this first case are shown. It is clear that using only the ESS is not a good option to meet the load demands, because the micro-grid has to pay 225.65€ to the electricity market in one year. With the optimal participation, the micro-grid is able to improve the exchange of electricity with the grid. Using the ESMS allows the system to earn 47.41€ more than the exchange with the grid participation.

Table 5. Annual benefit of the micro-grid for the case 1

Hypothesis	Benefit (€)
Grid	95.78
ESS	-225.65
Optimal participation	143.19

Case 2

In the second case, the same optimal participation algorithm has been studied, but a variable DC load has been introduced, to obtain more realistic results. The GE will not work at maximum power during all the year, because without a fixed load, it is more realistic that the GE follows the fluctuations of the load, reducing the generated power during the lower consumed demand. In Fig. 25, the power flow for the case 2 is shown.

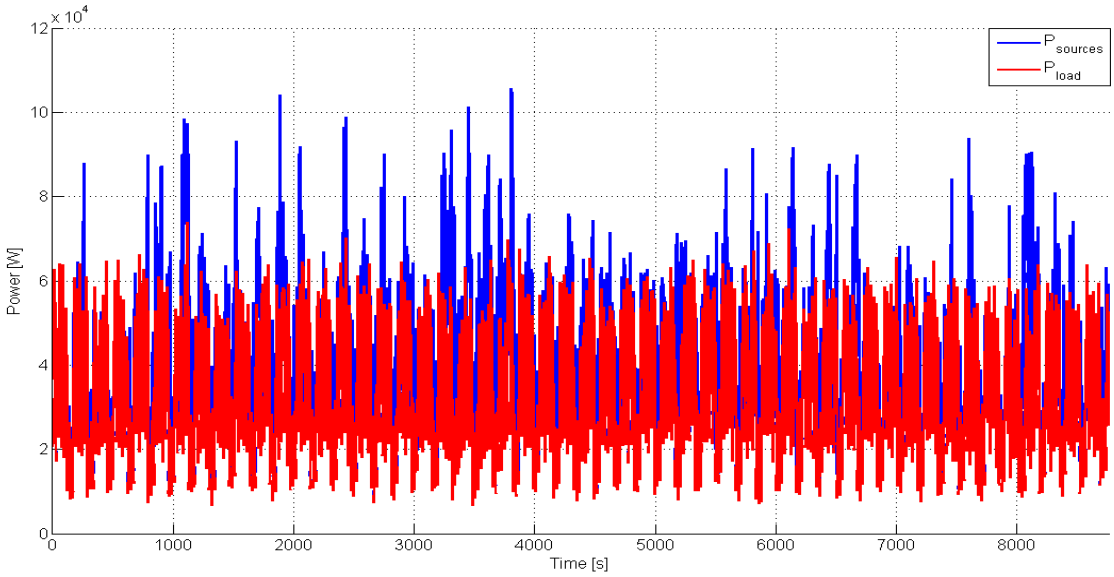

Fig. 25. Power flow of the case 2 with variable load

The three studied hypotheses are the same as the studied in the previous case. For the first one, exchanging energy only with the grid, the algorithm will compare the generated energy by the DGs with the consumed by the variable load, and the grid will supply or absorb the bulk energy.

In Fig. 26 shows the results for the ESS participation for two days of summer. In this case the fluctuations between the generated energy and the consumed by the variable load are smaller than in the studied case 1.

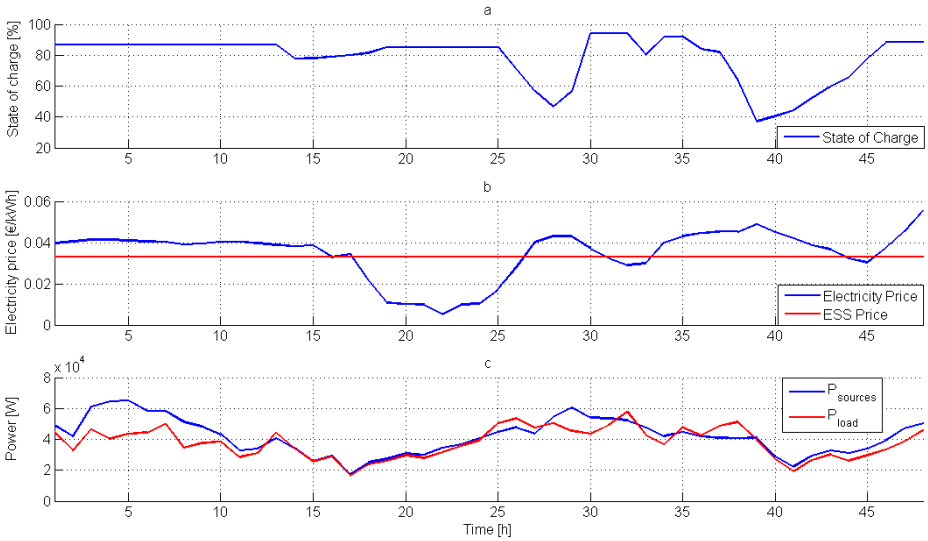

Fig. 26. Case 2, hypothesis B: a) SOC, b) comparison between electricity prices, c) comparison between power flow

Fig. 27, shows the values of the SOC, the electricity market and the power flow on the micro-grid for the third hypothesis, in this case the ESMS has been implemented to obtain the optimal participation with the grid.

The benefits of each hypothesis are shown in Table 6, in this case the benefits of the micro-grid are bigger than in the Case 1, due to the real behavior of the load, because with an uninterruptible load the difference with the energy generated by the DGs and the consumed by the fixed load increased during the night due to the PV array. In this case the three proposed hypothesis generates benefit for the system, but the optimal participation with the electricity market allows the system to increase profits in 115€.

As demonstrated by the proposed cases, an optimal participation allows using the ESS not only to control the system in islanded mode, but as a way to increase system revenues with the intelligent exchange of energy with the grid too.

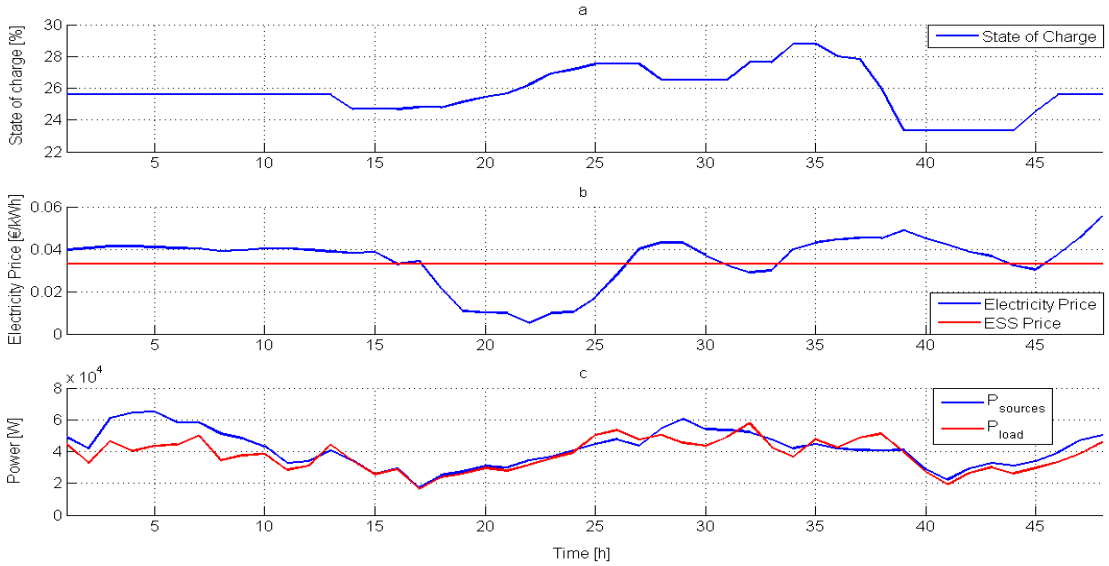

Fig. 27. Case 2, hypothesis C: a) SOC, b) comparison between electricity prices, c) comparison between power flow

Table 6. Annual benefit of the micro-grid for the case 2

Hypothesis	Benefit (€)
Grid	3008.80
ESS	2878.60
Optimal participation	3113.70

Case 3

The price arbitraging is the benefit to buy energy at low price and sell it again at higher price. The ESS is able to practice this application because it is able to charge from the grid when the electricity price is low and discharge this energy when the electricity market price is higher. For this application, the same ESS model as the used in both cases has been implemented, but the micro-grid has not been considered. Therefore the ESS interacts directly with the grid [39].

In this case, three hypotheses have been proposed depending the maximum duration of discharge operation at nominal power. The different discharge times analyzed are 3, 6 and 10 hours. The optimization has been considered for the hourly Denmark electricity market during one year.

In Fig. 28, the SOC and electricity prices values for the first 48 hours of the year in the case of 3 hours of maximum discharge are shown. When the electricity price is lower than the reference price for the ESS, the batteries are charged until reach a SOC of 95%, waiting until the electricity market price will be higher than the ESS price, and then the batteries are discharged.

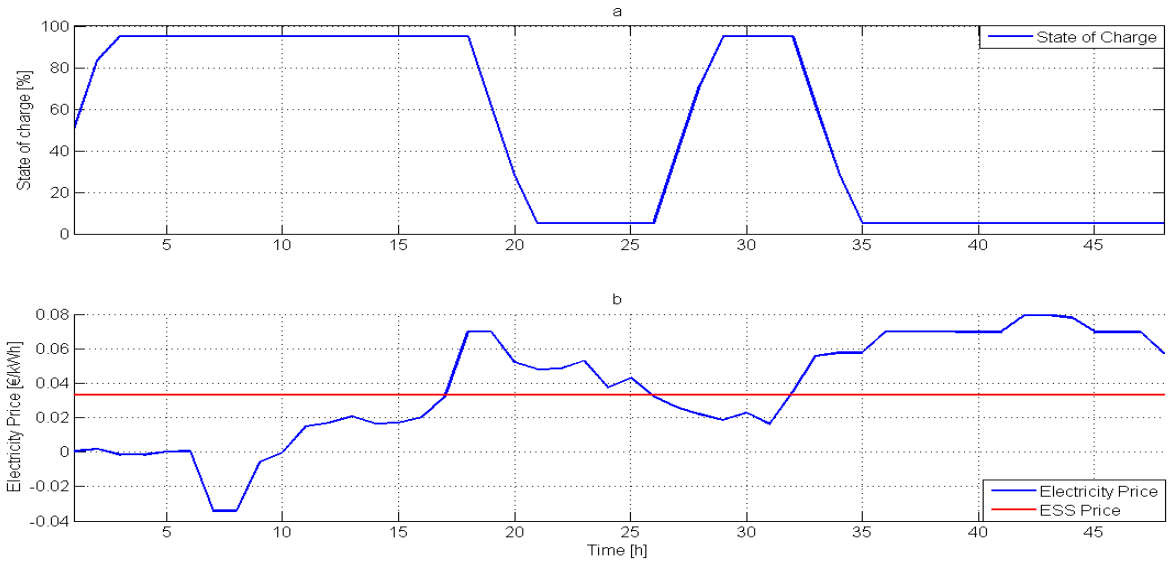

Fig. 28. Case 3, hypothesis 3h: a) SOC, b) comparison between electricity prices

The second hypothesis with a maximum discharge time of 6 hours is shown in Fig. 29, and the third one with a maximum discharge time of 10 hours is shown in Fig. 30. The variations of the SOC fluctuations are caused by the maximum discharge time, therefore when the SOC reach the 95%, it has to wait until the electricity price become higher.

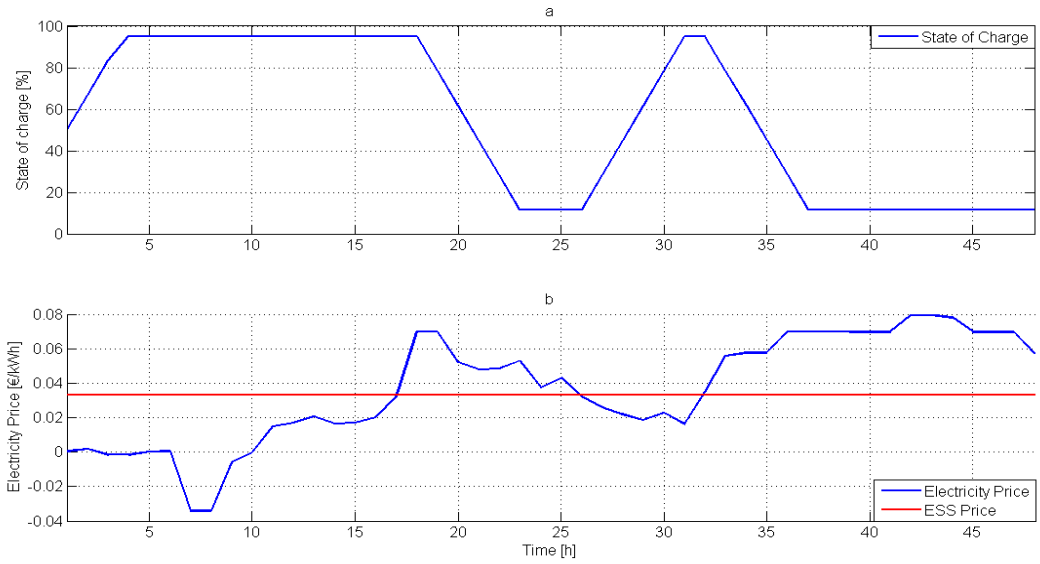

Fig. 29. Case 3, hypothesis 6h: a) SOC, b) comparison between electricity prices

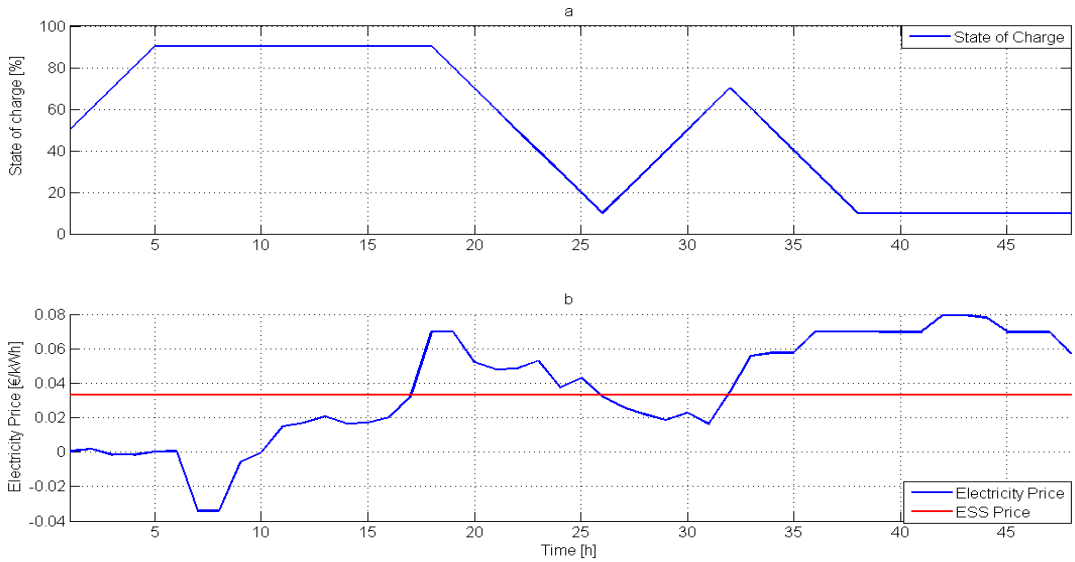

Fig. 30. Case 3, hypothesis 10h: a) SOC, b) comparison between electricity prices

Table 7. Annual benefit of the arbitraging application for 2011

Hypotheses	Benefit (€)
3h	325.04
6h	541.08
10h	671.13

As it was expected when the maximum discharge time increase the total benefits are bigger as shows the Table 7. This study shows how the arbitraging application can be used to obtain an economical benefit of the interaction between the ESS and the grid.

CHAPTER 4 – UNIT MODELS AND THEIR CONTROLS

4. Introduction

In the previous chapter the unit models used in the DC micro-grid are shown. After a detailed explanation about the unit models, the control of every DGs will be analyzed by highlighting how the power electronic systems are designed and controlled to achieve their purpose. Every proposed distribution is selected on the base of the studies about the specific area. The main DGs are WT, PV, GE and ES, that are controlled through DC-DC converters and AC-DC inverters. Particularly, the wind turbine is controlled by an active rectifier, the photovoltaic arrays by a boost converter, the energy storages by a bidirectional chopper and the gas engine by a boost converter through an universal bridge.

4.1 Energy Storages

Nowadays the energy storage is used in many fields, but of course one of the more interesting is in parallel with other energy source to obtain hybrid power systems. The Chemically and electrochemically storage are a large part of the ES as shown in Fig. 31

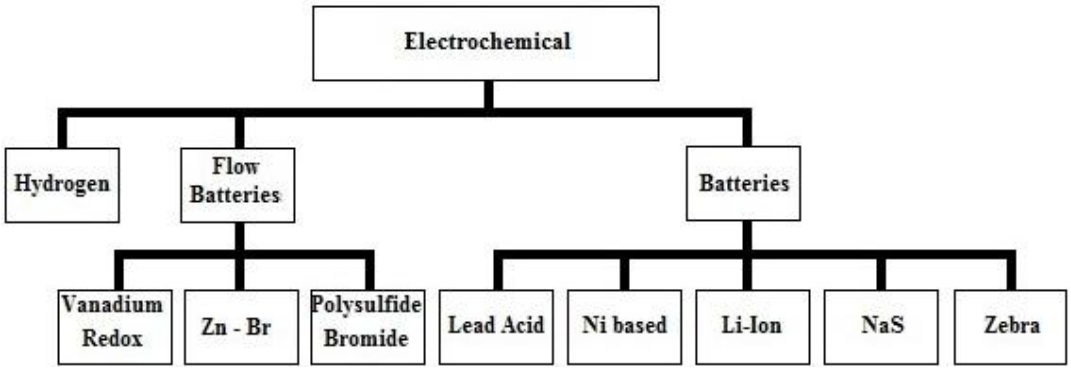

Fig. 31. Electrochemical batteries classification[40]

Prior to the detailed description for the considered batteries, some characteristic parameters which are discussed in the following sections and apply to the different technologies must be defined for clarity:

- *Power Capacity*: is the maximum instantaneous output that an ES device can provide, usually measured in kilowatts (kW) or megawatts (MW).
- *Energy Capacity:* is the amount of electrical energy the device can store usually measured in kilowatt-hours (kWh) or megawatt-hours (MWh).
- *Response Time:* is the length of time it takes the storage device to start releasing power from the moment it is activated.
- *Efficiency:* indicates the quantity of electricity which can be recovered as a percentage of the electricity used to charge the device.
- *Round-Trip Efficiency:* indicates the quantity of electricity which can be recovered as a percentage of the electricity used to charge and discharge the device.

In this thesis, two specific models of batteries are chosen on the base of the mostly used ones in the topic, the Lead acid and the Li-Ion, which will be explained below.

4.1.1 Model A

Lead Acid

This is the most common energy storage device in use at present. Its success is due to its maturity, relatively low cost, long lifespan and fast response. These batteries can be used for short-term applications that need discharging time in the range of seconds but also for long-term application with discharge time in the range of hours.

Fig. 32. Lead Acid Battery. Source: The battery rejuvenator website

Lead-Acid batteries are electrochemical cells based on chemical reactions involving lead and sulphuric acid. Both the power and energy capacities of lead-acid batteries are based on the size and geometry of the electrodes. The power capacity can be increased by increasing the surface area for each electrode, which means greater quantities of thinner electrode plates in the battery. However, to increase the storage capacity of the battery, the mass of each electrode must be increased, which means fewer and thicker plates. Consequently, a compromise must be met for each application. A LA battery set of typical parameters can be observed in Table 8.

Table 8. Typical parameters of LA Battery

Specific energy	30-40 Wh/kg
Energy density	60-75 Wh/Liter
Specific power	About 250 W/kg
Nominal cell voltage	2 V
Electrical efficiency	About 80%, depending on recharge rate and temperature
Recharge rate	About 8 hours (possible to quick recharge 90%)
Self-discharge	1-2% per day
Lifetime	About 800 cycles, depending on the depth of cycle

Advantages

As the other kinds of batteries, the most important advantages for the aim of this project is related to the possibility to use this kind of energy storage for both short and long term applications. Another important positive characteristic is the relatively low capital cost due to its maturity in the market.

Disadvantages

Lead Acid batteries are extremely sensitive to the environment, in particular to the temperature. The typical operating temperature is about 27°C, but a change in temperature of 5°C or more can cut the life of the battery by 50% [2]. The lifetime of this kind of batteries is an important point. It depends not only on the temperature but it depends strictly also to the DOD (depth of discharge). For DOD in the range of 2-5 %, typically, the lifetime in cycles of this battery is equal to 1000, with deep DOD this value decreases to 300-500 cycles. This is the worst disadvantage of the lead acid also because the self discharging reaches values around 40% per year.

Because of the high density of the materials used in these batteries, the typical energy densities are low and also the efficiency, compared with other kind of energy storage, is not so high.

About the environment impact, the lead is toxic and for this reason it has to be recycled. Also the sulphuric acid typically used as the electrolyte is corrosive and when overcharged the battery generates hydrogen which presents an explosion risk.

Applications

Due to the low cost, this kind of energy storage is used basically for power quality, UPS and some spinning reserve applications. Theoretically it can be used also for long term applications like energy management but in reality this application is limited by the short lifetime of these batteries.

Plants

Some plants in service used Lead Acid batteries are shown in the Table 9.

Table 9. LA storage systems larger than 1MWh**[41]**

Plant name& Location	Years of Installation	Rated Energy (MWh)	Rated Power (MW)	Cost in 1995 (€/kW)	Cost in 1995 (€/kWh)
CHINO California	1998	40	10	612	153
HELCO Hawai	1993	15	10	347	231
PREPA Porto Rico	1994	14	20	182	259
BEWAG Berlin	1986	8.5	8.5	537	537
VERNON California	1995	4.5	3	348	232

- The 8.5 MWh BEWAG plant in Berlin, was constructed in 1986 and it provided spinning reserve and frequency regulation functionality[42].
- The 5 MWh Vernon system cost $4 million and it was installed in 1995 and it is used primarily as an Uninterruptable Power Supply (UPS). The battery energy storage system instantly provides up to 5 MW of power to support critical infrastructure. The system can operate for up to one hour. The system is also used for peak shaving [43].
- The plant located in Chino, California, was a 10 MW storage plant, it consists of 4-hour-duration system to manage peak load from 1988 to 1996[43].
- The largest power capacity plant is the 20-MW/14-MWh plant in San Juan in Puerto Rico providing spinning reserve, frequency control and voltage control [44].

There are lots of manufacturers for this technology. Some of them are: Trojan Battery Company, C&D Technologies, Delco, Sunbright battery, Tudor Exide, EASTAR Batteries…

4.1.2 Model B

Lithium Battery (Li-ion)

This kind of battery consists of a cathode formed by a lithiated metal oxide, an anode node of graphitic carbon in layer structure and an electrolyte constituted by lithium slats dissolved in organic carbonates.

When the charging process takes place the lithium oxide in the cathode becomes lithium ions and migrates through the electrolyte to the anode where it is deposited as lithium atoms in the carbon layer. The discharging the process is reversed.

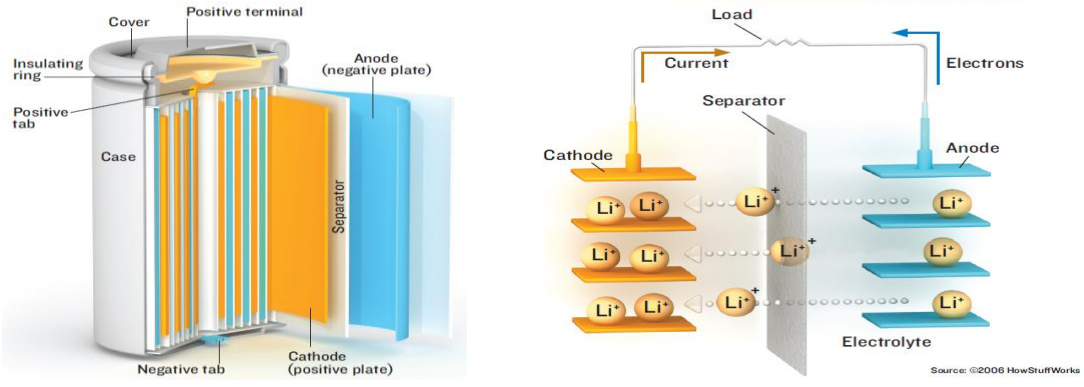

Fig. 33. Sketch of SAFT Li-ion[45]

There are nowadays mainly four different Li-ion batteries groups which are reflected in the Table 10.

Table 10. List of Li-Ion groups, Extracted from Battery University webpage

Specifications	**Li-cobalt $LiCoO_2$ (LCO)**	**Li-manganese $LiMn_2O_4$ (LMO)**	**Li-phosphate $LiFePO_4$ (LFP)**	**NMC $LiNiMnCoO_2$**
Voltage	3.60V	3.80V	3.30V	3.60/3.70V
Charge limit	4.20V	4.20V	3.60V	4.20V
Cycle life	500–1,000	500–1,000	1,000–2,000	1,000–2,000
Operating temperature	Average	Average	Good	Good
Specific energy	150–190Wh/kg	100–135Wh/kg	90–120Wh/kg	140-180Wh/kg
Specific power	1C	10C, 40C pulse	35C continuous	10C
Safety	Average. Requires protection circuit and cell balancing of multi cell pack. Requirements for small formats with 1 or 2 cells can be relaxed		Very safe, needs cell balancing and V protection.	Safer than Li-cobalt. Needs cell balancing and protection.
Thermal. Runaway	150°C (302°F)	250°C (482°F)	270°C (518°F)	210°C (410°F)
In use since	1994	1996	1999	2003
Researchers, manufacturers	Sony, Sanyo, GS Yuasa, LG Chem Samsung Hitachi, Toshiba	Hitachi, Samsung, Sanyo, GS Yuasa, LG Chem, Toshiba Moli Energy, NEC	A123, Valence, GS Yuasa, BYD, JCI/Saft, Lishen	Sony, Sanyo, LG Chem, GS Yuasa, Hitachi Samsung
Notes	Very high specific energy, limited power; cell phones, laptops	High power, good to high specific energy; power tools, medical, EVs	High power, average specific energy, elevated self-discharge	Very high specific energy, high power; tools, medical, EVs

Advantages

The main advantages of this kind of electrochemical batteries, compared to other types, consist of an high energy density, very high efficiency and long life cycle (3000 with a DOD equal to 80%) .

Disadvantages

On the other hand, these energy storage technologies have a high cost due to special packing these batteries need and also because of an internal protection system. This

system is necessary because the lithium batteries are sensitive to the over-temperature, over-charge and increase of pressure within the electrochemical cell. The cost is main challenge for this technology.

Applications

Currently, the main applications compatible with this energy storage technology are the field of power quality or short-duration peak shaving.

Plants

There are some interesting projects based on the applications of the Lithium batteries. In the USA the Department of Energy has sponsored a project to design two 100 kW/1 minute Li-ion battery systems to provide power quality for grid connected micro-turbines.

4.1.3 Control

Bidirectional dc/dc converter

The DC/DC converters are circuits that have as input and output a DC voltage with different values. Really the output is an average value, and Fig. 34 shows the general scheme of this converter topology.

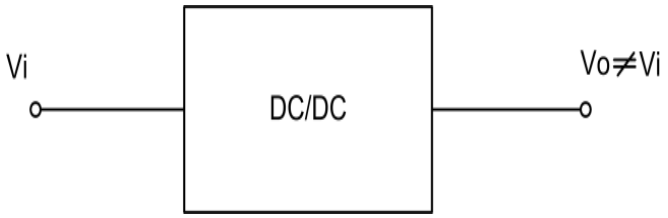

Fig. 34. General scheme DC/DC converter

The specific converter used with the batteries has the bidirectional buck-boost configuration.

It is able to work as a buck (step-down) when the battery has been charged and as a boost (step-up) in the case the battery has been discharged. It is called bidirectional to mean that it is able to flow the current in both ways, i.e. from the battery to the grid and vice-versa.

Fig. 35 shows the circuit of the used converter, it works in two modes. Charged mode and discharge mode.

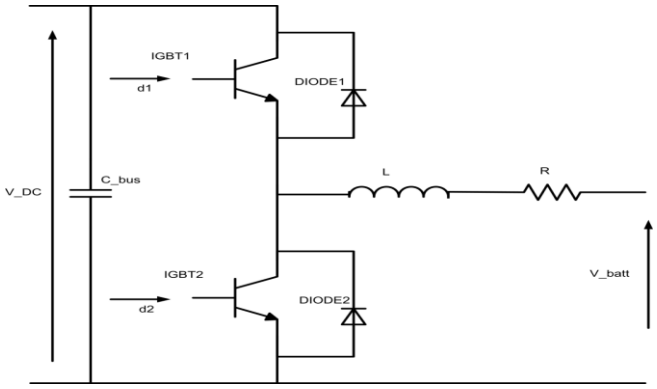

Fig. 35. DC/DC bidirectional converter configuration

In charge mode the upper IGBT1 is on and it is controlled through PWM signal *d*, at the same time the lower IGBT2 is off. In this time the converter keeps the voltage level on the micro-grid at 800V and it is able to supply the battery until it is charged.

In discharge mode the lower IGBT2 is on and it is controlled through PWM signal d_1, at the same time the IGBT1 is off In this time the converter keeps the voltage level on the micro-grid at 800V, it is able to supply the DC-link and the battery is discharging.

This converter configuration is able to supply a negative or positive current on the base of discharge or charge of the battery respectively, while the voltage level is always positive.

Analyzing the converter circuit is clear to see that it is consisting of two choppers (IGBT/DIODE) properly connected. The control of these two IGBTs is complementary, so when one is conduced the other one is off, so never the DC-link is effected of a short circuit ($V_{DC} = 0$).

The behavior of the converter to switch on the two modes should be interesting, so the battery is able to discharge the following condition is necessary:

$$V_m > 0,\ I_m > 0 \tag{4.1}$$

thus the upper chopper is working, in the other way the battery is able to charge on these conditions:

$$V_m > 0,\ I_m < 0 \tag{4.2}$$

thus the lower chopper is working.

Control of DC/DC converter

The goal of the control for the ES is to keep constant the level of the voltage on the DC-link, i.e. on the micro-grid. To have this, two loop control circuits are implemented, the first one to control the voltage and the second one to control the current. So, the

following control is implemented (Fig. 36), where the loops have to perform the control of voltage and current through the PI controls.

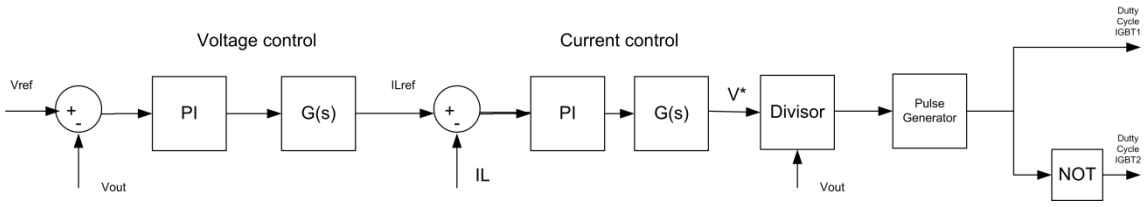

Fig. 36. Scheme of bidirectional converter control

The first loop allows having the average voltage value on the DC-link on 800V, but without the second loop, the low oscillations on the average voltage value increase and the system will be instable.

So to have a stable system the second loop is needed, thus the oscillations are removed and the voltage on the DC load is kept constant.

The values of K_p and K_i on both the PI controls are calculated considering the transfer functions G1(s) and G2(s) and by using the SISO tool in MATLAB for the following buck-boost circuit in Fig. 37 in small signal analysis.

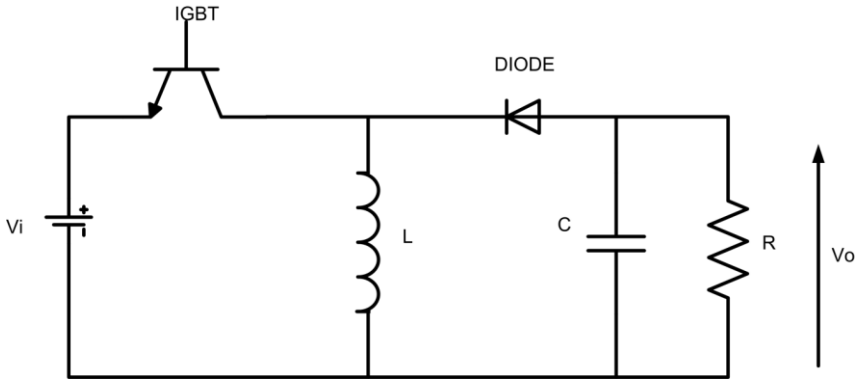

Fig. 37. Schematic of the buck-boost converter

For the buck-boost converter the line-to-output G1(s) and control-to-output G2(s) transfer functions are given from the literatures [46][47] and they are calculated by following shown method in the paragraph 4.2.2:

$$G1(s) = \frac{V}{D\,D'}\frac{\left(1-s\frac{DL}{D'^2R}\right)}{dem(s)} \tag{4.3}$$

$$G2(s) = \frac{D}{D'}\frac{1}{dem(s)} \tag{4.4}$$

where $dem(s) = 1 + s\frac{L}{D'^2R} + s^2\frac{LC}{D'^2}$, $D = \frac{Vo}{Vo-Vi}$ is the duty cycle and $D' = 1 - D$

4.2 Combined Heat and Power

In the past different definitions about the micro combined heat and power CHP were used. Since the directive in February 2004 [48] the following definitions were clarified for the European countries[49]:

"Cogeneration production includes the sum of produced electricity and mechanical energy and useful heat from the cogeneration units. This generally means that conventional heating systems are replaced by electricity generators equipped with heat exchangers to additionally use/recover the waste heat. The heat is used for space and water heating and possibly for cooling, the electricity is used within the building or fed into the grid."

- "micro-cogeneration unit shall mean a cogeneration unit with a maximum capacity below 50 kWe"
- "small scale cogeneration shall mean cogeneration units with an installed capacity below 1 MWe."

A lot of energy in the world is used for building heating[50]. Especially in USA, China and Western Europe are heated with a central heating system using CHP, Fig. 38 shows the capacity of CHP and its potential for the future in the most industrialized countries around the World.

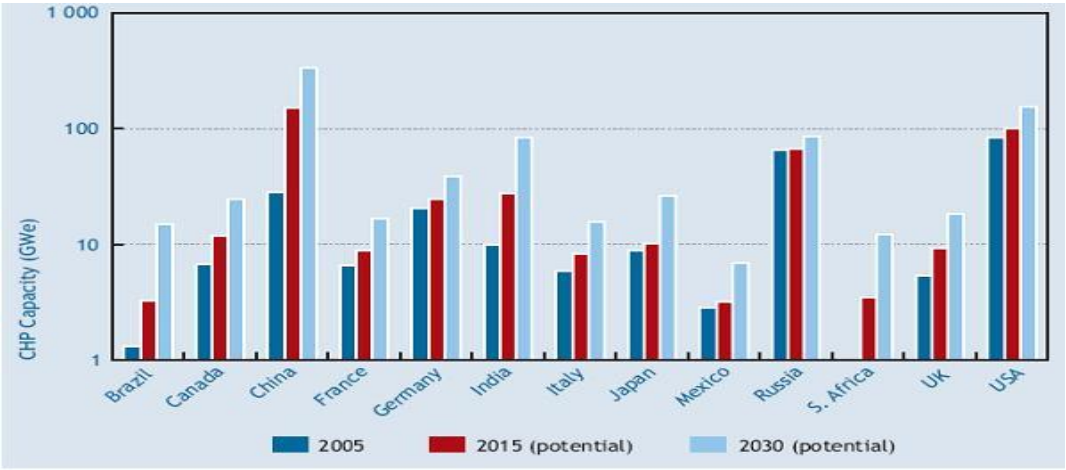

Fig. 38. CHP global capacity. Source: International Energy Agency

Nowadays different technologies of CHP are present in market with very different impacts on the reduction of primary energy use. Some of the most common CHP technologies are:

- Diesel engines
- Spark ignition engines
- Micro Gas Turbines
- Stirling Engines
- Organic Rankine Cycle – ORC
- Fuel Cell Technology

Gas engines seem to have the best performance and for this reason are considered in this thesis [50].

4.2.1 Model

Micro gas turbine

The basic technology of micro turbines is derived from diesel engine turbochargers, aircraft auxiliary power systems, and automotive designs[49]. So its basic components are the compressor, combustor, turbine generator and recuperator. Here, exhaust heat is used to preheat the air before it enters the combustion chamber. The combustion chamber then mixes the heated air with the fuel and bums it. This mixture expands through the turbine, which drives the compressor and generator. The combusted air is then exhausted through the recuperator before being discharged at the exhaust outlet [51]. An example of these units is shown in the next Fig. 39, where it is possible to see the Capstone's C30 micro turbine generator.

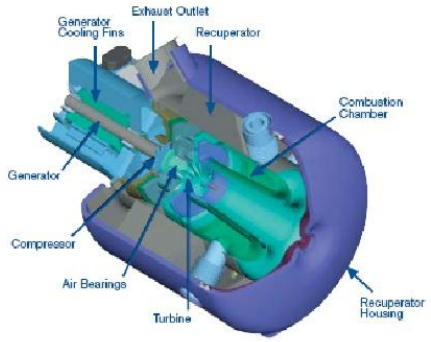

Fig. 39. Micro-gas turbine [49]

In this thesis the following model for the micro gas turbine is considered, Fig. 40. It is composed by the Gas Engine (GE), the PMSG, the universal bridge and the boost converter to connect to the DC micro-grid. The use of this system can increase the energy capture from the gas.

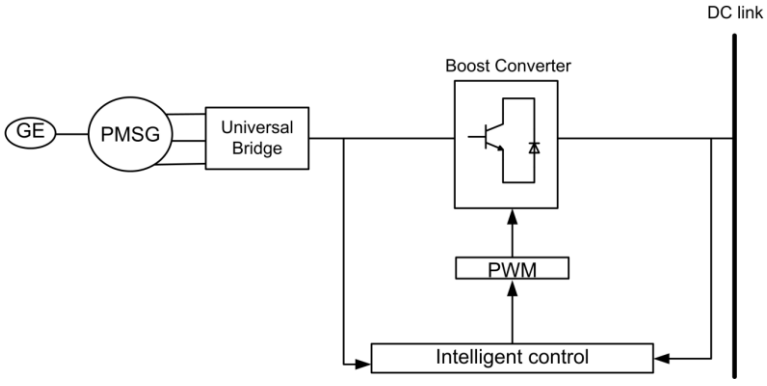

Fig. 40. GE energy system

The GE is connected to the PMSG with the output power of 40kW, the efficiency of the gas engine is supposed of 31% and the efficiency of PMSG is 97%, so by knowing the

lower heating values for the natural gas LHV= 35889.3 kJ/m^3 from the International Energy Agency in Norway, it is possible to calculate how many gas the engine needs to produce a power about 41.237 kW since 1[Ws]= 1[J]. From the Appendix D:

- Gas amount in one hour is 13.34 m^3
- Gas amount in one day is 320.16 m^3

4.2.2 Control

DC/DC boost converter

The PV unit considered in this work gives an output voltage value lower than the required DC micro-grid. Therefore, the voltage level has to be increased and the converter has to work in the boost mode.

Fig. 41 shows the schematic of the boost converter with a power flow from left to right, the main components are the inductor L, the output capacitor C, the switch IGBT, the diode, and the load R.

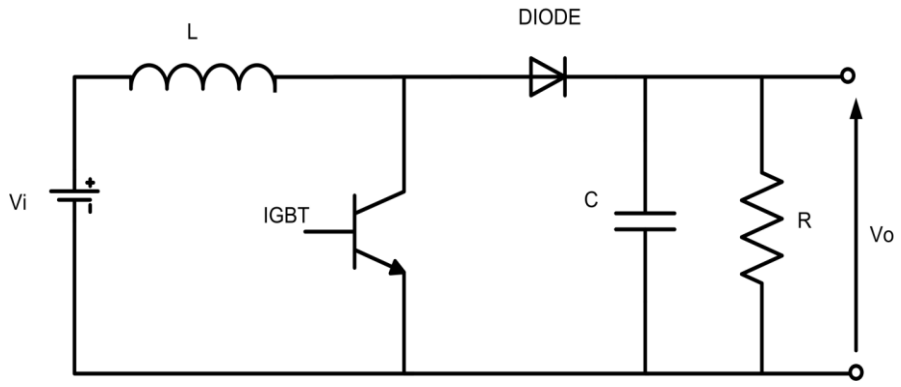

Fig. 41. Boost converter circuit

The Fig. 42 represents the main signals of a boost converter. PWM is the signal for the control stage and the voltage and the current in the inductance correspond to the power stage.

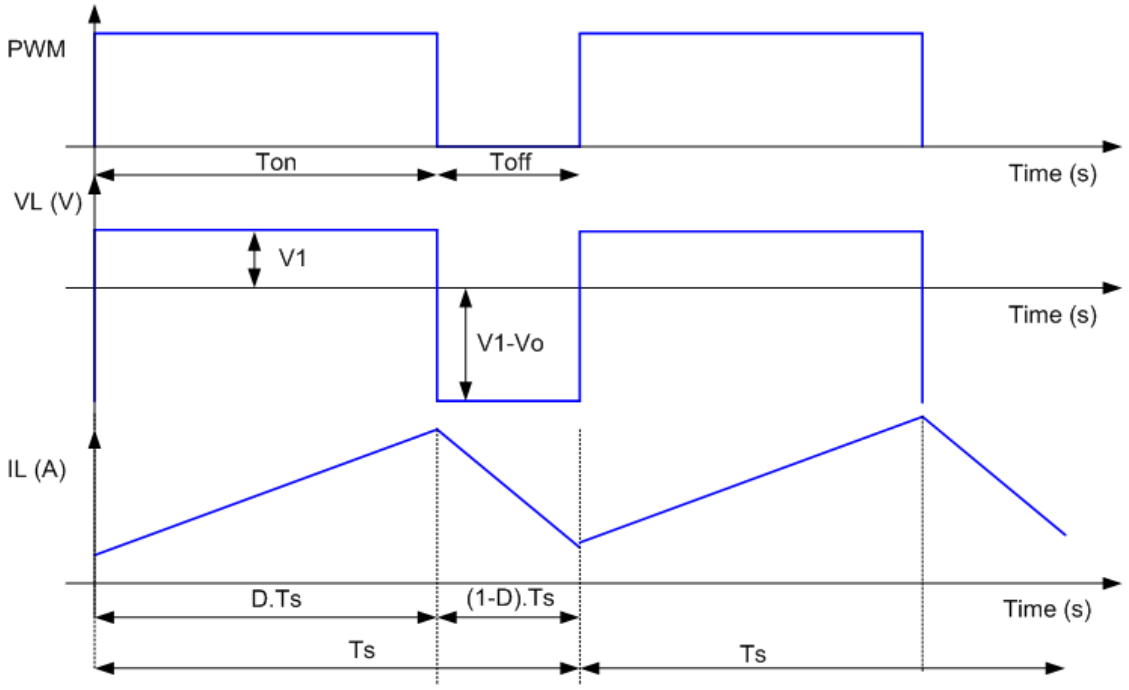

Fig. 42. Boost converter signals

In the literature[47][46] it is possible to found a complete mathematical analysis of the boost converter, therefore, in this section the most relevant formulas are only presented.

The voltage in the capacitor:

$$v_c = \frac{1}{C}\int_{t_1}^{t_2} i_c \, dt \tag{4.5}$$

where i_c is calculated since the relation between i_0 and i_L

The current through the inductor is:

$$i_L = \frac{1}{L}\int_{t_1}^{t_2} v_L \, dt \tag{4.6}$$

where v_L is equal to v_1 during T_{on} and $v_L = \ v_1 - v_0$ during T_{off}.

The relationship of voltage conversion in CCM for the boost converter is:

$$v_o = v_i \frac{1}{1-D} \tag{4.7}$$

Considering the average values, the relation between the inductor current and output current, working always in CCM for the boost converter is:

$$i_L = i_o \frac{1}{1-D} \tag{4.8}$$

so between output and input current the relationship will be:

$$i_o = i_1(1-D) \tag{4.9}$$

Control of Boost converter

The converter control diagram is presented in Fig. 43.The DC/DC converter is connected to the inverter and must maintain the input voltage for the inverter to the desired voltage. The control implements a fast inner current loop and a slower outer loop for setting the DC voltage.

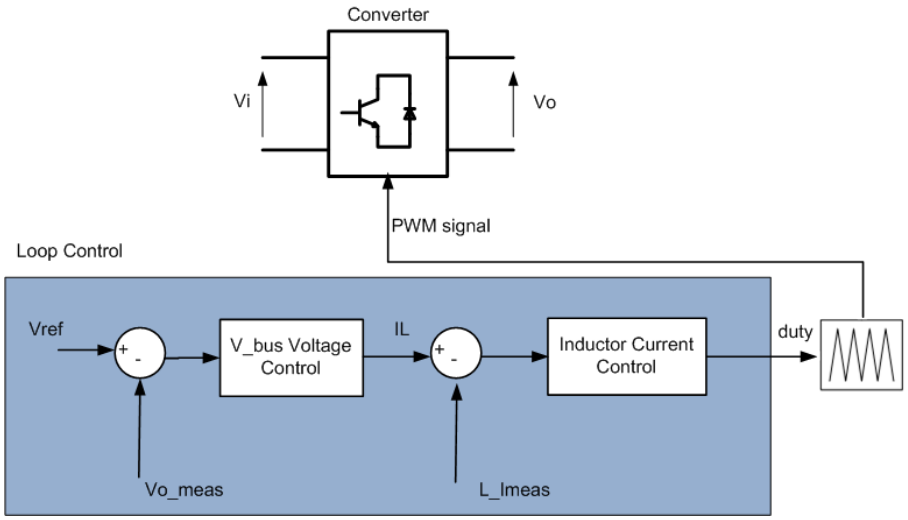

Fig. 43. Loop control for boost converter

Standard PI controllers are implemented for the entire control block, resulting the overall control structure described in Fig. 44.

The system is controlling DC voltage by sending references to an outer voltage control loop that generates an inductor current reference, which generates a duty cycle value, for PWM signal generation.

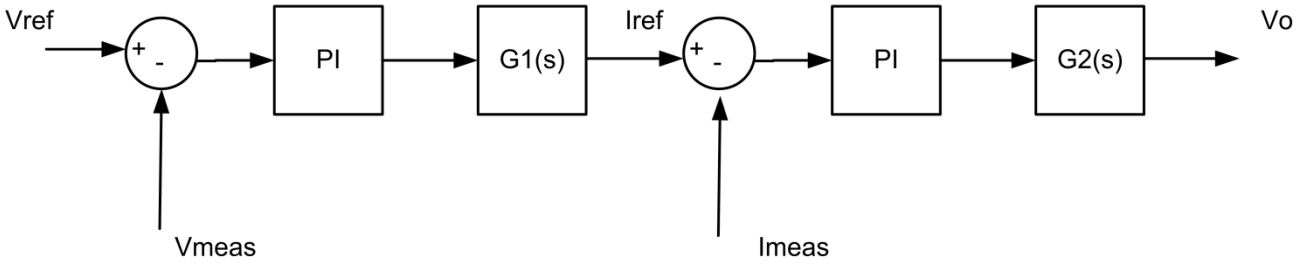

Fig. 44. PI control for boost converter

The input voltages V_i are lower than the output, thus they must be stepped up to have the required output voltage V_o through a controlled boost circuit.

The circuit in Fig. 41 is analyzed to found the transfer functions $G_2(s)$

The system has to be study in two intervals, the interval 1 is DT_s and the interval 2 is $(1-D)T_s$, it is supposed without perturbations.

$$\text{Interval 1}\begin{cases} L\frac{di_L}{dt} = v_1 \\ C_0\frac{dv_o}{dt} = -\frac{v_o}{R} \end{cases} \tag{4.10}$$

$$\text{Interval 2}\begin{cases} L\frac{di_L}{dt} = v_1 - v_o \\ C_0\frac{dv_o}{dt} = i_L - \frac{v_o}{R} \end{cases} \tag{4.11}$$

The average state-equations are:

$$L\frac{di_L}{dt} = (v_1 - v_o)(1-D) \tag{4.12}$$

$$C_0\frac{dv_o}{dt} = -\frac{v_o}{R}D + \left(i_L - \frac{v_o}{R}\right)(1-D) = i_L(1-D) - \frac{v_o}{R} \tag{4.13}$$

The small-signal model

$$L\frac{d\tilde{\imath}_L}{dt} = \tilde{v}_1 + V_o\tilde{d} - (1-D)\tilde{v}_o \tag{4.14}$$

$$C_0\frac{d\tilde{v}_o}{dt} = I_L\tilde{d} - (1-D)\tilde{\imath}_L - \frac{\tilde{v}_o}{R} \tag{4.15}$$

The transfer function

$$LsI_L(s) = V_1(s) + V_oD(s) - (1-D)V_o(s) \tag{4.16}$$

$$V_o(s) = \frac{R(1-D)}{CRs+1}I_L - \frac{RI_L}{CRs+1}D(s) \tag{4.17}$$

For $V_1(s) = 0$ the relation between the duty cycle and the inductor current is:

$$LsI_L(s) = V_oD(s) - (1-D)V_o(s) = V_oD(s) - (1-D)\left[\frac{R(1-D)}{CRs+1}I_L - \frac{RI_L}{CRs+1}D(s)\right] \tag{4.18}$$

$$\frac{I_L(s)}{D(s)} = \frac{V_oCRs+V_o+(1-D)RI_L}{CLRs^2+Ls+R(1-D)^2} \tag{4.19}$$

$$I_L = \frac{V_o}{R}\frac{1}{(1-D)} \tag{4.20}$$

$$G_2 = \frac{I_L(s)}{D(s)} = V_o\frac{2+CRs}{CLRs^2+Ls+R(1-D)^2} \tag{4.21}$$

By using SISO tool of MATLAB the PI control is designedand the root locus and bode diagrams are shown in Fig. 45 for the inner loop. The step response is shown to check that the system is fast stabe in the Fig. 46.

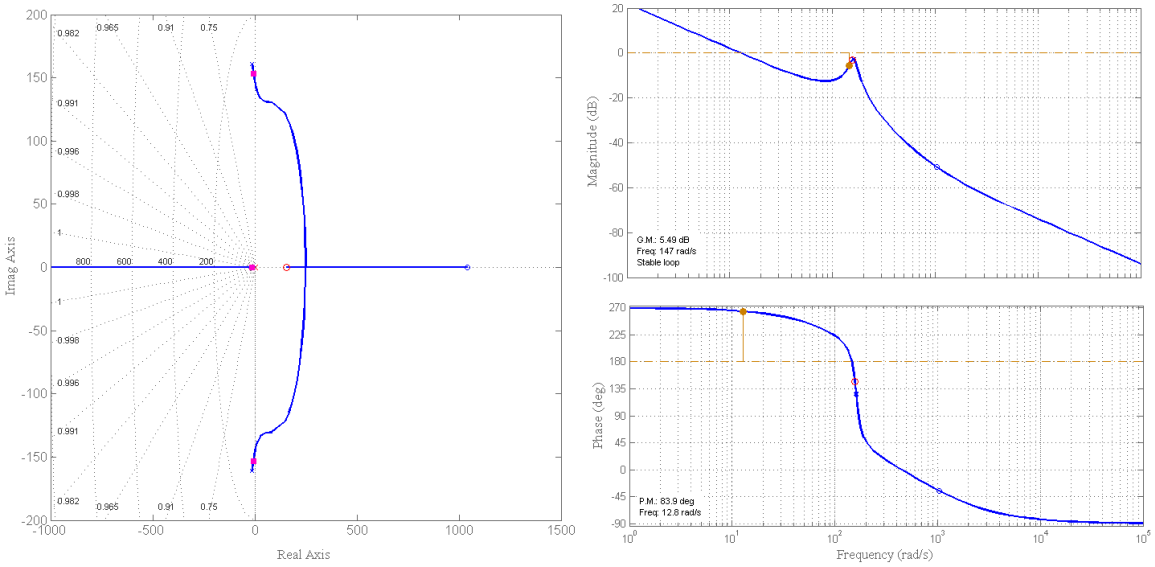

Fig. 45. Root Locus and Bode diagrams for internal open loop

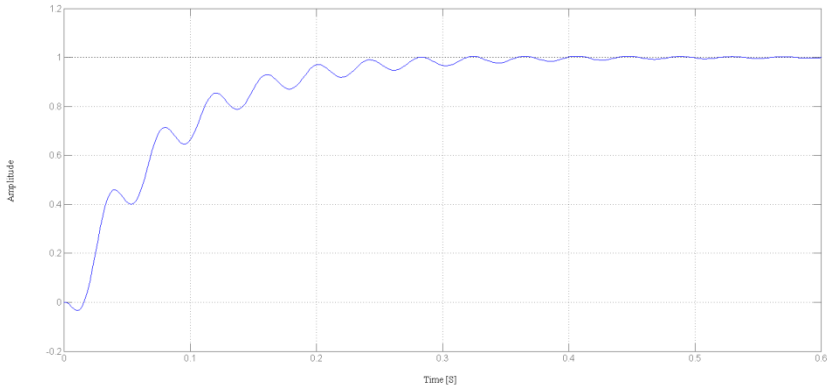

Fig. 46. Step Responce internal Loop

In the same way the transfer function for the outer loop is calculated by considering the circuit in Fig. 47:

$$G_1 = \frac{V_o}{I_L(s)} = V_o \cdot \frac{R_1}{R_1 C_1 s + 1} \cdot \frac{1}{D} \tag{4.22}$$

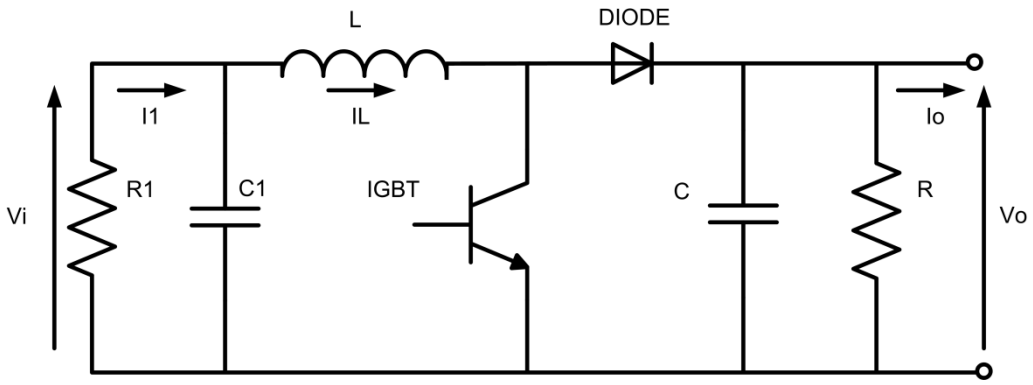

Fig. 47. Boost converter circuit for GE

The bode diagrams of the outer open loop, root locus and step response are shown in the Fig. 48 and Fig. 49 respectively to prove that the system is stable. In fact by the root locus diagram it is possible to see that the pole are in the half left region and by the bode diagrams of the open loop the marginal gain and the marginal phase are positive. The step response diagram shows the time that the system needs to reach stable.

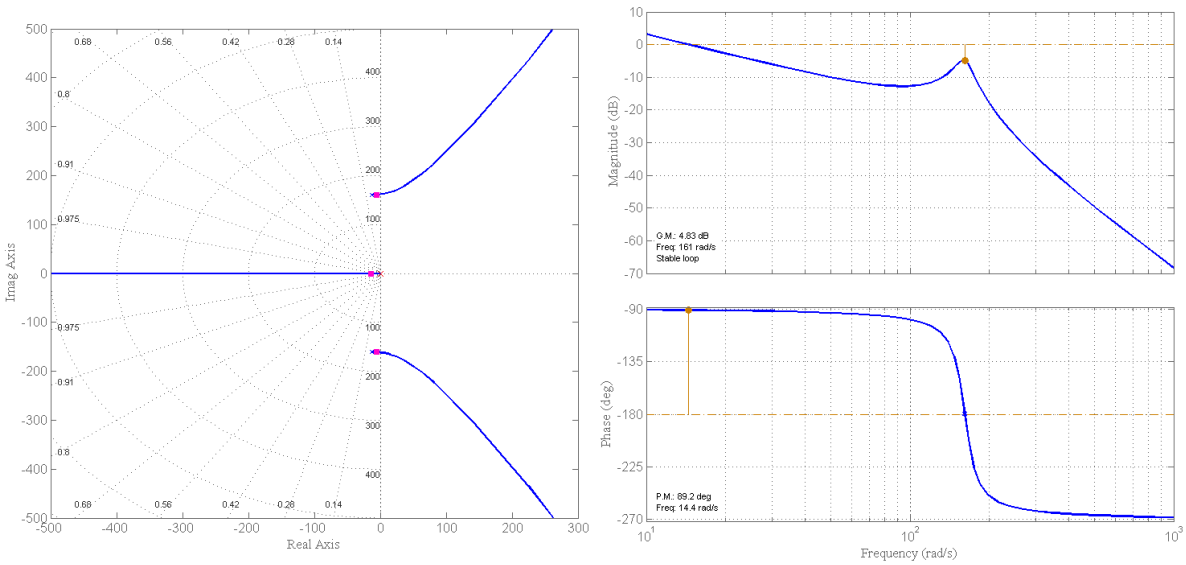

Fig. 48. Root Locus and Bode diagrams for outer loop

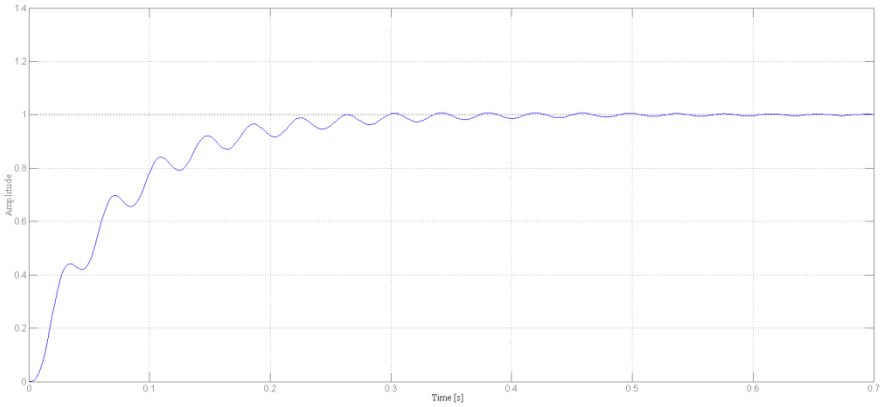

Fig. 49. Step response outer loop

4.3 Wind Turbine

One of the renewable sources that are growing rapidly in the world is the wind power; its penetration in the generation of electricity is going to reach very high percentages in several countries. In Fig. 50 it is possible to see the global installed wind capacity from 2005 to 2010.

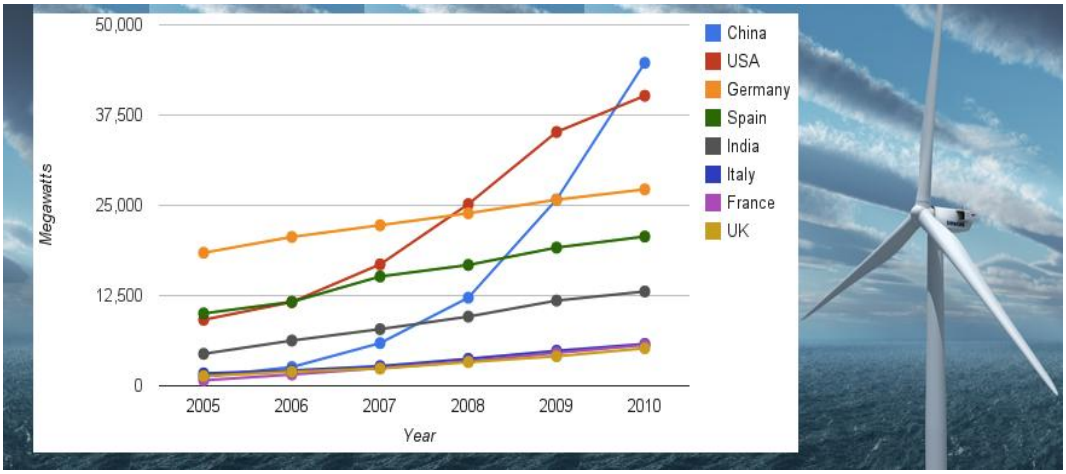

Fig. 50. Installed Wind World Capacity

In the last 30 years the development in wind turbine systems has been studied and nowadays the topologies of wind turbines are increased. The components of a wind turbine system can be spitted in two main parts. The first is the mechanical power section consisting of power conversion and its control and power transmission. These components are connected to the second section, the electrical power system. The section of electrical power consisting of generator, power converter, power transformer and supply grid[52].

Different generator systems are used for the wind turbine, on the base that the wind turbine works in fixed-speed or variable-speed. The common one for the fixed-speed is the induction generator. In the other way for the variable-speed some other topologies are used further. These other topologies are: Synchronous generator, Synchronous generator multi-pole, permanent magnet synchronous generator multi-pole, wounded rotor induction generator, doubly-fed inductor generator.

Some wind turbines use power electronic system as interfaces, i.e. a power electronic converter system is able to allow the variable electrical generator frequency be converted to the frequency of the grid.

Considering the different topologies of generators in fixed and variable speed and how the power electronic systems are used, nine different wind turbine systems are listed in the following Table 11[52].

Table 11. Wind Energy Systems[52]

System	I	II	III	IV	V	VI	VII	VIII	IX
Speed	Fixed	Fixed	Fixed	Limitede range	Limitede range	Variable	Variable	Variable	Variable
Generator	Induction	Induction	Induction	Wounded rotor Induction	Double -Fed Induction	Induction	Synchronous	Synchronous Multi-Pole	PM-Syncrhonous Multipole
Power converter	NO	NO	NO	Partially rated	Partially rated	Full-scale	Full-scale	Full-scale	Full-scale
Aerodynamic power control	Pitch	Stall	Active stall	Pitch	Pitch	Pitch	Pitch	Pitch	Pitch
Gear Box	Yes	Yes	Yes	Yes	Yes	Yes	Yes	NO	NO

4.3.1 Model

SYSTEM "IX"

The Wind Turbine considered in this thesis is H12.0-50kW model from *ANHUI HUMMER DYNAMO CO*. The characteristics are showed in the next Table 12.

Table 12. Wind Turbine data sheet

Rated Power (kW)	50
System output voltage (Vac)	380
Start-up wind (m/s)	2
Rated wind speed (m/s)	11
Working wind speed (m/s)	2-25
Wind energy utilizing ratio (Cp)	0.49
Blade diameter (m)	12

Since a small wind turbine is needed to implement the DC micro-grid, the best choice is the permanent magnet generator without gearbox that works in variable-speed [53].

The use of this system can increase the energy capture from the wind, improve the efficiency and resolve other problems as noise. For example, when the gearbox is used in the wind turbine system, additional cost, power losses, noise, and potential of mechanical failure can cause problems. In this way the use of variable-speed Permanent Magnet Synchronous Generator (PMSG) could be the best choice[54].

The model is composed by the WT, the PMSG, and through a AC/DC active rectifier is connected to the DC micro-grid as shown in Fig. 51.

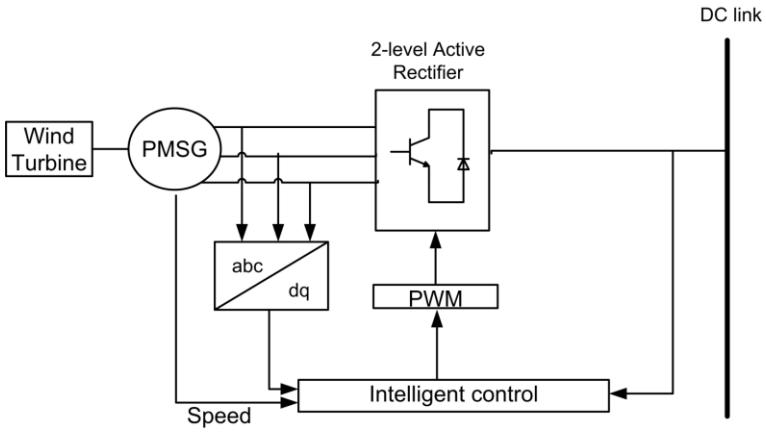

Fig. 51. Wind Energy system

The power converted by a wind turbine is given by the following equation[55]:

$$P_{WT} = \frac{1}{2}\rho C_p A U_w^3 \ [W] \tag{4.23}$$

where C_p is the power coefficient which is a function of tip speed ratio λ and the blade angle β, it is shown in the fig with fixed pitch, so $\beta = 0$. This relationship is usually provided by the manufacturer in the form of a set of no dimensional curves. U_w is the wind speed $[m/s]$, A is the wind turbine rotor swept area $[m^2]$, and the ρ is the air density $[kg \cdot m^3]$.

The Tip Speed Ratio (TSR) is given by:

$$\lambda = \frac{r \cdot \omega_m}{U_w} \tag{4.24}$$

where r is the radius of the rotor [m], and ω_m is the mechanical angular velocity of the generator [rad/s].

The dynamic equations of the PMSG are expressed in the "dq reference" frame by the Park's Transformation, as it is shown in the Appendix A. The model of electrical dynamic is given by the following equations in term of voltage and current, assuming that the q-axis is aligned with the stator terminal voltage phasor (i.e. $V_d = 0$) [56].

$$v_q = -\big(R + pL_q\big)i_q - \omega_r L_d i_d + \omega_r \emptyset_m \tag{4.25}$$

$$v_d = -(R + pL_d)i_d - \omega_r L_q i_q \tag{4.26}$$

where the R and L are respectively the resistance and inductance per phase, $\emptyset_m$ is the amplitude of the flux linkages established by the permanent magnet, i_q and i_d are the two axis machine currents, v_q and v_d are the two-axis machine voltages, and $p = \frac{d}{dt}$.

The expression for the electromagnetic torque in the rotor is the following:

$$T_e = \left(\frac{3}{2}\right)\left(\frac{P}{2}\right)\left[(L_q - L_d\ )\, i_q i_d - \emptyset_m i_q\right] \tag{4.27}$$

where P is the number of poles of the PMSG, and T_e is the electrical torque from the generator.

The relationship between the mechanical angular velocity of the rotor ω_m and the angular frequency of the stator ω_r is expressed as:

$$\omega_r = \frac{P}{2}\omega_m \tag{4.28}$$

The power coefficient in this numerical approximation ascribed by (Slootweg et al., 2003)[57] is given by:

$$c_p = \\ = c_1 \cdot \left(c_2 \cdot \frac{1}{(\lambda + c_8 \cdot \theta_{pitch}) - \frac{c_9}{1+\theta_{pitch}^3}} - c_3 \cdot \theta_{pitch} - c_4 \cdot \left(\theta_{pitch}^{c_5} - c_6\right) \cdot \right. \\ \left. \cdot\ e^{\left(-c_7 \cdot \frac{1}{(\lambda + c_8 \cdot \theta_{pitch}) - \frac{c_9}{1+\theta_{pitch}^3}}\right)}\right) \tag{4.29}$$

Where from c_1 to c_9 are parameters of the WT given by the manufacturer and θ_{pitch} is the pitch angle.

4.3.2 Control

Active Rectifier

Using an active rectifier (Fig. 52.) as a Voltage Source Converter (VSC) can give some advantages such the possibility of full control of the dc voltage.

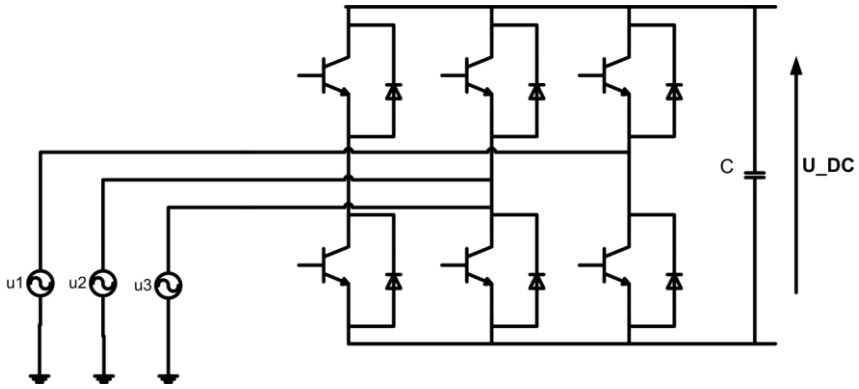

Fig. 52. Active rectifier for WT

The ratio of the blades is fixed; the wind speed depends on the weather conditions, so the only variable able to be controlled is the rotor speed. The TSR value depends on the rotor speed and the wind speed, from the equation (4.22). In Fig. 53, the relationship between the power coefficient (Cp) and the TSR are shown.

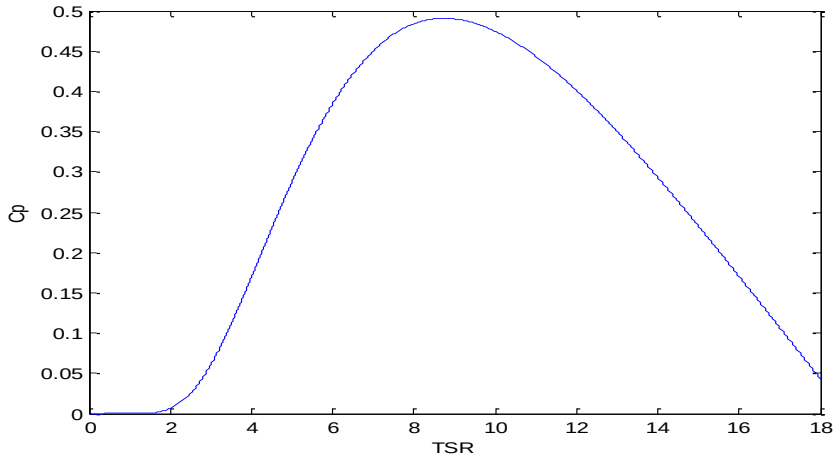

Fig. 53. Power Coefficient vs Tip speed Ratio

The designed control for wind speeds below the nominal one pursues the WT operation at the maximum power coefficient, setting reference rotational speeds proportional to the wind speeds. Instead for stronger winds the method ensures the nominal power production as shown in the flat region of the optimal tracking curve of Fig. 54.

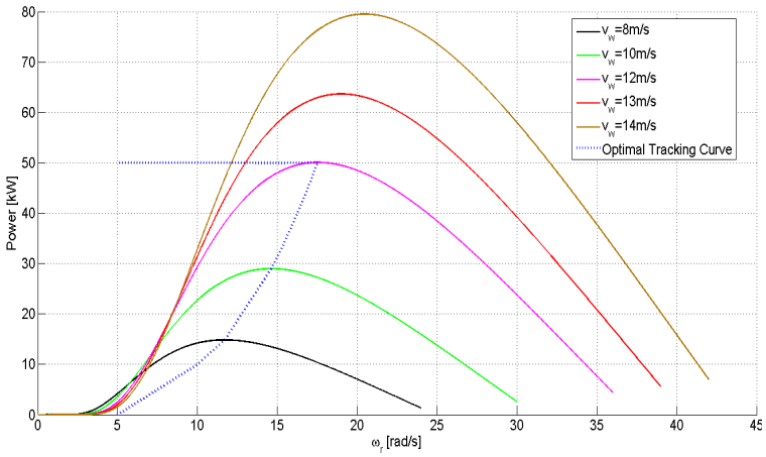

Fig. 54. Wind Turbine Optimal Tracking Curve

This is achieved by setting a reference rotational speed fulfilling the proper reduction of the power coefficient. Such speed regulation is attained with a PI regulator in an outer speed loop applied to the inverter control. This operates with inner loops controlling the machine currents transformed in a reference frame rotating at the PMSG electrical speed. Such speed can be easily obtained with an encoder and known the number of pair poles of the machine. The overall control scheme is reported in Fig. 55.

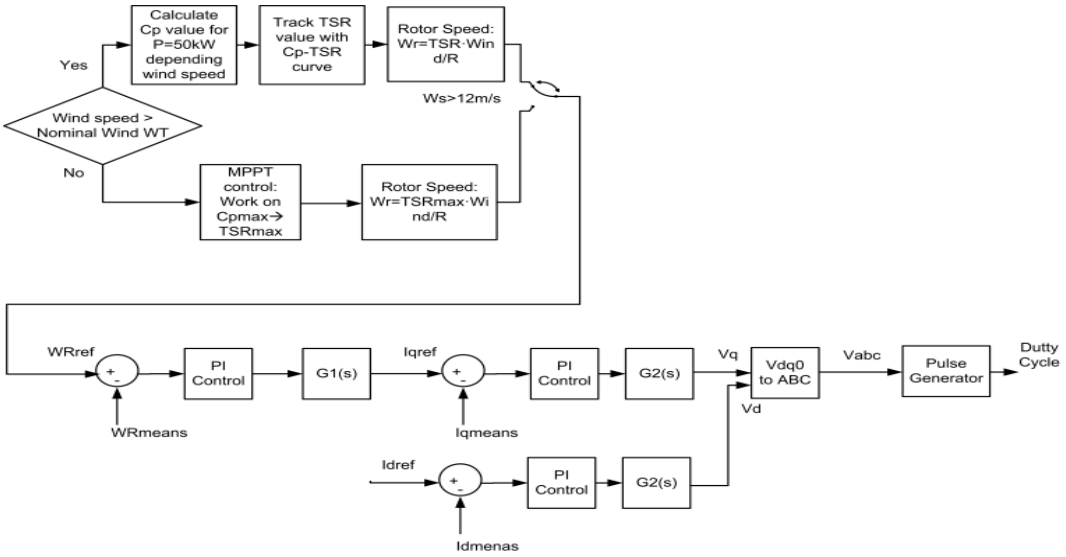

Fig. 55. Control for WT

4.4 Photovoltaic

The PV is growing rapidly in the world; its penetration in the generation of electricity is going to reach very high percentages in several countries, Fig. 56 shows the global cumulative installed PV solar capacity.

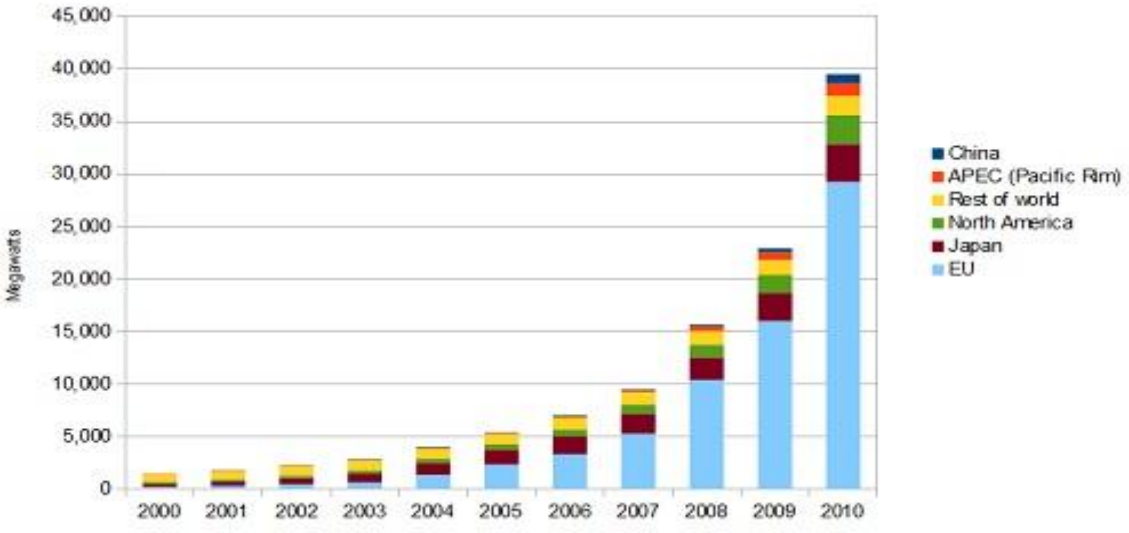

Fig. 56. Global cumulative installed PV solar capacity. Source: International Energy Agency

Photovoltaic cell are devices that transform the sun irradiance into DC current, the common types of PV Cells produced are[58]:

- Monocrystalline Silicon Cells
- Multicrystalline Silicon Cells
- Thin film Silicon
- Amorphous Silicon

In Fig. 57 a simplified equivalent circuit model of the PV is presented. The output current of a PV module can be obtained from the below equation,

$$I = I_{SC} - I_D - I_{Rp} = I_{SC} - I_0\left[e^{q\frac{V+IR_S}{nV_T}} - 1\right] - \frac{V+IR_S}{R_p} \tag{4.28}$$

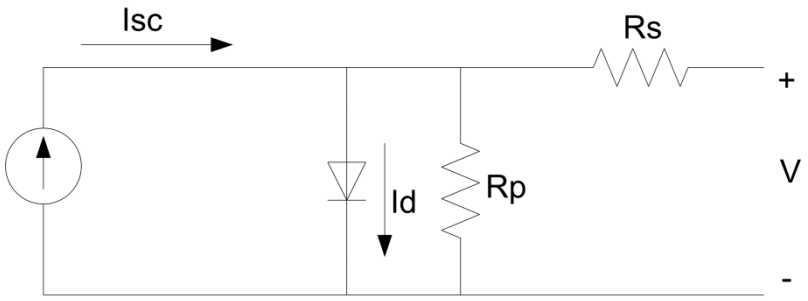

Fig. 57. Equivalent circuit model for a PV

The effect of parallel resistance (*Rp*) is very small in a single module because its value is close to ∞, therefore it doesn't affect the PV current value.

Usually a PV array consists of a group of PV modules for obtaining high power. Those modules in a PV array are connected in series-parallel combinations[11]. The output current, if R_p is considered ∞, of a PV array can be obtained from equation

$$I = N_p I_{SC} - N_p I_D = N_p I_{SC} - N_p I_0\left[e^{q\frac{V+IR_S}{nN_S V_T}} - 1\right] \tag{4.29}$$

where N_p and N_s are the number of cell in parallel and in series respectively.

The current versus voltage and power versus voltage characteristics of a PV array are similar as the characteristics of a single module shown in Fig. 58.

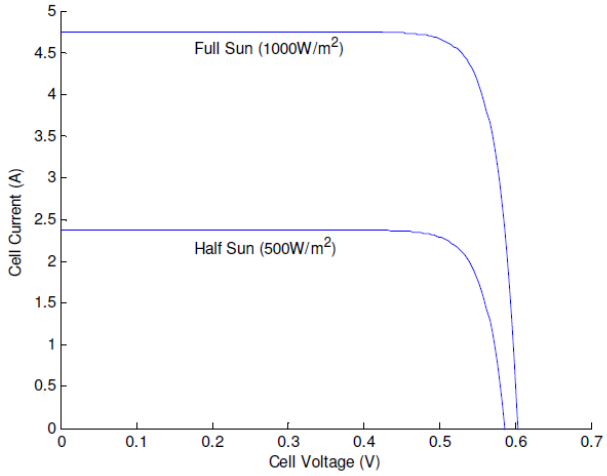

Fig. 58. I-V characteristics of PV

4.4.1 Model

For the PV array, the SX190W‘s model from BP Solar manufacturer has been chosen. The parameters are shown in next Table 13:

Table 13. PV data sheet

Maximum Power (Pmax)	190W
Voltage at Pmax (Vmppt)	24.3V
Current at Pmax (Imppt)	7.82A
Short-circuit current (Isc)	8.5A
Open-circuit voltage (Voc)	30.6V
Temperature coefficient of Isc	(0.065±0.015)%/ºC
Temperature coefficient of Voc	-(111±10)mV/ºC
Temperature coefficient of power	-(0.5±0.05)%/ºC
NOCT (Air 20ºC; Sun 0.8kW/m^2; wind 1m/s)	47±2ºC
Number of series connected modules	12
Number of parallel strings	11
Maximum Power	25Kw

The PV model considering in this thesis is composed by 11 parallel strings, each one devised by 12 modules connected in series, for an overall nominal power of 25kW. The aggregated PV cell module is defined by a Four-Parameter Model.

4.4.2 Control

The optimal operation of the PV is ensured by the Incremental Conductance Maximum Power Point Tracking (MPPT) algorithm, fitting to rapidly changing irradiance conditions[59]. It aims “climbing” the typical hill-shaped P-V curve, pursuing the zero slope condition:

$$\frac{dP}{dV} = 0 \tag{4.30}$$

The equation (4.30 in turns allows achieving the Maximum Power Point (MPP) when:

$$\left.\frac{dI}{dV}\right|_{\substack{i=I_{MPP}\\ v=V_{MPP}}} = -\frac{I_{MPP}}{V_{MPP}} \tag{4.31}$$

Therefore the algorithm conceived in [60] and shown in Fig. 59 is used to drive the boost converter interfacing the PV system to the DC micro-grid.

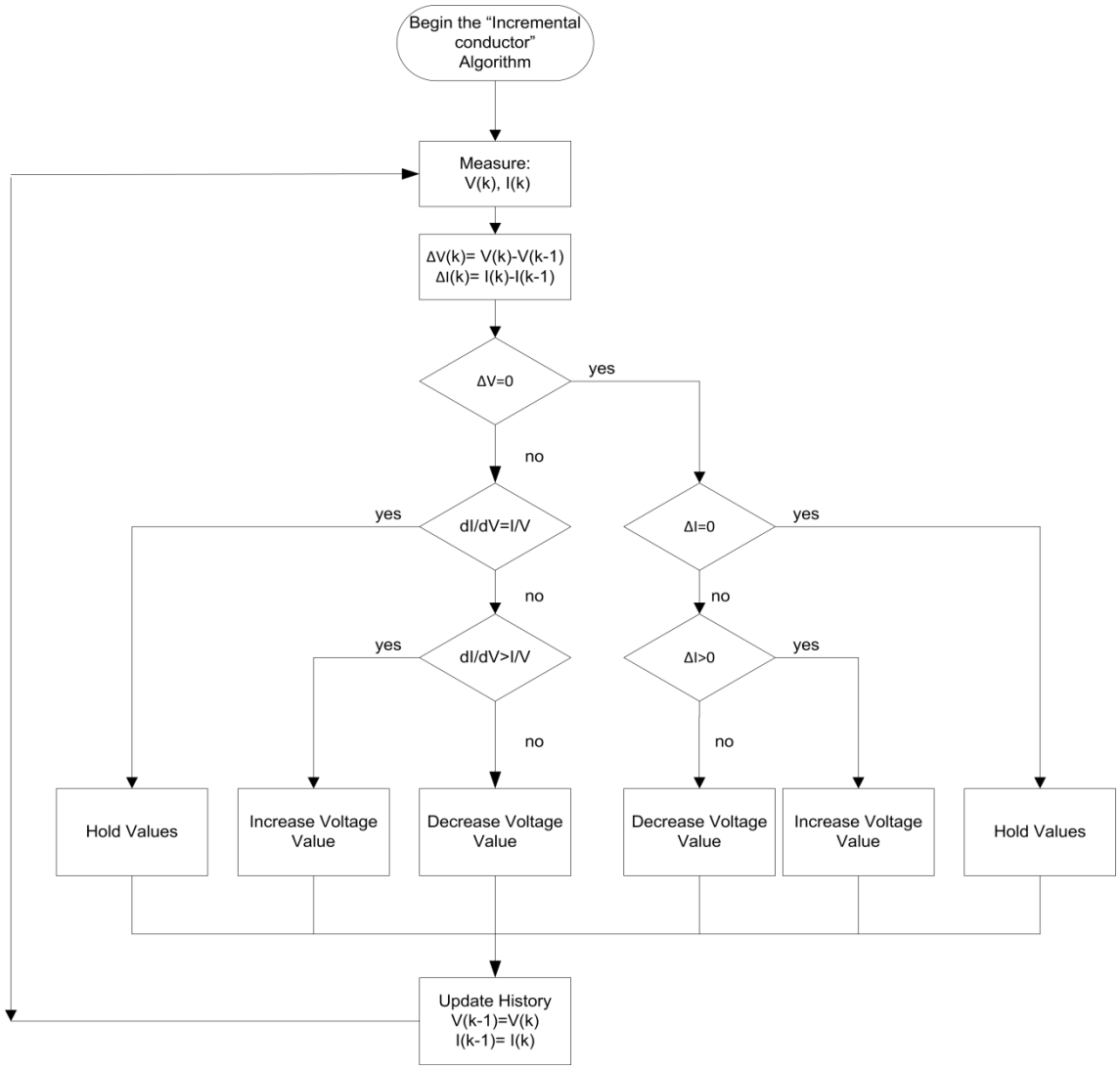

Fig. 59. Flow chart MPPT for PV

Fig. 60 shows the PV energy system configuration, where it is possible to see that the PV arrays are connected to the DC-DC boost, the DC-DC boost converter model analysis was presented in the paragraph 4.2.2.

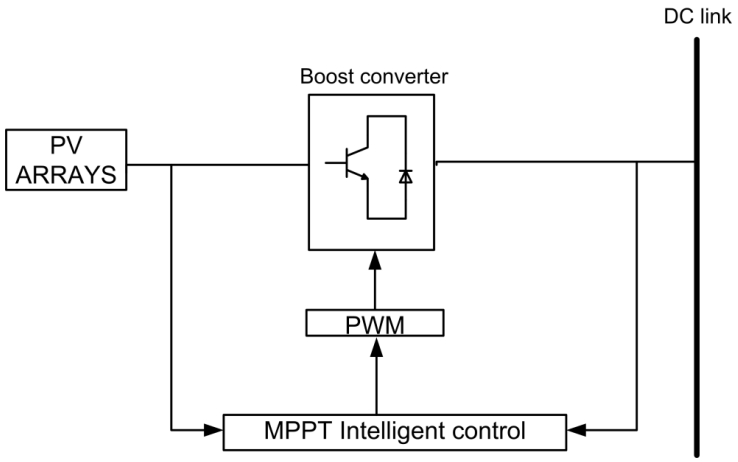

Fig. 60. PV Energy system

The converter is controlled by the implementation of the MPPT algorithm as it is presented in the Fig. 61.

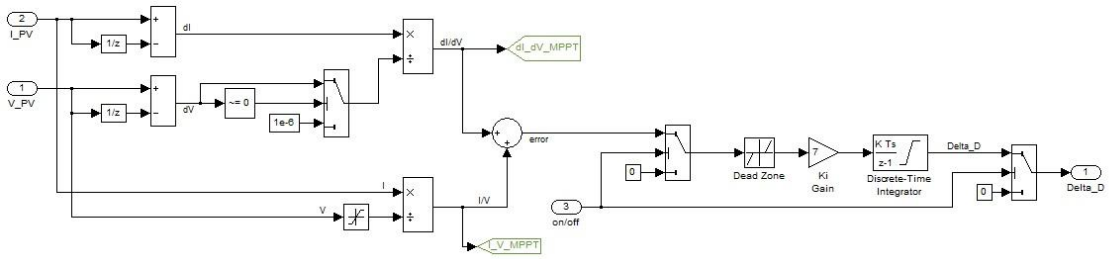

Fig. 61. Boost control in PV system

Chapter -5-SIMULATIONS

5.1 Introduction

The objective of the simulations cases studies is to verify that the proposed micro-grid simulation model can operate in different modes with high DER penetration, and to analyze the performance of the system in different scenarios. The implemented model of the DC micro-grid is shown in Fig. 62.

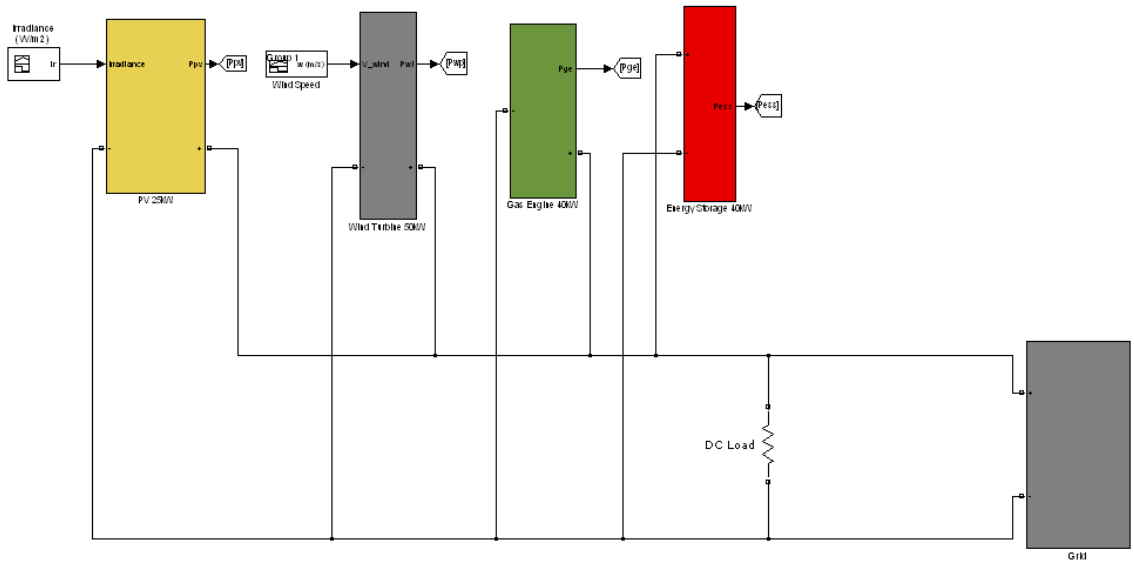

Fig. 62. Implemented DC micro-grid by Simulink

Four study cases have been implemented by MATLAB/Simulink and in this chapter will be shown the results, Table 14 shows the different study cases.

Table 14. Study cases implemented by MATLAB/Simulink

Case 1	Islanded Mode
Case 2	Grid Connected Mode
Case 3	Three Master units working
Case 4	Cascade faults

5.2 Case 1

In the first case the micro-grid is implemented to work in islanded mode, where the ESS acts as the “master”, to control the voltage level on the DC bus and to balance the power flow. In this scenario the input of the PV is the fluctuation of the irradiance and the input of the WT is the wind speed variation and in both units the MPPT methods are implemented which are illustrated in the chapter 4.3.2 and 4.4.1 .

In Fig. 63, the power supplied by the WT source and the wind speed is shown. In this first simulation, the wind speed starts at 10 m/s and increase until arrive at the nominal speed value of 12 m/s at the time 1.5s. When the wind reaches the 13m/s at the time 3s, it starts to decrease until 8.5 m/s at 9s. In the power fluctuation, the power increase at

0.5 (same time as the wind speed increase from 10m/s), until arrive at the nominal power at 1.5s. The power remains at 50kW until 4.5s (when the wind speed is lower than 12 m/s). After 4.5s the power decrease until arrive to 18.5kW at the time 9s. The speed control of the WT will be shown to point out the two transients that occur at 1.5s and 4.5s.

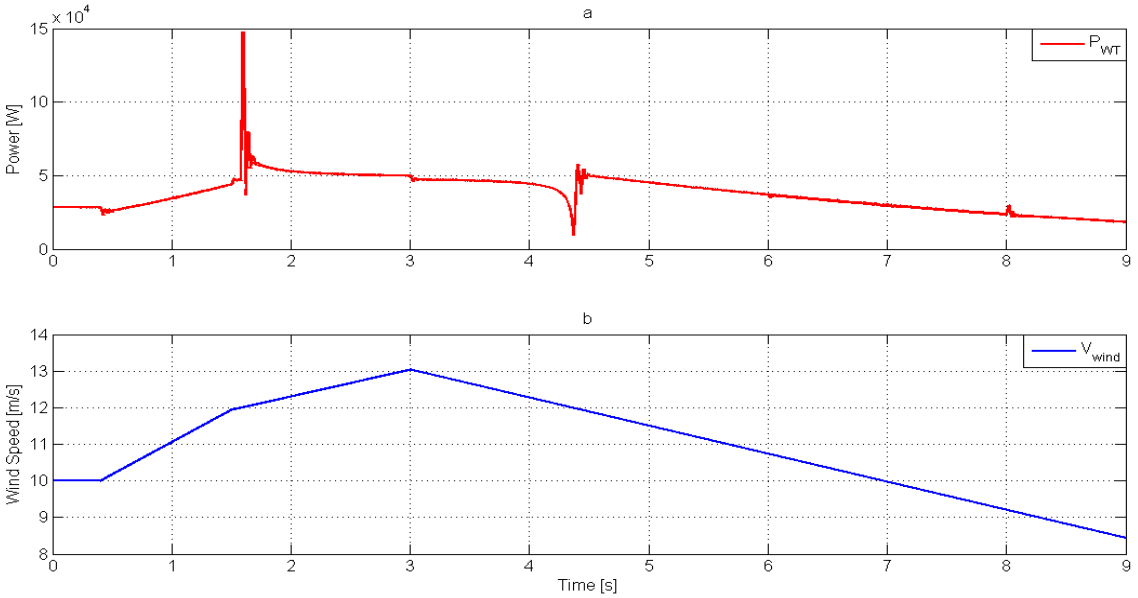

Fig. 63. a) Power injected by the WT depending on b) wind speed

In Fig. 64, the rotor speed is compared with the reference speed designed in the MPPT control. The highest rotor speed occurs at 1.5 and 4.5s at a wind speed of 12 m/s. When the wind speed is higher than the nominal value, the speed control reduces the rotor speed to remain the supplied power at 50kW. In Fig. 65, the power generated by the WT is compared with the error of the shown comparator in Fig. 64. It is clear that the transients are caused by the speed control, due to a fast variation of the rotor speed. The high peak of the transient is caused by the sudden kinetic energy release occurring whenever the wind speed reaches the nominal value.

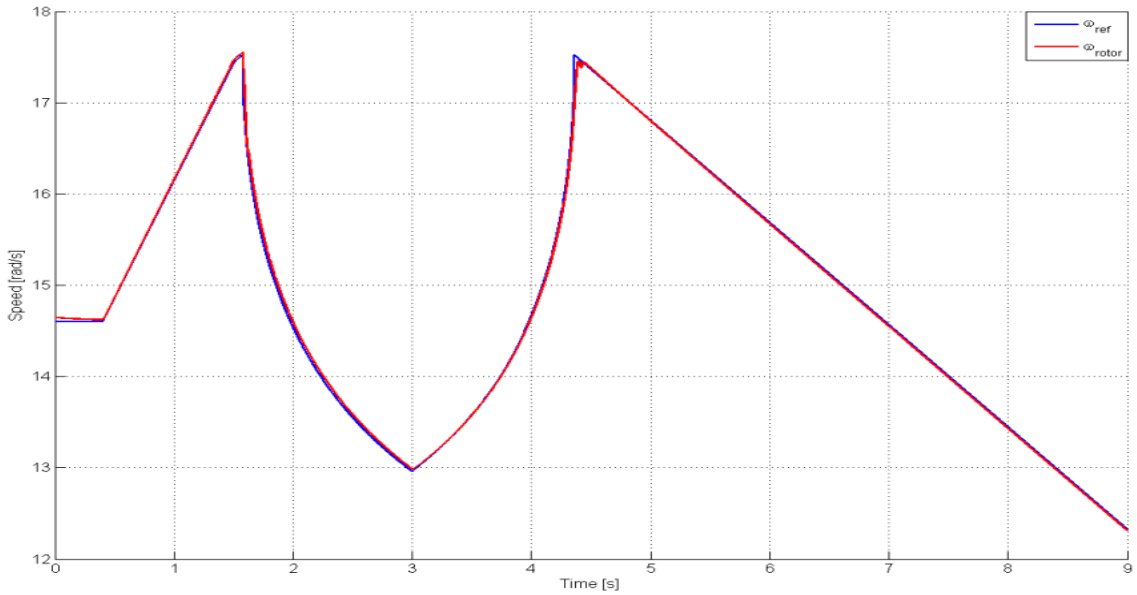

Fig. 64. Speed control for the WT model

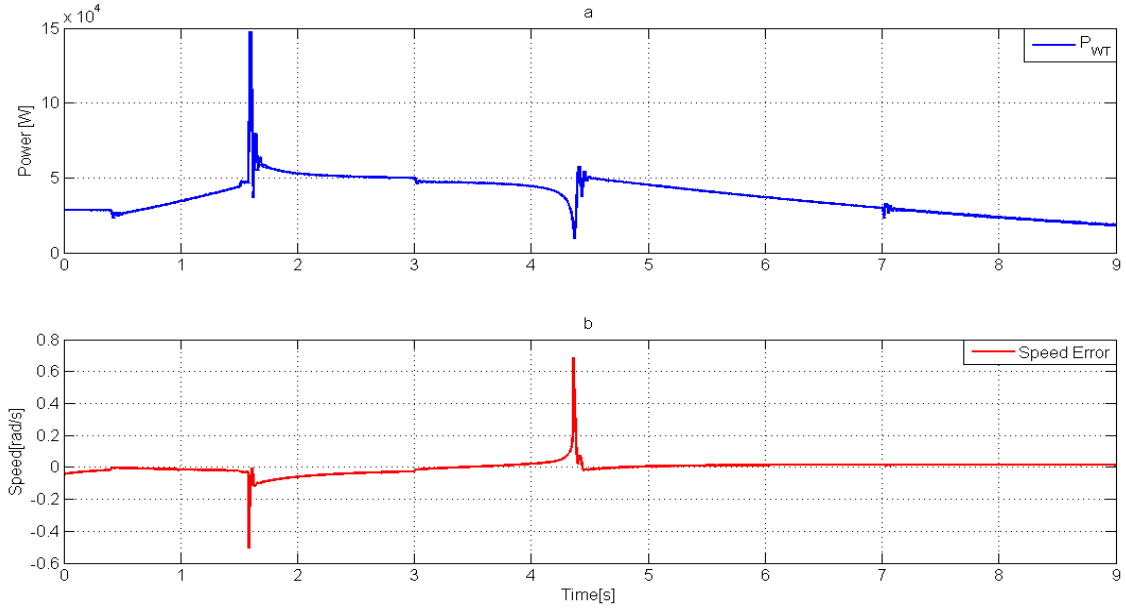

Fig. 65. Comparison between a) Power generated by the WT, b) speed error

In the PV model, the irradiance value and the power generated by the PV array fluctuate as illustrates Fig. 66. The generated power reaches the nominal value when the irradiance is 1000 W/m^2. Therefore the MPPT control works properly to allow the model to supply the maximum power for every irradiance value. This MPPT control has been explained in chapter 4.4.1. Fig. 67 illustrates the comparison between *dI/dV* and *I/V*. Where the error is near to zero during the entire region except with the minimum irradiance value, where there is a peak when the irradiance stops decreasing and starts to increase.

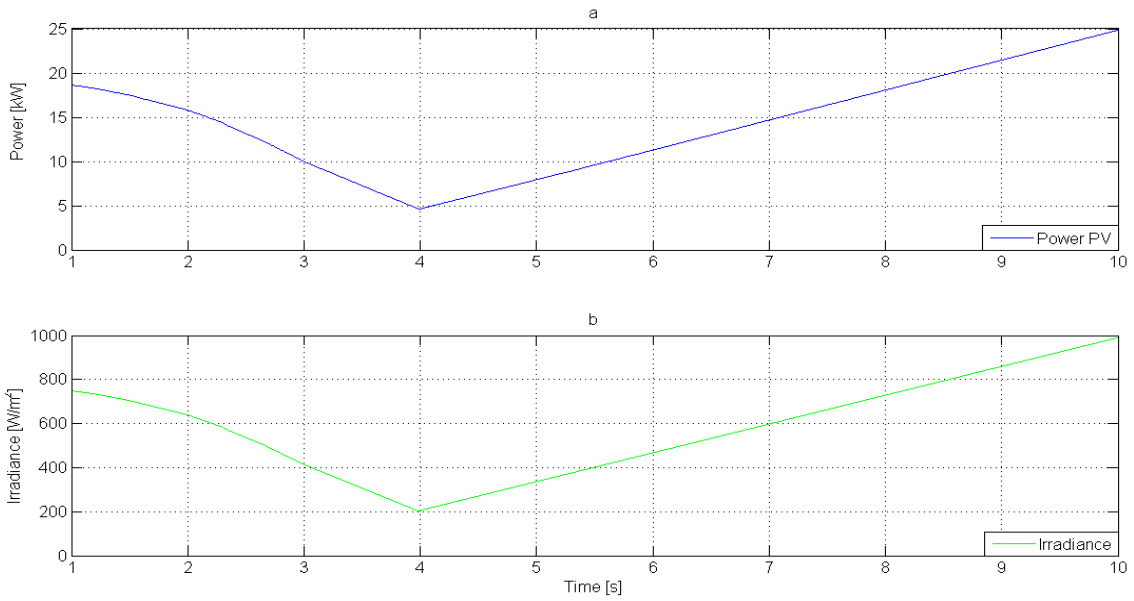

Fig. 66. Comparison between a) Power generated by the PV, b) irradiance value

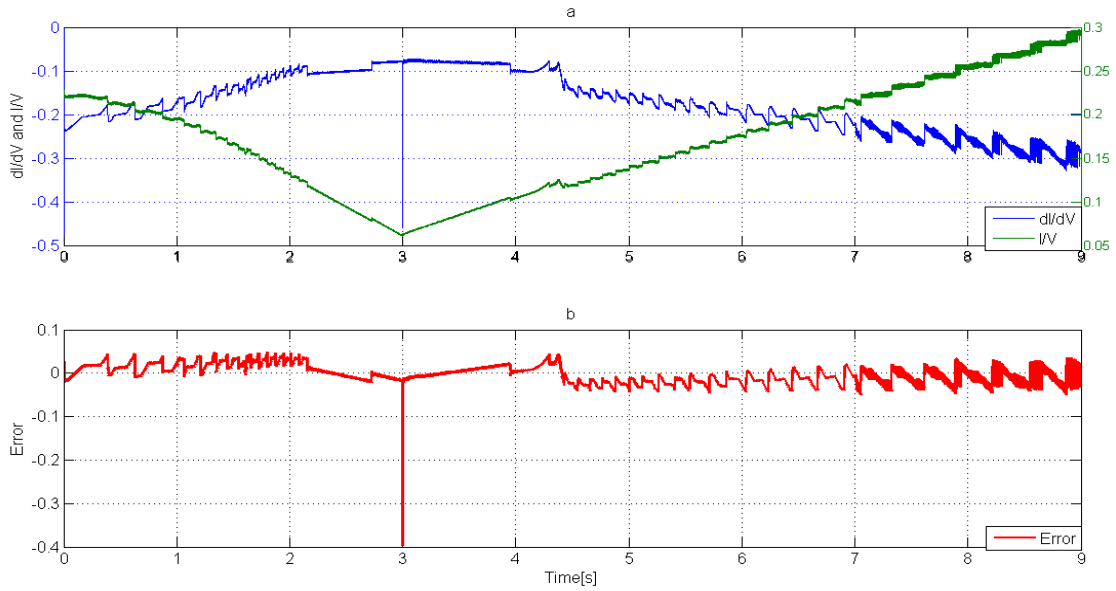

Fig. 67. Control of the PV MPPT mode. a) Comparison between dI/dV and I/V b)Error

In this study case, the ESS controls the power flow and the DC voltage bus. The reference voltage has been chosen in chapter 3.1, with a value of 800V. In Fig. 69, the comparison between the DC bus voltage and the reference voltage is shown. The ESS remains the voltage value at 800V, except at 1.5s and 4.5s (when appear the transients caused by the WT).

The ESS controls the power flow on the micro-grid shown in Fig. 68 by injecting and consuming power by the bi-directional converter. The power flow in the DC system is displayed in Fig. 68, here it is interesting noticing the ESS power flow variation at time 3s, when a second DC load is connected to the micro-grid. In particular the ESS copes

with the power unbalance passing from charging to discharging mode. Also the fluctuation of the WT, due to the inertia of the PMSG, is regulated by the ESS. Fig. 69 illustrates the SOC value and the voltage of the batteries. The voltage on the batteries increase when the ESS is charging, and decrease when a second DC load is connected and the ESS discharge energy to balance the power flow. The SOC value changes slightly due to the limited time simulation. To be able to show a completely discharge cycle the simulation time has to be longer than one hour.

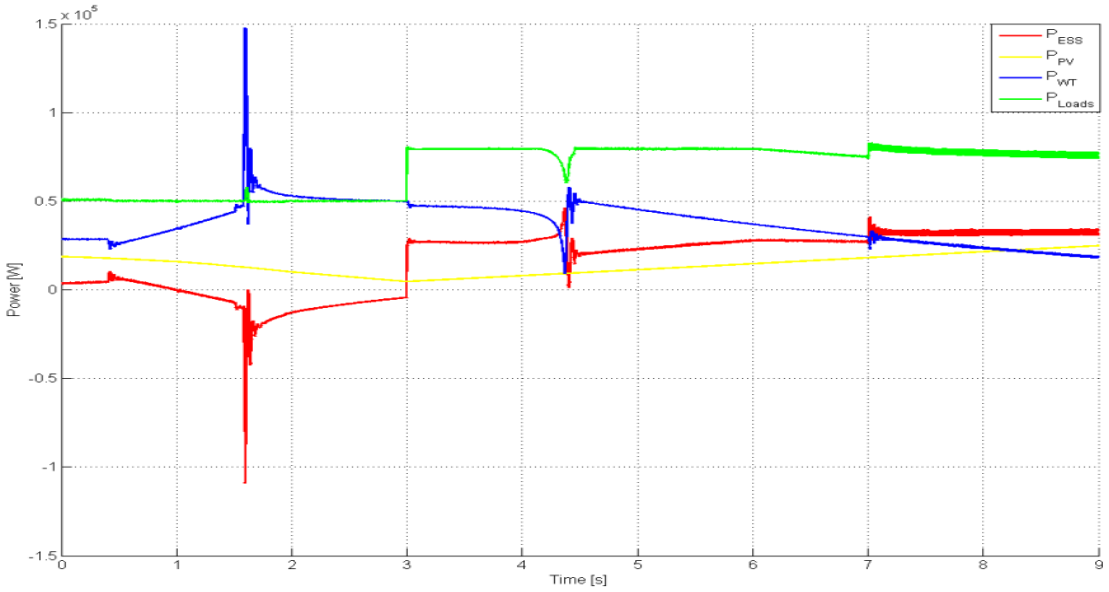

Fig. 68. Power flow in the micro-grid for the Case 1

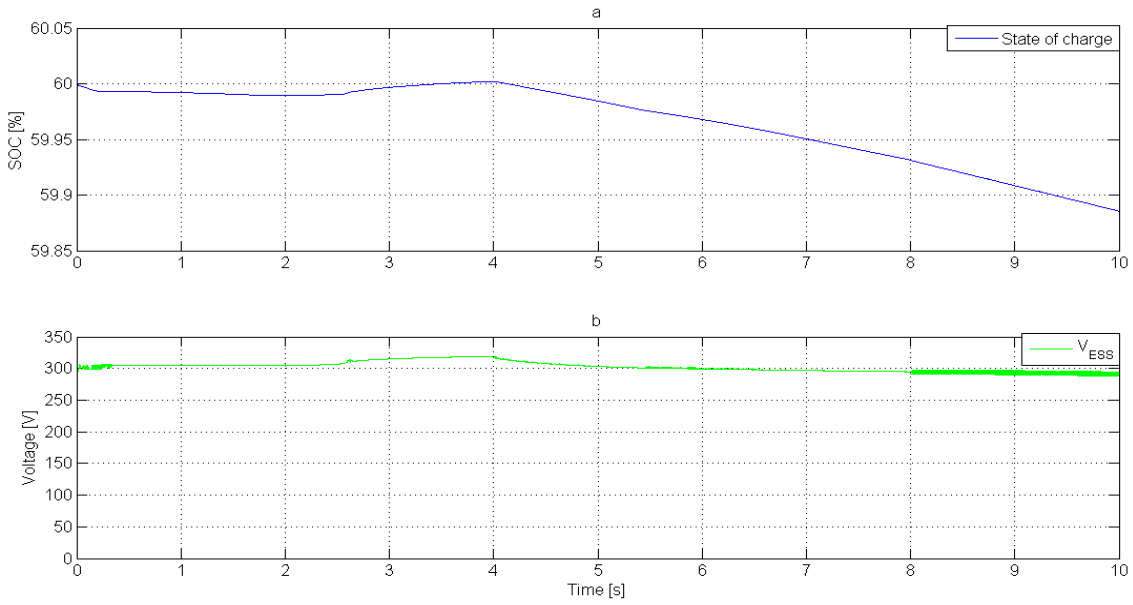

Fig. 69 ESS characteristics : a) SOC , b) Voltage

The voltage in the DC micro-grid is shown in Fig. 70, this is constant with a fluctuation around 2% except when the WT transients appear.

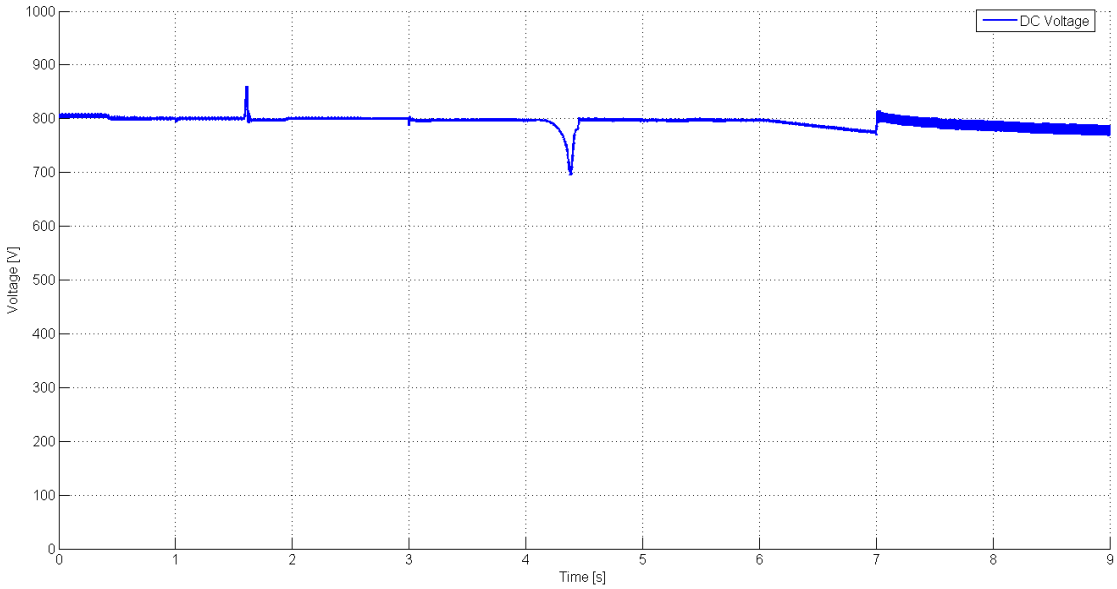

Fig. 70 DC voltage level on the micro-grid for the Case 1

5.3 Case 2

In the case two, the micro-grid is implemented to work in grid connected where the VSC is the "master" controller, to control the voltage level on the grid and on the DC micro-grid bus and to balance the power flow. In this scenario, it is supposed that the PV and WT are working in nominal power without fluctuations in the wind speed and in the irradiance.

In Fig. 71 the power flow on the DC micro-grid is displayed when it is connected with the grid. When the units start to generate power, the grid injects power to control the fluctuations due to the PMSG of the WT, when the system works on the steady state the power injected by the grid is near to zero. In Fig. 72 is shown the DC voltage level after the first 0.5 seconds, when due to the PMSG transients the voltage is higher than the reference value.

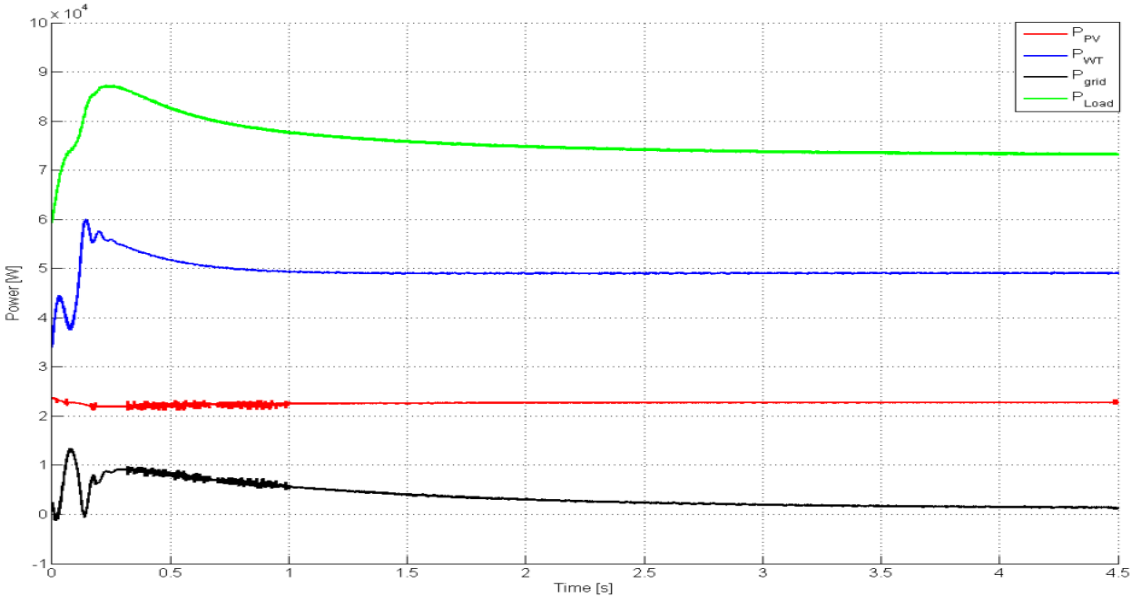

Fig. 71. Power flow in the micro-grid for the Case 2

The DC voltage fluctuates around 5%, this could be improved modifying the parameters of the VSC, finding the transfer function for the voltage and current loop.

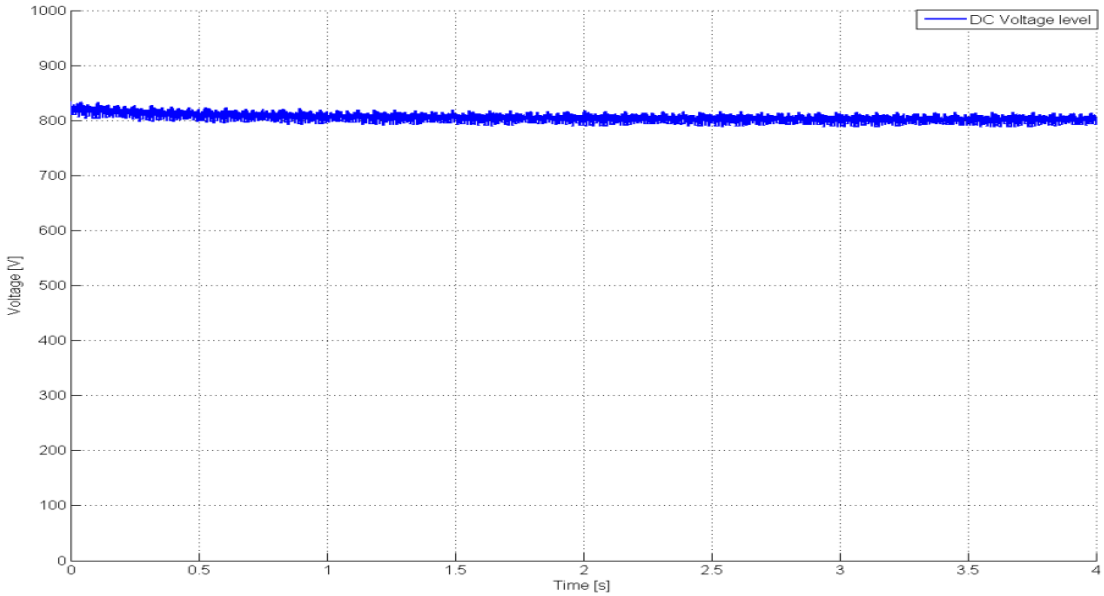

Fig. 72. DC voltage level for the Case 2

Fig. 73 illustrates the current flow of the system, due to a fix DC voltage, it is clear to see that the trend of the power flow in the Fig. 71 depends from the current flow.

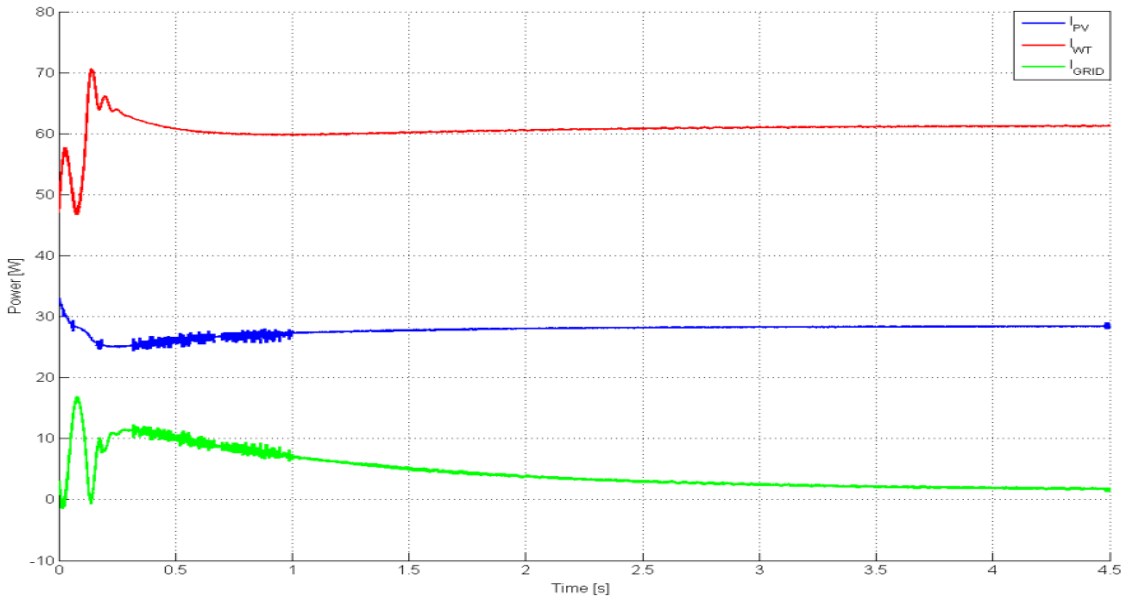

Fig. 73. Current flow in the grid for the Case 2

The VSC inverter output is shown in the Fig. 74 a) and the output of LC filter in the Fig. 74 b) with a peak voltage of 565V and a frequency of 50Hz. The AC voltage supplied to the grid presents small disturbance due the time sample of the simulation. The commutation frequency of the inverter is 10kHz and the time sample of the simulation is 1µs. Therefore the duty cycle accuracy is ±1%.

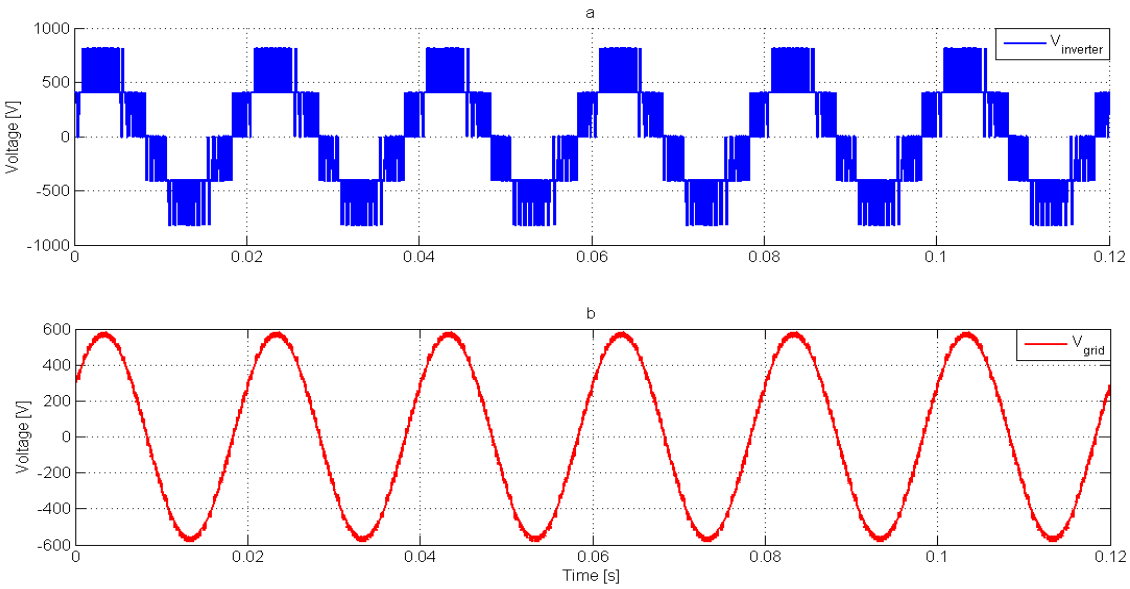

Fig. 74. Voltage in the a) AC side of the inverter, b) Grid Voltage

5.4 Case 3

In chapter 3.2 it has been explained that the used DC micro-grid configuration works properly in case that only one unit is able to work such a master. In this paragraph the results when more master units are working in the same time will be displayed and the problem within the micro-grid will be pointed out in grid connected. .

In Fig. 75, it is shown how the DC voltage level works properly. Concluding that working with 3 master units the DC voltage is balanced in the desired value with a fluctuation around the 5%.

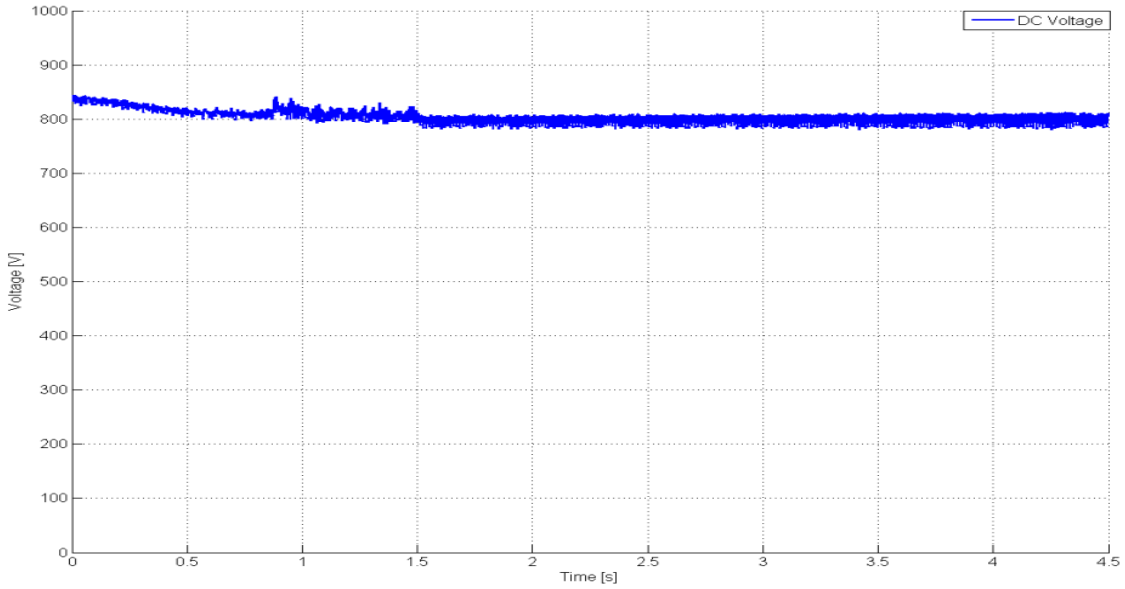

Fig. 75. DC voltage bus level with 3 Master units

The PV and the WT models still working as slaves units, injecting only current to the system. Therefore the generated power will be the same as shown on chapter 5.3. Fig. 76 shows the power flow on the load, the PV and the WT. The fluctuation of the WT is due to the PMSG. To understand the fluctuations of the load, Fig. 77 illustrates the fluctuation of the power generated by the ESS and the GE. Where the power delivered by the ESS fluctuates more than 100kW and the GE almost 50kW. This happens because the two different controllers pursuing the same set point with different dynamics causing current peak. Therefore, the injected current fluctuates making the system unstable because the ESS and the GE can’t work properly in this way and the power quality on the load is not acceptable.

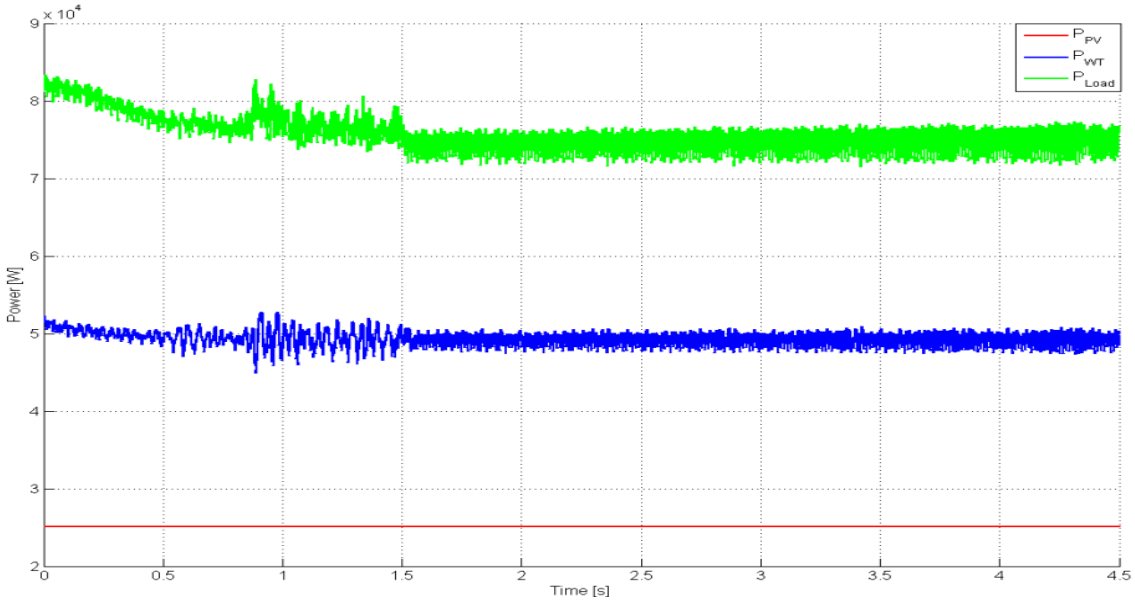

Fig. 76. Power flow in the load, PV and WT for Case 3

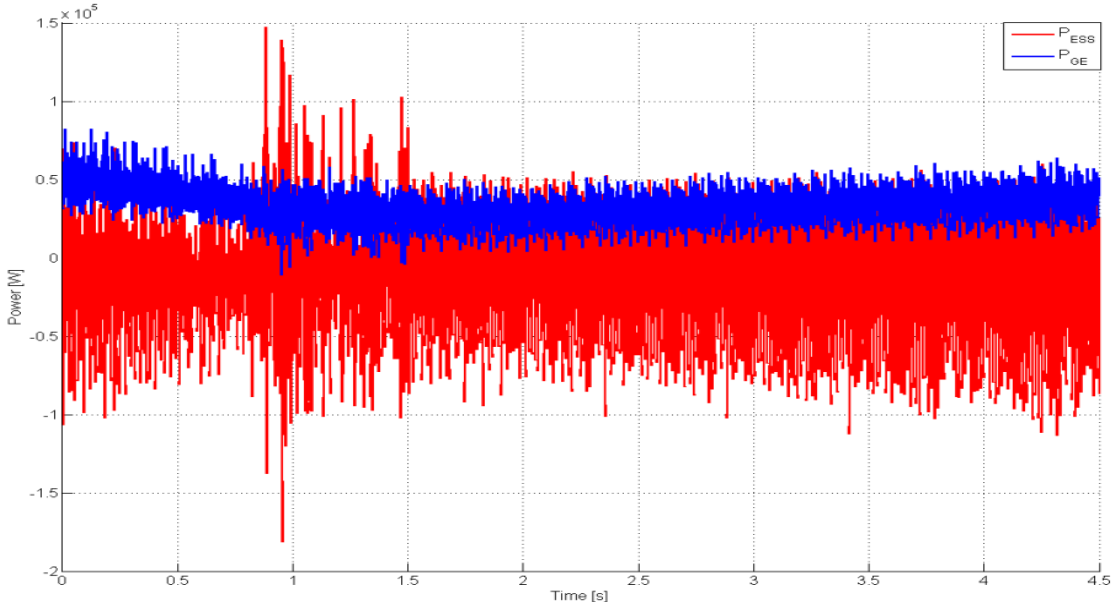

Fig. 77. Power flow in the GE and ESS for Case 3

Fig. 78 shows the current injected by the PV and the WT with small fluctuations. As whereas, Fig. 79 displays the current injected by the GE and the ESS, where the fluctuations are higher than 100A.

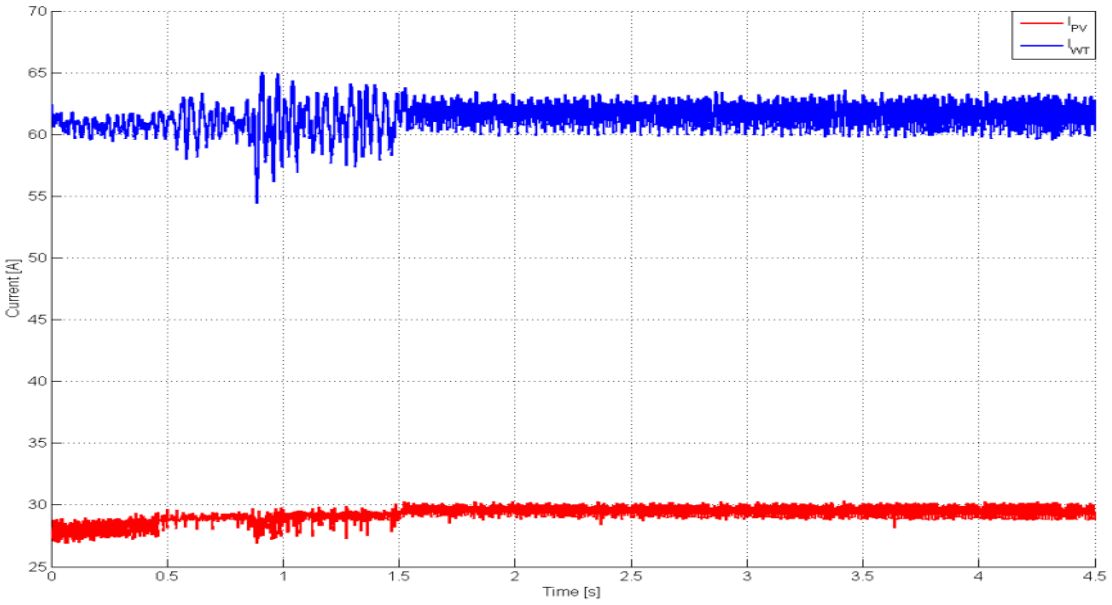

Fig. 78. Current injected by the PV and the WT for Case 3

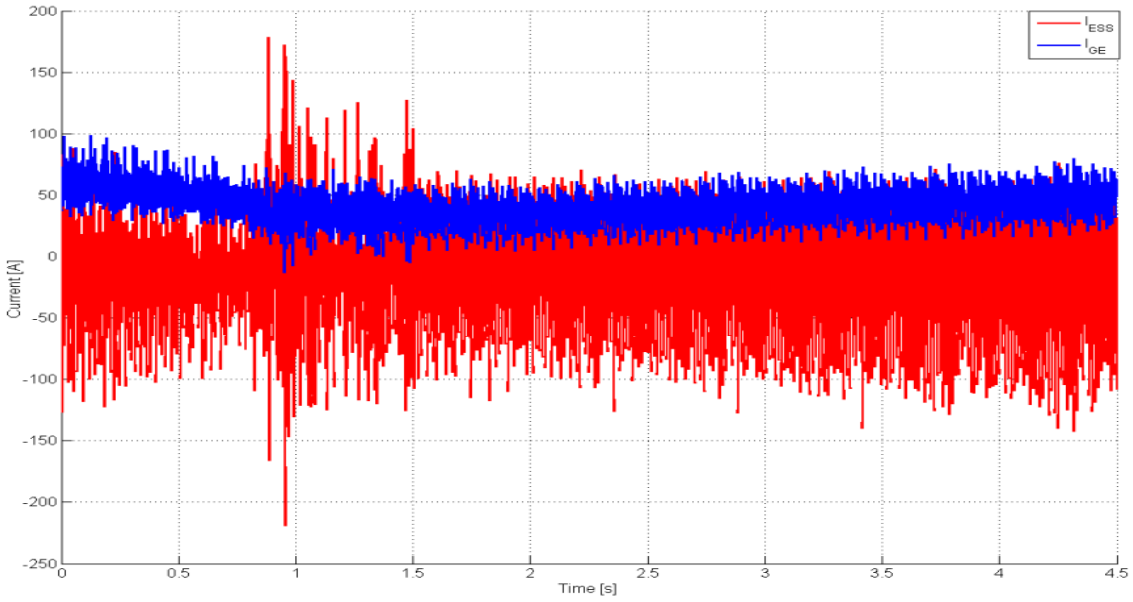

Fig. 79. Current injected by the ESS and the GE for the Case 3

5.5 Case 4

To improve the reliability of the system and to avoid the problem shown in Case 3, the micro-grid is controlled by using only one unit as a "master". The devices in charge to make this are the grid, the ESS and the GE. In the other hand this case shows how the intelligent control is able to maintain the voltage level and the power flow of the micro-grid in case of cascaded faults in the AC-grid and in ESS.

In this case, until the time 2s the micro-grid is connected to the AC-grid, therefore the VSC is operating as “master” unit to control the voltage level. At time 2s a fault in the grid is hypothesized and the micro-grid is disconnected from the AC-grid and controlled by the bidirectional converter of the ESS as a “master” controller. Finally at the time 3.5s the GE is called such “master” by disconnecting the ESS. Fig. 80 shows the DC voltage bus profile. In the first region there is a slight oscillation due to the grid tied inverter regulators. While in the intermediate one the voltage profile looks flat when the ESS acts as a “master”. The transition between the ESS mastering to the GE one is affected by an initial transient which is damped in less than 100 ms.

Fig. 81 shows the behaviors of the power for all the units in the system in the three different scenarios.

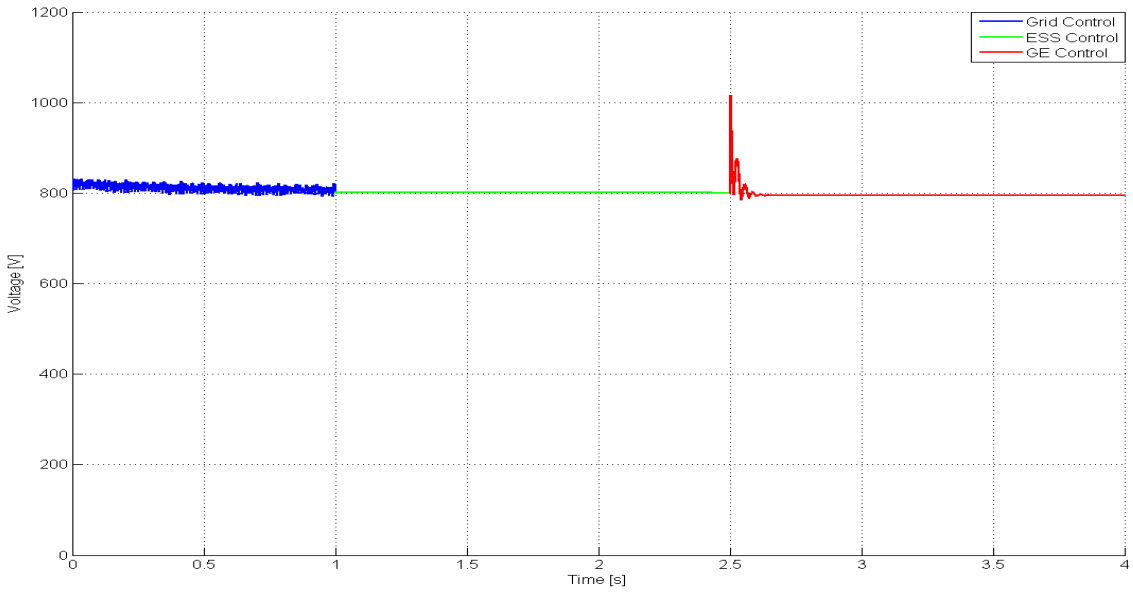

Fig. 80. DC Voltage level for every Master Control period

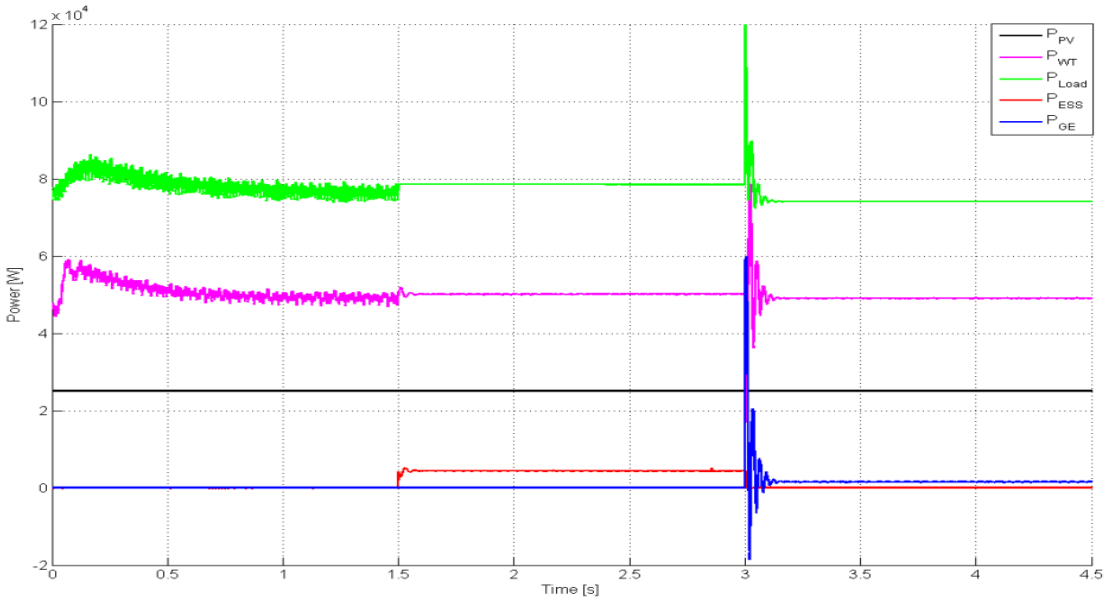

Fig. 81. Power flow in the micro-grid for the Case 4

Chapter-6-CONCLUSIONS AND FUTURE WORK

6.1 Introduction

In this last chapter, the conclusions derived from this thesis are presented. The main goals and contributions are summarized and the possible future work of research proposed from this thesis will be discussed.

6.2 Summary

After a general introduction in the chapter one, in the second chapter a review of the state of art of the micro-grids was shown considering the development of the electrical networks in the last years and the introduction of DER sources, taking into account the following points:

- The concept and micro-grids state of art.
- Currently control topology methods for micro-grids.
- Different implemented micro-grids and control topology used.

In the third chapter the implemented DC micro-grid has been presented, with the chosen voltage level and its intelligent control strategy. Also the participation of the micro-grid in the electricity market was considered and its economical profit was studied with an intelligent economical control. The main contribution of this chapter was:

- Implemented DC micro-grid.
- Voltage level configuration.
- Control strategy implemented in the system.
- Election of the optimal ESS technology from the economical point of view.
- Economical strategy to implement an optimal participation.
- Proposed study cases.

In the fourth chapter, the DER units are shown with different kinds of control methods used for each unit, showing:

- The fundamental concept of every technology used in the implemented micro-grid.
- The chosen model for the implemented system.
- Different kinds of control methods to increase the injected power, balance the power flow and the voltage level of the micro-grid.
- The chosen power electronics for each unit

Finally in the fifth chapter, the implemented simulations with Simulink are shown, four study cases are presented to show the behaviour of the DC micro-grid in different scenarios.

- Islanded mode: ESS as a master regulating voltage and power flow.
- Grid connected mode: The VSC inverter regulates the voltage and the power flow.
- Three Master units: VSC inverter, ESS and GE works at same time as “Master” units.
- Cascade faults

6.3 Key Contributions

This thesis presents a DC micro-grid based power generation system with a PV, WT, GE and ESS generation connected to the grid. Different kinds of control methods are proposed to increase the injected power, balance the power flow and the voltage level of the micro-grid. The proposed control strategy based on the MPPT control for the PV and WT models and the voltage and power control for the GE and the ESS has been implemented in Simulink. The design of the bidirectional converter and the boost converter were done by considering the equivalent circuit and its transfer functions. Finally the control of the boost converter were proven thanks the bode diagrams, root locus, and step response by SISOtool/MATLAB implementation. About the economical point of view, an Intelligent Economical Control has been implemented to evaluate the participation of the micro-grid with the electricity market by using the ESS. Three study cases were conducted by MATLAB, from the obtained results, various observations were made:

- The micro-grid is able to obtain a benefit by an optimal participation of the system with the electricity market.
- The Lead-Acid batteries with enhanced carbon electrodes are optimal to exchange energy with the grid by an optimal participation or an arbitraging application.

Using the DC micro-grid developed model in this work, four study cases were conducted. From the simulation results, various observations were made:

- It is confirmed that the PV and the WT can work in MPP mode.
- The ESS is able to balance the power flow and stabilize the voltage level.
- Only one unit can work as a “Master” unit to ensure the correct behavior of the system.
- If there is a fault on the ESS or almost out of charge the GE converter is able to ensure the secured power supply and efficient operation of the micro-grid in islanded mode.

6.4 Future Work

The aforementioned conclusions in this thesis lead to several proposals for the future work being developed at present.

First of all, the technical limitation of the hardware should be settled by using a more powerful computer, so a longer simulation could provide scenarios more realistic, on the behavior of micro-grid, i.e. the SOC of the batteries or/and the behavior of the WT.

In the implemented simulations, the sample time was fixed at 1μs (for technical limitations) and the switch frequency at 10kHz (100 μs), so the accuracy not was suitable. For the future, the use of a smaller simple time could give better results.

The VSC inverter of the grid was obtained from a MATLAB demo model, therefore it wasn't suitable to control the power flow of the system. For future work, the implementation of another controller inverter could be interesting, to study the possibilities of the exchange power flow between the grid and the micro-grid system (i.e. ESS).

The model could be further validated with pole-to-neutral loads and with the operation of weather dependant units in master mode, as long as provided by a proper control.

Take the natural gas price into account, the study about the economical part could be extended on the use of GE for the optimal participation in the electricity market.

REFERENCES

[1] "Good Energy.cl." [Online]. Available: http://www.goodenergy.cl/eng_renewable_energy.html. [Accessed: 01-Mar-2012].

[2] Kyohei Kurohane, Akie Uehara, Tomnonobu Senjya, Atsushi Yona, Naomitsu Urasaki, Toshihisa Funabashi, and Chul-Hwan Kim, "Control strategy for a distributed DC power system with renewable energy," *2011*, vol. 36, pp. 42–49.

[3] Y. Ito, Y. Zhongqing, and H. Akagi, "DC microgrid based distribution power generation system," in *Power Electronics and Motion Control Conference, 2004. IPEMC 2004. The 4th International*, 2004, vol. 3, pp. 1740–1745.

[4] H. Kakigano, Y. Miura, T. Ise, and R. Uchida, "DC Micro-grid for Super High Quality Distribution—System Configuration and Control of Distributed Generations and Energy Storage Devices—," in *Power Electronics Specialists Conference, 2006. PESC'06. 37th IEEE*, 2006, pp. 1–7.

[5] H. Kakigano, Y. Miura, T. Ise, and R. Uchida, "DC voltage control of the DC micro-grid for super high quality distribution," in *Power Conversion Conference-Nagoya, 2007. PCC'07*, 2007, pp. 518–525.

[6] Michael A. Hyams, "Microgrid: An Assessment of rhe Value, Opportunities and Barriers to Deployment in New York State." Sep-2010.

[7] F. Kanellos, A. I. Tsouchnikas, and N. Hatziargyriou, "Micro-grid simulation during grid-connected and islanded modes of operation," in *International Conference on Power Systems Transients*, 2005, vol. 6.

[8] E. Commission and others, "European SmartGrids technology platform: vision and strategy for europe's electricity networks of the future," *European Commission, Brussels, Belgium, Tech. Rep. UR*, vol. 22040, 2006.

[9] "The Smart Grid: An Introduction." [Online]. Available: http://energy.gov/oe/downloads/smart-grid-introduction-0. [Accessed: 14-Apr-2012].

[10] R. E. Brown, "Impact of Smart Grid on distribution system design," 2008, pp. 1–4.

[11] Z. Chu, "PSCAD/EMTDC-based Modeling and Analysis of a Microgrid with Renewable Energy Sources," Texas A&M University, 2010.

[12] R. H. Lasseter and P. Paigi, "Microgrid: A conceptual solution," in *Power Electronics Specialists Conference, 2004. PESC 04. 2004 IEEE 35th Annual*, 2004, vol. 6, pp. 4285–4290.

[13] Peter Asmus, Adam Cornelius, and Clint Wheelock, "Microgrids Islanded Power Grids and Distributed Generation for Community, Commercial, and Institutional Applications," PikeResearch.

[14] J. Lee, B. Han, and N. Choi, "DC micro-grid operational analysis with detailed simulation model for distributed generation," in *Energy Conversion Congress and Exposition (ECCE), 2010 IEEE*, 2010, pp. 3153–3160.

[15] J. M. Guerrero, J. C. Vasquez, J. Matas, M. Castilla, and L. G. de Vicuna, "Control strategy for flexible microgrid based on parallel line-interactive UPS systems," *Industrial Electronics, IEEE Transactions on*, vol. 56, no. 3, pp. 726–736, 2009.

[16] M. Barnes, J. Kondoh, H. Asano, J. Oyarzabal, G. Ventakaramanan, R. Lasseter, N. Hatziargyriou, and T. Green, "Real-world microgrids-an overview," 2007, pp. 1–8.

[17] J. Stevens, *Characterization of microgrids in the United States*. 2005.

[18] F. Ktiraei, R. Iravani, N. Hatziargyriou, and A. Dimeas, "Microgrids management-controls and operation aspects of microgrids," *IEEE Power Energy*, vol. 6, no. 3, pp. 54–65, 2008.
[19] M. C. Chandorkar, D. M. Divan, and R. Adapa, "Control of parallel connected inverters in standalone ac supply systems," *Industry Applications, IEEE Transactions on*, vol. 29, no. 1, pp. 136–143, 1993.
[20] S. Morozumi, "Micro-grid demonstration projects in Japan," in *Power Conversion Conference-Nagoya, 2007. PCC'07*, 2007, pp. 635–642.
[21] J. M. Guerrero, J. C. Vasquez, J. Matas, L. G. de Vicuna, and M. Castilla, "Hierarchical control of droop-controlled AC and DC microgrids—a general approach toward standardization," *Industrial Electronics, IEEE Transactions on*, vol. 58, no. 1, pp. 158–172, 2011.
[22] R. Lasseter, A. Akhil, C. Marnay, J. Stephens, J. Dagle, R. Guttromson, A. Meliopoulous, R. Yinger, and J. Eto, "The CERTS microgrid concept," *White paper for Transmission Reliability Program, Office of Power Technologies, US Department of Energy*, 2002.
[23] J. Lynch, *Northern power system update on Mad River microgrid and related activities*. .
[24] A. Denda, "Shimizu's microgrid research activities," 2006.
[25] Y. Kojima, M. Koshio, S. Nakamura, H. Maejima, Y. Fujioka, and T. Goda, "A demonstration project in hachinohe: Microgrid with private distribution line," 2007, pp. 1–6.
[26] K. Hirose, T. Takeda, and S. Muroyama, "Study on field demonstration of multiple power quality levels system in Sendai," 2006, pp. 1–6.
[27] Y. Ito, Y. Zhongqing, and H. Akagi, "DC microgrid based distribution power generation system," 2004, vol. 3, pp. 1740–1745.
[28] E. Borioli, M. Brenna, R. Faranda, and G. Simioli, "Comparison between the electrical capabilities of the cables used in LV AC and DC power lines," in *Harmonics and Quality of Power, 2004. 11th International Conference on*, 2004, pp. 408–413.
[29] J. Y. Kim, J. H. Jeon, S. K. Kim, C. Cho, J. H. Park, H. M. Kim, and K. Y. Nam, "Cooperative control strategy of energy storage system and microsources for stabilizing the microgrid during islanded operation," *Power Electronics, IEEE Transactions on*, vol. 25, no. 12, pp. 3037–3048, 2010.
[30] J. D. Kueck, R. H. Staunton, S. D. Labinov, and B. J. Kirby, "„Microgrid Energy Management System ", CERTS project report ORNL," TM-2002/242.
[31] G. Celli, F. Pilo, G. Pisano, and G. G. Soma, "Optimal participation of a microgrid to the energy market with an intelligent EMS," in *Power Engineering Conference, 2005. IPEC 2005. The 7th International*, 2005, pp. 663–668.
[32] N. D. Hatziargyriou, A. Dimeas, A. G. Tsikalakis, J. A. . Lopes, G. Karniotakis, and J. Oyarzabal, "Management of microgrids in market environment," in *Future Power Systems, 2005 International Conference on*, 2005, p. 7–pp.
[33] S. M. Schoenung and J. Eyer, "Benefit/Cost Framework for Evaluating Modular Energy Storage."
[34] J. M. Eyer, J. J. Iannucci, and G. P. Corey, "Energy Storage Benefits and Market Analysis Handbook, A Study for the DOE Energy Storage Systems Program," *Sandia National Labratories*, 2004.
[35] S. M. Schoenung, "Energy Storage Systems Cost Update," *SAND2011-2730*, 2011.

[36] A. Nourai, “Installation of the first distributed energy storage system (DESS) at american electric power (AEP),” *Sandia National Laboratories, SAND2007-3580*, 2007.
[37] U. E. A. Committee and others, “Bottling electricity: Storage as a strategic tool for managing variability and capacity concerns in the modern grid,” 2009, 2009.
[38] A. Price, G. Thijssen, and P. Symons, “Electricity Storage, A Solution in Network Operation?,” *Distributech Europe*, 2000.
[39] Michele Martino and Group WPS2-851, “Suitability Study of a Hybrid Energy Storage System,” May 2011.
[40] M. Swierczynski, R. Teodorescu, C. N. Rasmussen, P. Rodriguez, and H. Vikelgaard, “Overview of the energy storage systems for wind power integration enhancement,” in *Industrial Electronics (ISIE), 2010 IEEE International Symposium on*, pp. 3749–3756.
[41] “Lead-acid storage system plants.” [Online]. Available: http://electricitystorage.org/tech/technologies_technologies_leadacid.htm. [Accessed: 04-Apr-2011].
[42] “Lead Acid Batteries.” [Online]. Available: http://www.electricitystorage.org/ESA/technologies/lead-acid_batteries/. [Accessed: 13-Apr-2011].
[43] C. Naish, I. McCubbin, O. Edberg, and M. Harfoot, “Outlook of Energy Storage Technologies,” Feb. 2008.
[44] Y. V. Makarov, B. Yang, J. G. DeSteese, S. Lu, C. H. Miller, and P. N. N. L. (US), “Wide Area Energy Storage and Management System to Balance Intermittent Resources in the Bonneville Power Administration and California ISO Control Areas,” 2008.
[45] J. Voelcker, “Lithium batteries take to the road,” *Spectrum, IEEE*, vol. 44, no. 9, pp. 26–31, 2007.
[46] N. Mohan and T. M. Undeland, *Power electronics: converters, applications, and design*. Wiley-India, 2007.
[47] R. W. Erickson and D. Maksimović, *Fundamentals of power electronics*. Springer, 2001.
[48] E. Commission and others, “Directive 2004/8/EC of the European Parliament and of the Council of 11 February 2004 on the promotion of cogeneration based on a useful heat demand in the internal energy market and amending Directive 92/42/EEC,” *EEC*, 2004.
[49] G. R. Simader, R. Krawinkler, and G. Trnka, “Micro CHP systems: state-of-the-art,” *Final Report, Deliverable*, vol. 8, 2006.
[50] M. De Paepe, P. D’Herdt, and D. Mertens, “Micro-CHP systems for residential applications,” *Energy conversion and management*, vol. 47, no. 18, pp. 3435–3446, 2006.
[51] D. N. Gaonkar and S. Nayak, “Modeling and performance analysis of microturbine based Distributed Generation system,‘a review’,” in *Energytech, 2011 IEEE*, 2011, pp. 1–6.
[52] F. Blaabjerg and Z. Chen, *Power electronics for modern wind turbines*, vol. 1. Morgan & Claypool, 2006.
[53] J. R. Bumby, N. Stannard, and R. Martin, “A permanent magnet generator for small scale wind turbines,” *Proceedings of ICEM 2006*, 2006.
[54] R. Esmaili, L. Xu, and D. K. Nichols, “A new control method of permanent magnet generator for maximum power tracking in wind turbine application,” in *Power Engineering Society General Meeting, 2005. IEEE*, 2005, pp. 2090–2095.

[55] K. Tan and S. Islam, “Optimum control strategies in energy conversion of PMSG wind turbine system without mechanical sensors,” *Energy Conversion, IEEE Transactions on*, vol. 19, no. 2, pp. 392–399, 2004.
[56] B. S. Borowy and Z. M. Salameh, “Dynamic response of a stand-alone wind energy conversion system with battery energy storage to a wind gust,” *Energy Conversion, IEEE Transactions on*, vol. 12, no. 1, pp. 73–78, 1997.
[57] R. Melício, V. M. . Mendes, and J. P. . Catalão, “Wind Turbines with Permanent Magnet Synchronous Generator and Full-Power Converters: Modelling, Control and Simulation.”
[58] M. Martino and intro group-736 Aalborg University, *Efficiency Improvement for Photovoltaic Inverters*. 2010.
[59] K. H. Hussein, I. Muta, T. Hoshino, and M. Osakada, “Maximum photovoltaic power tracking: an algorithm for rapidly changing atmospheric conditions,” in *Generation, Transmission and Distribution, IEE Proceedings-*, 1995, vol. 142, pp. 59–64.
[60] A. Oi, “Design and simulation of photovoltaic water pumping system,” California Polytechnic State University, 2005.

APENDIX A - IMPLEMENTED MICRO-GRID in SIMULINK

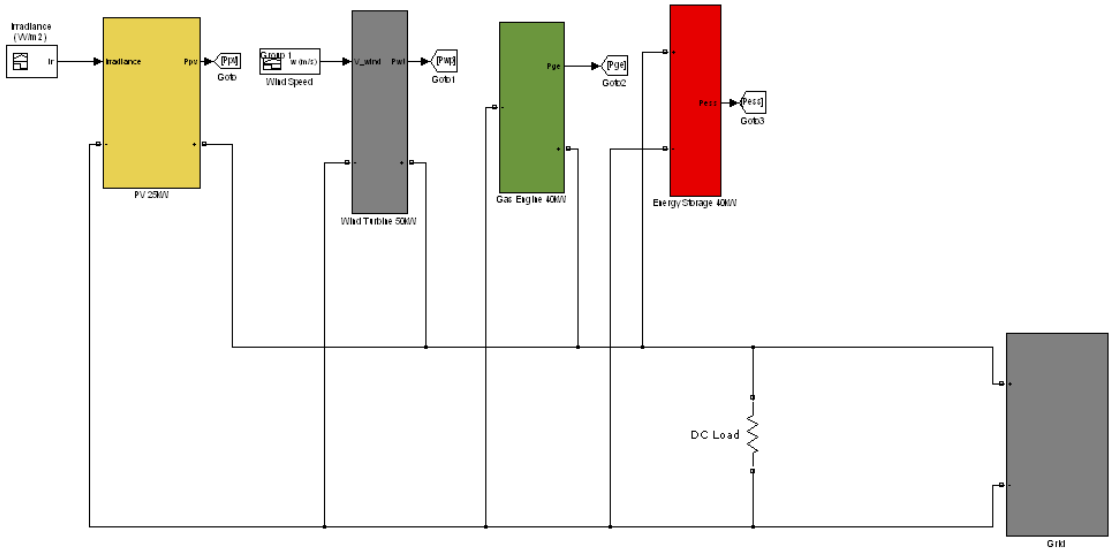

1. PV model:

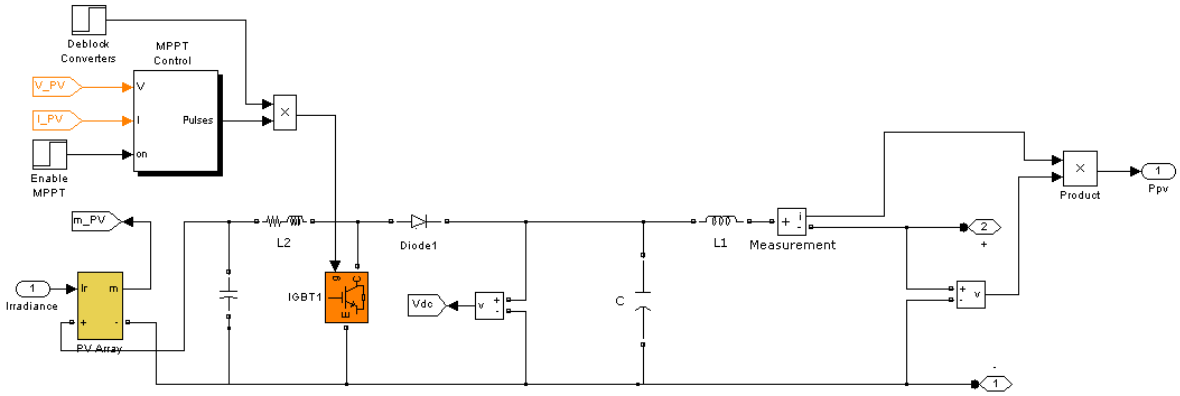

1.1 PV Array:

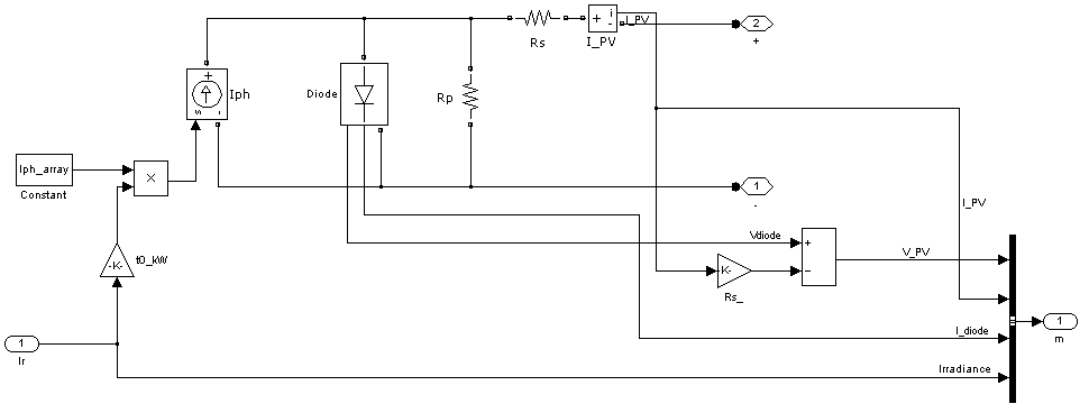

1.2 MPPT Control:

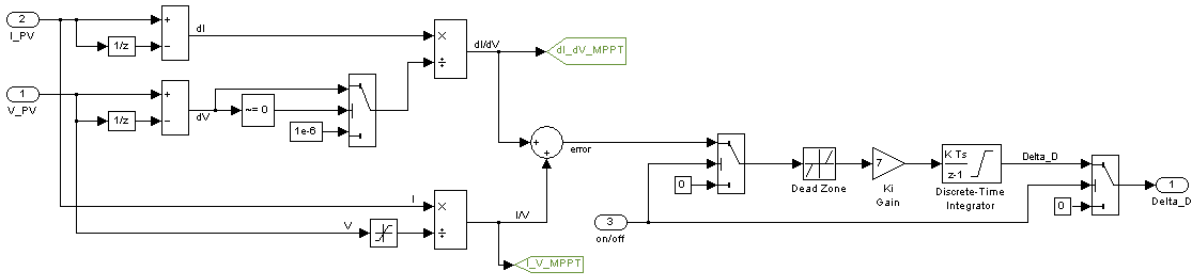

2. WT model:

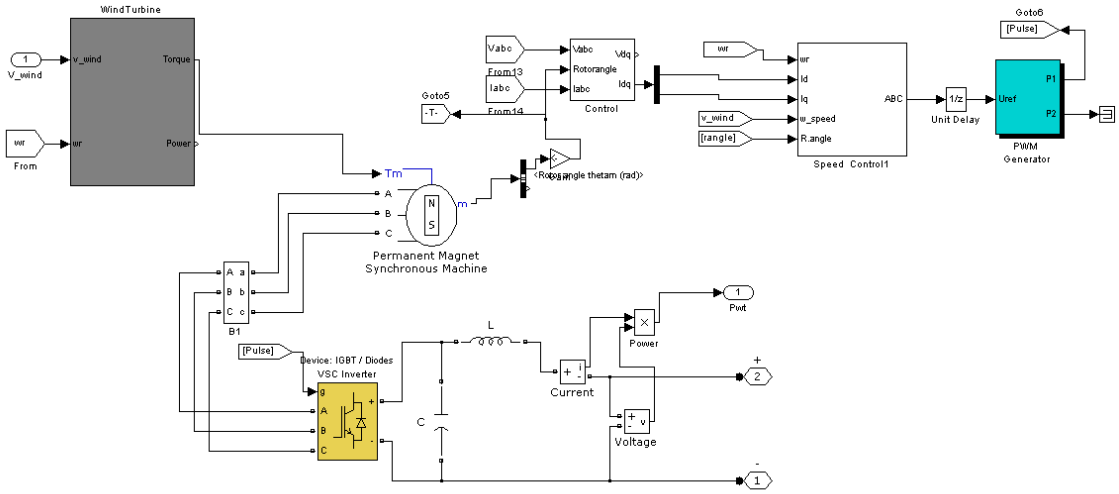

2.1 Wind Turbine :

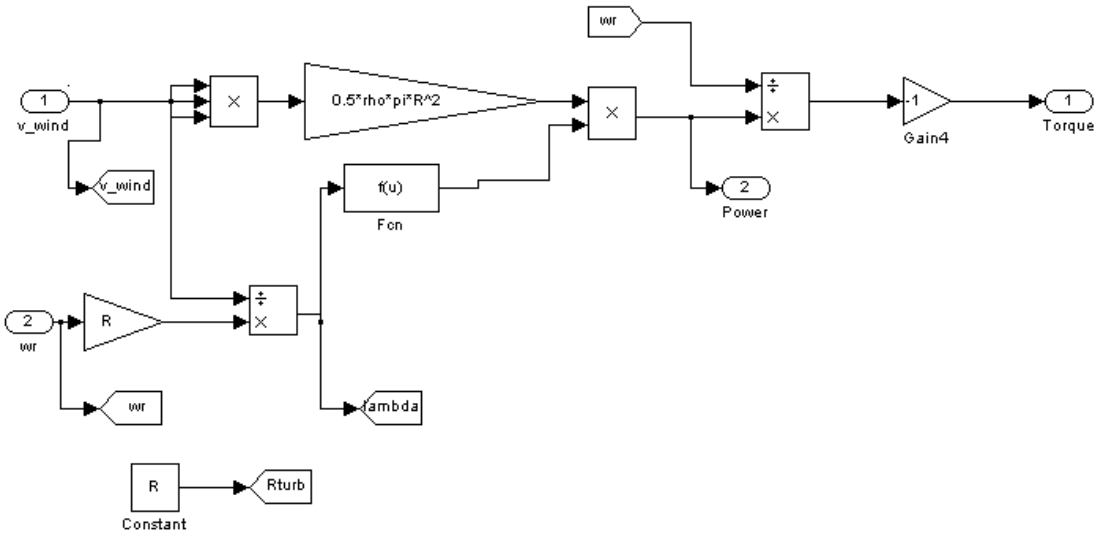

2.2 Speed Control:

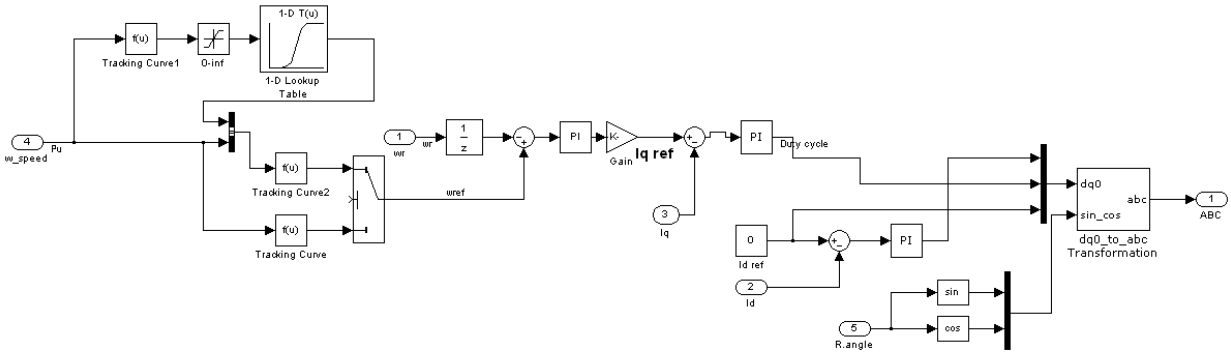

3. GE Model:

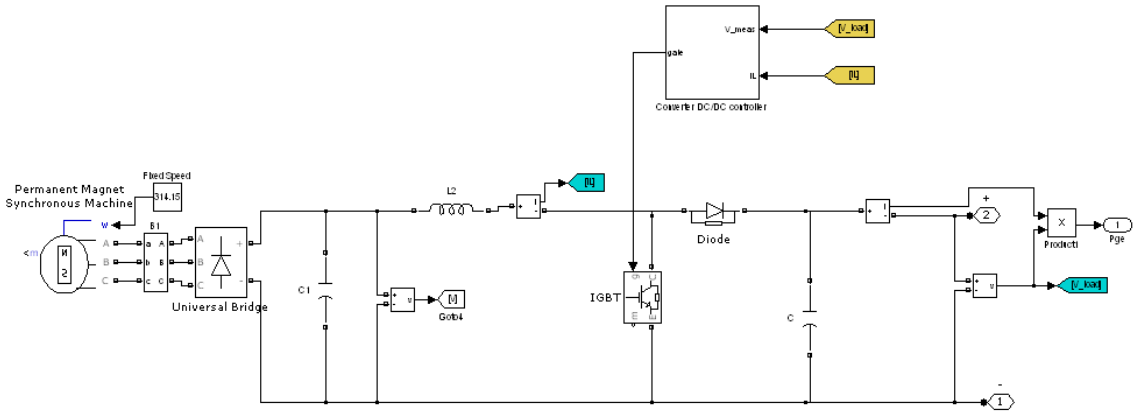

3.1 Voltage Control:

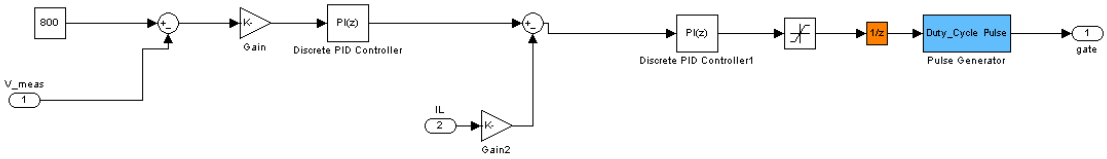

4. ESS model:

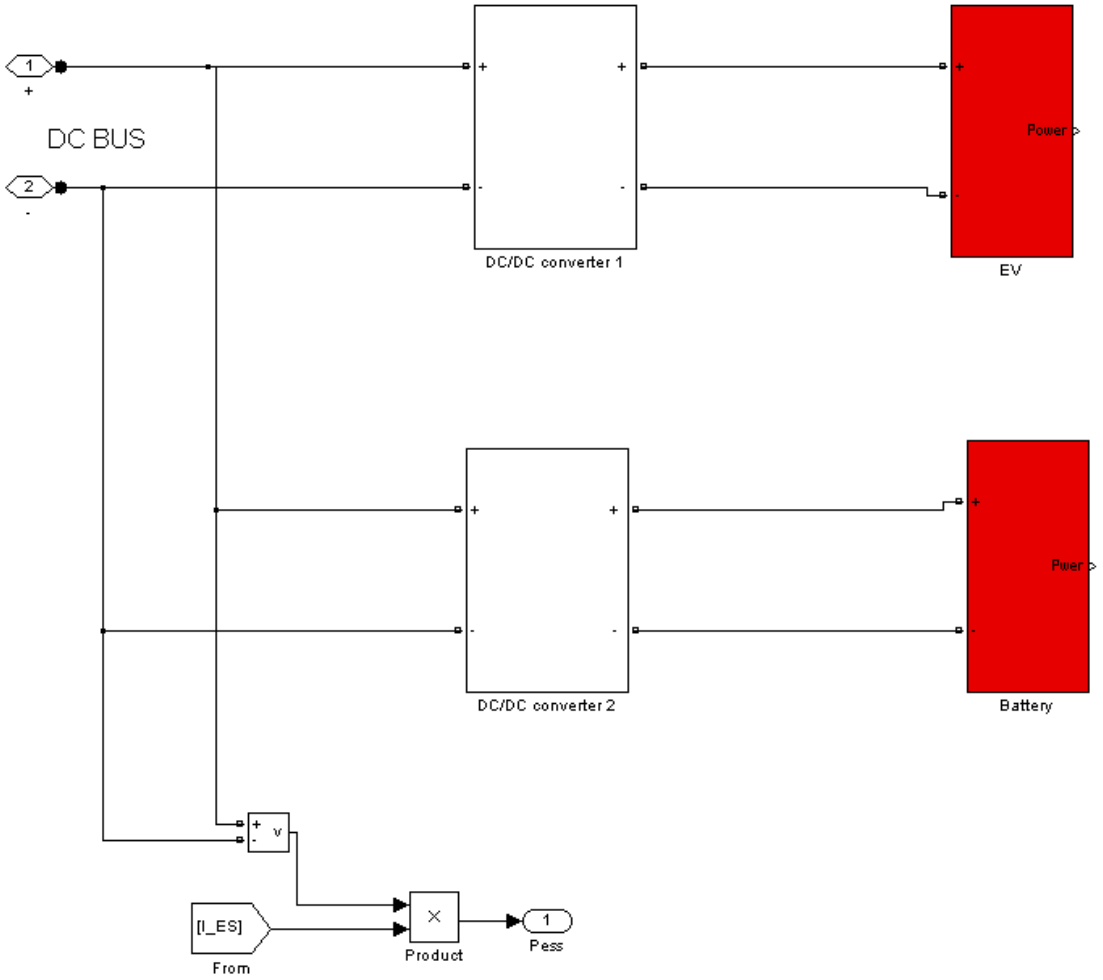

4.1 Battery model:

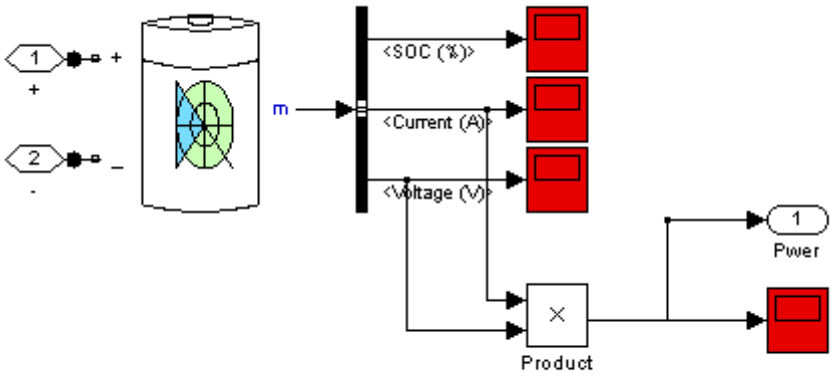

4.2 Bi-direccional Converter:

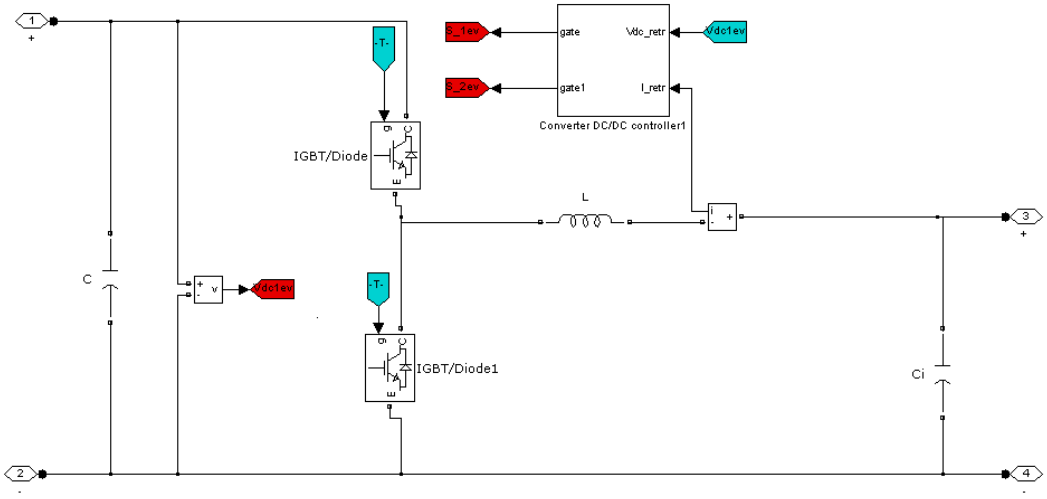

4.3 Bi-direccional Control:

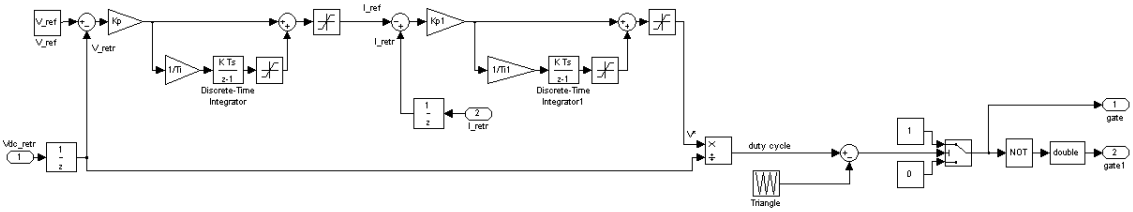

5. Grid Model:

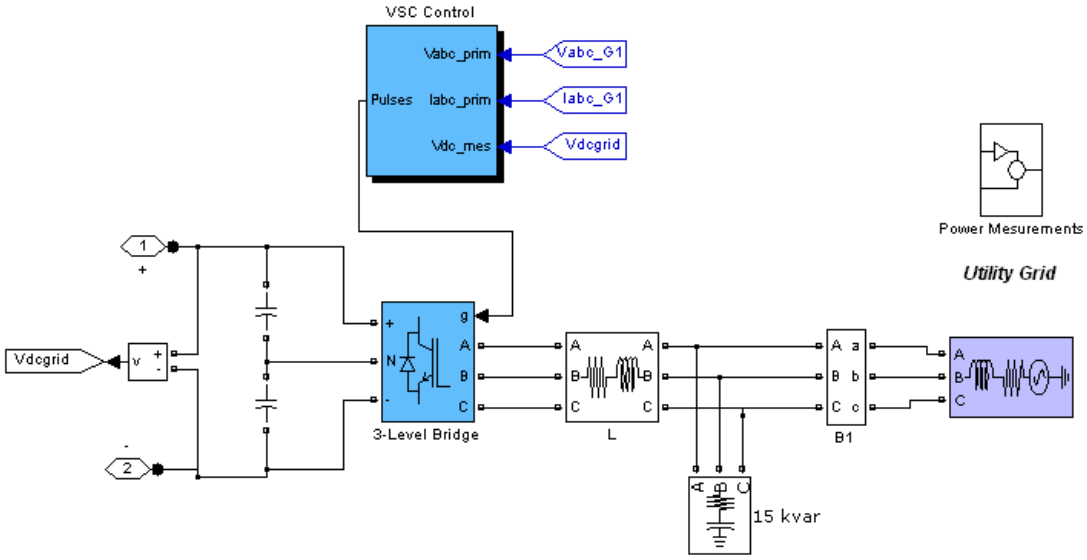

5.1 VSC Control:

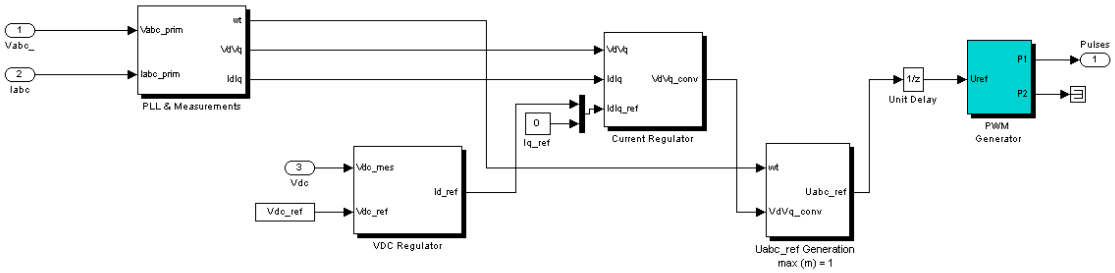

APENDIX B - ECONOMICAL STUDY CASES in MATLAB

The proposed study cases in chapter 3.3 have been implemented with MATLAB, the designed programs used to evaluate the different cases are shown below:

For the Case 1:

```
Vspeed=load('WindSpeed1.txt');
irradiance=load('Irradiance.txt');
Electricityprice=load('ElectricityPrice.txt');
Eprice=Electricityprice(:,1)/1000;    % Electricity market price array
Vs=Vspeed(:,1);                       % Annual wind speed array
N=1:1:length(Vspeed); %
Irr=irradiance(:,1); %                % Annual Irradiance array
Pwt=0.5*pi*36*1.0443*0.4906*(Vs).^3; % Annual WT power array
Ppv=Irr*25000;                        % Annual PV power array
Pge=40000;                            % Annual GE power array
Eref=0.0331;                          % Refference ESS kWh price
Money1=0;
Money2=0;
Money3=0;
SOC=50:(1/8759):51;
Y=1:1:8761;
%Pload=75000;
for i=1:length(Vspeed)
Pload(i)=50000;                       % Fixed annual DC load
    if Pwt(i)>50000                    % Correction of WT power to never
raise 50kW
        Pwt(i)=50000;
    end
end
Psource=Pwt+Pge+Ppv;


%%       &&&&&&&&&&&       Hypothesis       1-Grid       Participation
&&&&&&&&&&&&&&&&&&&&&&&&

for k=1:length(Vspeed)
    Pgrid(k)=(Psource(k)-Pload(k))/1000; %Power flow in kW
    Money1=Money1+Pgrid(k)*Eprice(k);
end


%%       &&&&&&&&&&&       Hypothesis       2-ESS       Participation
&&&&&&&&&&&&&&&&&&&&&&&&

for k=1:length(Vspeed)
    Pgrid(k)=Psource(k)-Pload(k);

    if Pgrid(k)>0
            if SOC(k)>85
            Money2=Money2+Pgrid(k)/1000*Eprice(k);
            SOC(k+1)=SOC(k);
```

```
            else
                SOC(k+1)=SOC(k)+(100*Pgrid(k)/40000);
                if SOC(k+1)>95
                    SOC(k+1)=95;
                end
            end

        end

    if Pgrid(k)<0
            if SOC(k)>15
                Money2=Money2+Pgrid(k)/1000*Eref;
                SOC(k+1)=SOC(k)+(100*Pgrid(k)/40000);
                if SOC(k+1)<1
                    SOC(k+1)=1;
                end
            else
                Money2=Money2+Pgrid(k)/1000*Eprice(k);
                SOC(k+1)=SOC(k);
            end
        end
      if Pgrid(k)==0
          SOC(k+1)=SOC(k);
        end
%%      &&&&&&&&&&&      Hypothesis      3-Optimal      Participation
&&&&&&&&&&&&&&&&&&&&&&&&

for k=1:length(Vspeed)
    SOC(1)=50;
    Pgrid(k)=(Psource(k)-Pload(k));
    if Pgrid(k)>0
        if Eprice(k)>Eref
            if SOC(k)>15
            Money3=Money3+Pgrid(k)/1000*Eprice(k);
            SOC(k+1)=SOC(k);
            else
             SOC(k+1)=SOC(k)+(10*Pgrid(k)/40000);
                if SOC(k+1)>95
                    SOC(k+1)=95;
                end
            end
        end

        if Eprice(k)<Eref
            if SOC(k)<85
                SOC(k+1)=SOC(k)+(10*Pgrid(k)/40000);
                if SOC(k+1)>95
                    SOC(k+1)=95
                end

            else
              Money3=Money3+Pgrid(k)/1000*Eprice(k);
              SOC(k+1)=SOC(k);
            end

        end
    end
    if Pgrid(k)<0
        if Eprice(k)>Eref
            if SOC(k)>15
```

```
                SOC(k+1)=SOC(k)+(10*Pgrid(k)/40000);
                if SOC(k+1)<5
                    SOC(k+1)=5;
                end

            else
                Money3=Money3+Pgrid(k)/1000*Eprice(k);
                SOC(k+1)=SOC(k);
            end
        end
        if Eprice(k)<Eref
            if SOC(k)<85
                Money3=Money3+Pgrid(k)/1000*Eprice(k);
                SOC(k+1)=SOC(k);

            else
                SOC(k+1)=SOC(k)+(100*Pgrid(k)/40000);
                if SOC(k+1)<5
                    SOC(k+1)=5;
                end
            end
        end
    end
    if Pgrid==0
        SOC(k+1)=SOC(k);
    end
end
Money1
Money2
Money3
```

For the Case 2:

```
Vspeed=load('WindSpeed1.txt');
irradiance=load('Irradiance.txt');
Electricityprice=load('ElectricityPrice.txt');
Eprice=Electricityprice(:,1)/1000;    % Electricity market price array
Vs=Vspeed(:,1);                       % Annual wind speed array
N=1:1:length(Vspeed); %
Irr=irradiance(:,1); %                % Annual Irradiance array
Pwt=0.5*pi*36*1.0443*0.4906*(Vs).^3; % Annual WT power array
Ppv=Irr*25000;                        % Annual PV power array
Pge=40000;                            % Annual GE power array
Eref=0.0331;                          % Refference ESS kWh price
Money1=0;
Money2=0;
Money3=0;
SOC=50:(1/8759):51;
Y=1:1:8761;
DCl=load('variabledcload.txt');      % Variable annual DC load
DCload=DCl*1000000;
Pge=DCl*1000000;
%Pload=75000;
for i=1:length(Vspeed)

    if Pwt(i)>50000                   % Correction of WT power to never
raise 50kW
```

```
        Pwt(i)=50000;
    end
    if Pge(i)>40000                    % Correction of GE power to never
raise 40kW
        Pge(i)=40000;
    end
end
Psource=Pwt+Pge+Ppv;


%%       &&&&&&&&&&&       Hypothesis       1-Grid       Participation
&&&&&&&&&&&&&&&&&&&&&&&&

for k=1:length(Vspeed)
    Pgrid(k)=(Psource(k)-DCload(k))/1000; %Power flow in kW
    Money1=Money1+Pgrid(k)*Eprice(k);
end


%%       &&&&&&&&&&&       Hypothesis       2-ESS       Participation
&&&&&&&&&&&&&&&&&&&&&&&&

for k=1:length(Vspeed)
    Pgrid(k)=Psource(k)-DCload(k);

    if Pgrid(k)>0
            if SOC(k)>85
            Money2=Money2+Pgrid(k)/1000*Eprice(k);
            SOC(k+1)=SOC(k);
            else
                SOC(k+1)=SOC(k)+(100*Pgrid(k)/40000);
                if SOC(k+1)>95
                    SOC(k+1)=95;
                end
            end

        end

    if Pgrid(k)<0
            if SOC(k)>15
                Money2=Money2+Pgrid(k)/1000*Eref;
                SOC(k+1)=SOC(k)+(100*Pgrid(k)/40000);
                if SOC(k+1)<1
                    SOC(k+1)=1;
                end
            else
                Money2=Money2+Pgrid(k)/1000*Eprice(k);
                SOC(k+1)=SOC(k);
            end
        end
      if Pgrid(k)==0
          SOC(k+1)=SOC(k);
        end
%%       &&&&&&&&&&&       Hypothesis       3-Optimal       Participation
&&&&&&&&&&&&&&&&&&&&&&&&

for k=1:length(Vspeed)
    SOC(1)=50;
    Pgrid(k)=(Psource(k)-DCload(k));
```

```
    if Pgrid(k)>0
        if Eprice(k)>Eref
            if SOC(k)>15
            Money3=Money3+Pgrid(k)/1000*Eprice(k);
            SOC(k+1)=SOC(k);
            else
             SOC(k+1)=SOC(k)+(10*Pgrid(k)/40000);
                if SOC(k+1)>95
                    SOC(k+1)=95;
                end
            end
        end

        if Eprice(k)<Eref
            if SOC(k)<85
                SOC(k+1)=SOC(k)+(10*Pgrid(k)/40000);
                if SOC(k+1)>95
                    SOC(k+1)=95
                end

            else
              Money3=Money3+Pgrid(k)/1000*Eprice(k);
              SOC(k+1)=SOC(k);
            end

        end
    end
    if Pgrid(k)<0
        if Eprice(k)>Eref
            if SOC(k)>15
                SOC(k+1)=SOC(k)+(10*Pgrid(k)/40000);
                if SOC(k+1)<5
                    SOC(k+1)=5;
                end

            else
                Money3=Money3+Pgrid(k)/1000*Eprice(k);
                SOC(k+1)=SOC(k);
            end
        end
        if Eprice(k)<Eref
            if SOC(k)<85
                Money3=Money3+Pgrid(k)/1000*Eprice(k);
                SOC(k+1)=SOC(k);

            else
                SOC(k+1)=SOC(k)+(100*Pgrid(k)/40000);
                if SOC(k+1)<5
                    SOC(k+1)=5;
                end
            end
        end
    end
    if Pgrid==0
        SOC(k+1)=SOC(k);
    end
end
Money1
Money2
Money3
```

For the Case 3:

```
Electricityprice=load('ElectricityPrice.txt');
Eprice=Electricityprice(:,1)/1000;  %Annual Electricity Price
Eref=0.0331;                        % Reference ESS kWh price
N=1:1:length(Eprice); %
Money1=0;
Money2=0;
Money3=0;
SOC=50:(0.1/8759):50.1;
Y=1:1:8761;

arb10=100/10;
arb6=100/6;
arb3=100/3;

%%   &&&&&&&&&&&   Hypothesis   1-   3   hours   maximum   discharge
&&&&&&&&&&&&&&&&&&&&&&&&

for k=1:length(N)
    SOC(1)=50;
    Eref1(k)=0.0331;
        if Eprice(k)>Eref
            if SOC(k)>15
            Money=Money+40*Eprice(k);
            SOC(k+1)=SOC(k)-arb3;
             if SOC(k+1)<5
                    SOC(k+1)=5;
                end
            else

                SOC(k+1)=SOC(k);

            end

        end
        if Eprice(k)<Eref
            if SOC(k)<85
                Money=Money-40*Eprice(k);
                SOC(k+1)=SOC(k)+arb3;
                if SOC(k+1)>95
                    SOC(k+1)=95
                end
            else
                SOC(k+1)=SOC(k);


            end



    end
```

```
    if Eprice(k)==Eref
        SOC(k+1)=SOC(k);
    end

end

%%   &&&&&&&&&&&   Hypothesis   2-   6   hours   maximum   discharge
&&&&&&&&&&&&&&&&&&&&&&&&

for k=1:length(N)
    SOC(1)=50;
    Eref1(k)=0.0331;
        if Eprice(k)>Eref
            if SOC(k)>15
            Money=Money+40*Eprice(k);
            SOC(k+1)=SOC(k)-arb6;
             if SOC(k+1)<5
                    SOC(k+1)=5;
                end
            else

                SOC(k+1)=SOC(k);

            end

        end
        if Eprice(k)<Eref
            if SOC(k)<85
                Money=Money-40*Eprice(k);
                SOC(k+1)=SOC(k)+arb6;
                if SOC(k+1)>95
                    SOC(k+1)=95
                end
            else
                SOC(k+1)=SOC(k);


            end



    end


%%   &&&&&&&&&&&   Hypothesis   3-   10   hours   maximum   discharge
&&&&&&&&&&&&&&&&&&&&&&&&

for k=1:length(N)
    SOC(1)=50;
    Eref1(k)=0.0331;
        if Eprice(k)>Eref
            if SOC(k)>15
            Money=Money+40*Eprice(k);
            SOC(k+1)=SOC(k)-arb10;
             if SOC(k+1)<5
                    SOC(k+1)=5;
                end
```

```
            else

                SOC(k+1)=SOC(k);

            end

        end
        if Eprice(k)<Eref
            if SOC(k)<85
                Money=Money-40*Eprice(k);
                SOC(k+1)=SOC(k)+arb10;
                if SOC(k+1)>95
                    SOC(k+1)=95
                end
            else
                SOC(k+1)=SOC(k);


            end



    end


Money1
Money2
Money3
```

APENDIX C - USED TABLE

Properties of the Natural Gas depending the source [IEA]

	Higher Heating Value (kJ/m^3)	Lower Heating Value (kJ/m^3)
Algeria	42.000	37.800
Bangladesh	36.000	32.400
Canada	38.200	34.380
Indonesia	40.600	36.540
Netherlands	33.320	29.988
Norway	39.877	35.889
Pakistan	34.900	31.410
Russia	38.231	34.408
Arabia Saudi	38.000	34.200
United Kingdom	39.710	35.739
United States	38.416	34.574
Uzbekistan	37.889	34.099

APPENDIX D - GAS AMOUNT

The relationship of the Energy in Joule is:

1Ws= 1J ……(1)

1kWh= 3600 kJ (2)

Since the property of the natural gas, tableX, the lower heating value is:

$$H_L = 35889\ {}^{kJ}/_{m^3} \tag{3}$$

From the literature the efficiency of the PMSG is around 97%, so to have an output of $P_{in\_PMSG} = 40\text{kW}$ it needs the following input:

$$P_{in\_PMSG} = \frac{40kW}{0.97} = 41.237kW \tag{4}$$

P_{in_PMSG} is the output power of the Gas Engine. From the literature the efficiency of the GE is around 31 %, so it needs the following input power:

$$P_{in\_GE} = \frac{41.237kW}{0.31} = 133kW \tag{5}$$

So the amount of gas per second is:

$$Q_g = \frac{P_{in\_GE}}{H_L} = 0.0037\ m^3s \tag{6}$$

and its amount per hours is:

$$Q_g \cdot 3600 = 13.34\ m^3h \tag{7}$$

APPENDIX E – PROPORTIONAL AND INTEGRAL TERMS

In this appendix the constant control values will be shows in the tableX

Unit	Power Electronics Device	Control	Ki_1	Kp_1	Ki_2	Kp_2
WT	Boost	Speed(MPPT)	500	484	2.64	10
ESs	Bidirectional-Converter	Voltage / Flow Power	90.9	35	90.9	3.5
PV	Boost-converter	MPPT	1	7	-	-
Grid	Voltage Source Converter	Voltage / Flow Power	1	0.5	20	0.3

Where Ki_1 and Kp_1 are the terms of the outer loop, instead Ki_2 and Kp_2 are related to the inner loop.